Convention on Long-range Transboundary Air Pollution

emep

Co-operative programme for monitoring and evaluation of the long-range transmission of air pollutants in Europe

STATUS REPORT 4/2012

Transboundary particulate matter in Europe

Status Report 4/2012

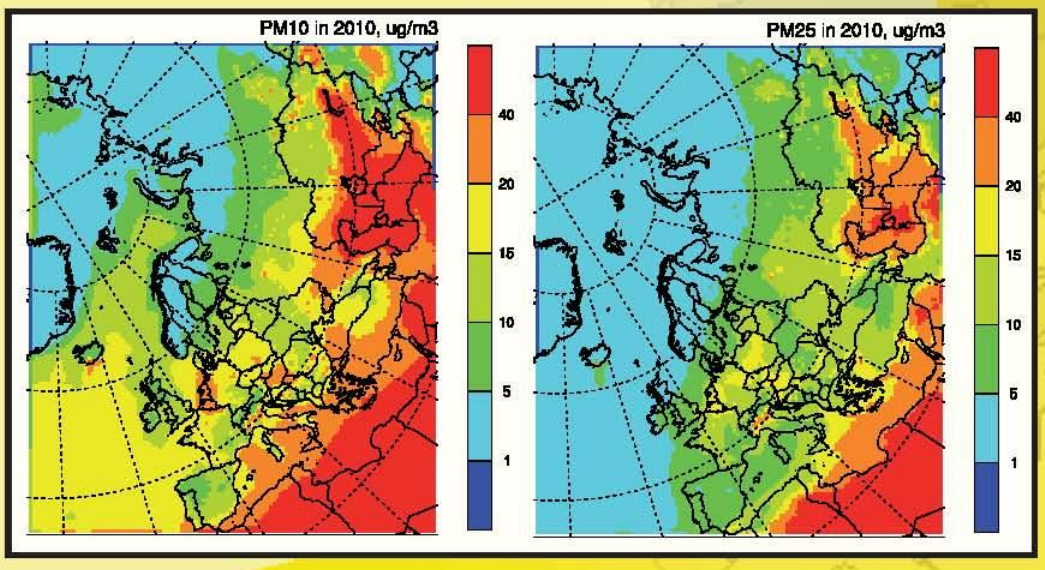

ccc & msc-w & ceip & ciam

NILU: EMEP Report 4/2012
REFERENCE: O-7726
DATE: AUGUST 2012
ISSN: 1504-6109 (print)
1504-6192 (online)

EMEP Co-operative Programme for Monitoring and Evaluation of the Long-Range Transmission of Air Pollutants in Europe

Transboundary particulate matter in Europe Status report 2012

Joint CCC, MSC-W, CEIP and CIAM Report 2012

Norwegian Institute for Air Research
P.O. Box 100, NO-2027 Kjeller, Norway

Norwegian Meteorological Institute
P.O. Box 43 Blindern, NO-0313 Oslo, Norway

Umweltbundesamt GmbH
Spittelauer Lände 5, AT-1090 Vienna, Austria

IIASA – International Institute for Applied Systems Analysis
Schlossplatz 1, AT-2361 Laxenburg, Austria

List of Contributors

Karl Espen Yttri[1], Wenche Aas[1], Kjetil Tørseth[1], Nina Iren Kristiansen[1], Cathrine Lund Myhre[1], Svetlana Tsyro[2], David Simpson[2,5], Robert Bergström[6,7], Katarína Marečková [3], Robert Wankmüller[3],Zbigniew Klimont[4], Markus Amman[4], Giorgos N. Kouvarakis[8], Paolo Laj[9], Gelsomina Pappalardo[10], André Prévôt[11]

1) Norwegian Institute for Air Research, Kjeller, Norway
2) Norwegian Meteorological Institute, Oslo, Norway
3) Umweltbundesamt, Vienna, Austria
4) International Institute for Applied Systems Analysis, Laxenburg, Austria
5) Chalmers University of Technology, Gothenburg, Sweden
6) Swedish Meteorological and Hydrological Institute, Norrköping, Sweden
7) Department of Chemistry, University of Gothenburg, Sweden
8) Environmental Chemical Processes Laboratory. Department of Chemistry - University of Crete, Greece
9) Laboratoire de Glaciologie et Géophysique de l'Environnement (CNRS-LGGE), France
10) The Institute of Methodologies for Environmental Analysis of the National Research Council of Italy (IMAA-CNR), Potenza, Italy
11) Paul Scherrer Institute, The Laboratory of Atmospheric Chemistry (LAC), Villigen, Switzerland

[1] EMEP Chemical Coordinating Centre
[2] EMEP Meteorological Synthesizing Centre – West
[3] EMEP Centre on Emission Inventories and Projections
[4] EMEP Centre on Integrated Assessment Modelling

Contents

Page

Executive Summary

The current report presents the status and progress of the emission reporting, observations and modelling activities undertaken under EMEP in relation to particulate matter in the European rural background environment. It also includes a special section related to volcanic ash eruption at the Eyjafjallajökull volcano in April and May 2010 which caused episodes with enhanced levels of PM and SO_2 at the European continent. A small section is devoted the EU infrastructures project ACTRIS (Aerosols, Clouds, and Trace gases Research InfraStructure Network), which is an important projects supporting the EMEP programme.

The main findings in the status for 2010 are described below.

Emission reporting

The number of Parties providing primary particulate matter emissions data increased by one from 2009 to 2010, and the total number of Parties was 36; out of 51 Parties to the Convention. Rather limited information is provided for Turkey, Central Asia and the Caucasus regions.

Emissions of particulate matter have been reported to CLRTAP from 2000 and earlier. PM emissions trends vary quite considerably among the Parties to the Convention. For most countries which have reported data, PM emissions have decreased since 2000; there are a few exceptions though. For the last year however (from 2009 to 2010), $PM_{2.5}$ and PM_{10} emissions rose in 21 Parties, with the most substantial increase in Serbia and the Russian Federation (about 30% increase).

The most significant source of PM emission is the combustion of fossil fuels, contributing about 50% of PM emissions. Not all Parties do report emissions from all the emissions sectors, and especially countries outside EU/EFTA region there is a relatively low contribution of "Small Combustion" to the total PM emissions, indicating that emissions from this sector are potentially underestimated. Another important source of PM emissions is the transport sector with contributions of 13 to 26% to national totals.

Revision of the Gothenburg Protocol

In May 2012, Parties to the LRTAP Convention reached an agreement on a revision of its Gothenburg multi-pollutant/multi-effect protocol. For the first time in a multilateral environmental agreement, the adverse effects of particulate matter (PM) on health have been considered and emission reduction commitments for emissions of fine primary particles ($PM_{2.5}$) were included. Also, for the first time in an international treaty, the revised Protocol reflects upon the close linkages between regional air pollution and global climate change by including black carbon (BC), a short-lived climate forcer.

Measurement and model assessment of particulate matter

For 2010, mass concentrations of PM are reported for 69 regional or global background sites (67 for PM_{10} and 43 for $PM_{2.5}$); four more than in 2009. During the past year, the EMEP/MSC-W model has been through an extensive revision

and update process with the purpose of improving model's general performance and in particular the representation of PM. As a result, several parameterisations of chemical and physical processes have been implemented or improved. One of the major improvements to PM calculations was due to implementation of secondary organic aerosols (SOA) in the standard model.

In general, modelling of organic aerosol is subject to much larger problems than those of many other pollutants, something which inevitably follows from the complexity of organic aerosol itself, and our lack of understanding of the underlying science. One of the major uncertainties to build or evaluate reliable SOA models is the current emission estimates. Emission inventories for especially biogenic volatile organic compounds (BVOC) and primary organic aerosols (POA), including residential wood-combustion (RWC) should be priority areas.

Combined maps of EMEP model results and measurements show a pronounced north to south gradient, with the annual mean PM_{10} concentrations varying from 1-5 μg m^{-3} in Northern Europe to 15-25 μg m^{-3} in Southern Europe. The average observed annual mean PM_{10} concentration for all sites was 15.5 μg/m^3, ranging from 2.2 μg/m^3 at the high altitude global site Jungfraujoch in Switzerland, to 30.4 μg/m^3 at Ayia Marina in Cyprus. On average about 50% of the urban background concentration is likely to be attributed to the mean rural background concentration of PM_{10}.

The observed PM_{10} levels in 2010 and 2009 are quite comparable. On average there was a small decrease of 3%. For $PM_{2.5}$ on the other hand, there was an average increase of 4% for all sites. When comparing the modelled results, PM_{10} and $PM_{2.5}$ concentrations in 2010 are respectively 0.5-5 μg/m^3 and 0.5-3 μg/m^3 higher in 2010 than in 2009 in most of EMEP area, using the same and updated EMEP model version. In arid areas in southern/south-eastern parts of the domain, PM_{10} and $PM_{2.5}$ in 2010 exceed by 5-7 μg/m^3 those in 2009, which is due to windblown dust. Only in Mediterranean region and Norway, calculated 2010 concentrations are 0.5-2 μg/m^3 lower than those in 2009. The large-scale differences in annual mean maps of PM concentrations are to a large extent due to meteorological conditions, especially differences in the annual amount of precipitation in 2009 and 2010. In a longer time perspective, there is a relatively clear decrease in the PM_{10} mass concentration. From twenty four sites, with measurements from 2000 (or 2001) to 2010 show an average decrease of 21% ±13%. 54% of the sites show a significant decrease. Similar numbers are observed for $PM_{2.5}$; an average decrease of 27 ±14%, at thirteen sites with measurements from 2000 or 2001.

The combined model and observation maps show that the annual mean regional background PM_{10} concentrations were below the EU limit value of 40 μg/m^3 over all of Europe in 2010, with the exception of the south most areas in Europe and the EECCA (Eastern Europe, Caucasus and Central Asia) countries affected by desert dust outbreaks. However, the annual mean PM_{10} concentrations calculated by the model exceed the WHO recommended AQG of 20 μg/m^3 in the Benelux countries, Hungary and the Po Valley in addition to the southern and south-eastern parts of the Mediterranean basin, in the Caucasus and in the EECCA countries. The regional background annual mean $PM_{2.5}$ concentrations were above

the WHO recommended AQG value of 10 μg/m^3 in many parts of Central, Eastern and South-Eastern Europe, in the Po Valley and the EECCA area.

Chemical composition data is essential to evaluate aerosol mass concentrations. There are clear geographical differences in the importance of different components in PM_{10} concentrations. As calculated by the model, SIA dominates in Central Europe comprising 40-50% of PM_{10}, while organic aerosols (OA) prevail in Northern Europe and northern/mid-latitude part of Russia (30-55% of PM_{10}) and particularly in Siberian areas of Russia (up to 60% of PM_{10}). Similar distribution is seen in the measurements. The average contribution of SIA from the fifteen sites with concurrent measurements of SO_4^{2-}, NO_3^- and NH_4^+ is 35±12%, where Central Europe had the highest SIA contribution with around 50%.

Twelve sites reported measurements of EC and OC for 2010, which are two more than for 2009. In addition to increased number of sites, the quality of the EC/OC data has improved with respect to more sites using the EUSAAR-2 reference protocol, and better data capture including year-round measurements at increased number of sites. The carbonaceous aerosol concentration was found to range by more than one order of magnitude within the European rural background environment. Elevated concentrations were observed in northern Italy and in Eastern Europe. Concentrations observed at sites in Scandinavia and at high altitude sites in western/south-western Europe, were substantially lower.

ACTRIS -Aerosols, Clouds and Trace gases Research InfraStructure Network

To strengthen the monitoring activities at supersites in Europe, collaboration and integration with other networks and frameworks working on observation of atmospheric constituents is essential for the EMEP programme. The ACTRIS EU FP7 infrastructure project will thus bring important support to EMEP in the coming years, by establishing high quality observations of aerosols, clouds and short-lived trace gases. One of the main objectives of ACTRIS is hence to provide long-term observational data relevant to climate and air quality research on the regional scale produced with standardized or comparable procedures throughout the network. The close link between ACTRIS and EMEP is also illustrated in the ongoing EMEP intensive measurement periods (IMP) for the summer 2012 and winter 2013. The campaign has further been coordinated with other relevant projects like ChArMEx and PEGASOS.

Volcanic eruption from the Eyjafjallajökull volcano

The eruption of the Eyjafjallajökull volcano in April and May 2010 released large amounts of volcanic ash and gases high into the atmosphere. It was transported eastward and southwards to the European mainland in the days after the eruption onset and caused closure of airports all over Europe. Several stations in the EMEP monitoring network and other measurement sites revealed time periods with volcanic aerosol impact in April and May 2010. I.e. at Schauinsland (DE0003) the concentration at 19-20 April (24h average) was 71.5 μg/m^3. The EMEP/MSC-W chemical transport model was shortly after the start of the Eyjafjallajökull eruption, adapted for calculating volcanic PM by implementing a first provisional scheme. In the following year, the volcano module was further developed and

improved, and calculations for volcanic emissions have been included in the operational version of the model. Other models, i.e. the FLEXPART transport model has also been used for evaluation the transport of volcanic ash over the European continent. The models were able to reproduce the occurrence of most of pollution episodes associated with emissions from the Eyjafjallajökull eruption in April-May 2010. However, the levels of PM_{10} concentrations are not always calculated accurately, and in some cases model calculated episodes (or concentration peaks) are slightly shifted in time compared to observations. There are also cases when modelled volcanic ash episodes are not found in observational data, or oppositely. Good quality of meteorological input is crucial for the transport model to correctly predict the direction and speed of ash cloud propagation. Also, good estimates of volcanic emissions are important for accurate modelling of the effects of volcanic eruption clouds on air pollution.

1 Status of emissions

By Katarína Marečková, Robert Wankmüller

1.1 PM emission reporting under the LRTAP Convention

Particulate matter (PM_{10} and $PM_{2.5}$) emissions should be reported to the Convention annually[1], as a minimum for the years from 2000 onwards. 2012 was also a reporting year for gridded emissions and large point sources (LPS). All information should be provided in standardized formats in accordance with the EMEP Reporting Guidelines (UNECE, 2009; EMEP/EEA, 2009).

1.2 Status of reporting in 2012

44[2] Parties (out of 51) to the LRTAP Convention submitted inventories for 2010, and one Party (Albania) submitted inventories only until 2009. Of these 44 Parties, only 36 provided PM emissions. Data submitted by the Parties can be accessed via the CEIP website at http://www.ceip.at/overview-of-submissions-under-clrtap/2012-submissions.

Completeness, consistency, comparability and transparency of reported emissions are analyzed in an annual review process[3]. Feedback is provided to the Parties in the form of individual country reports and summary findings are published in the EEA & CEIP technical report *Inventory Review 2012 (*http://www.ceip.at/review-of-inventories/review-2012) (EMEP/EEA, 2011).

1.3 PM emission trends

PM emissions trends (as reported) vary quite considerably among the Parties to the CLRTAP. For most countries which have reported data, PM emissions have decreased since 2000. However, there are a few exceptions where Parties reported increased emissions: PM_{10} have risen in 10 Parties, $PM_{2.5}$ emissions in fourteen Parties. The biggest increases in $PM_{2.5}$ emissions have been reported by the Republic of Moldova (210%), Serbia (41%), Albania (26%) and Bulgaria (22%).

From 2009 to 2010, $PM_{2.5}$ and PM_{10} emissions rose in 21 Parties, with the most substantial increase in Serbia (36% in $PM_{2.5}$ and 21% in PM_{10}) and the Russian Federation (34% in $PM_{2.5}$ and 29% in PM_{10}) (see Table 1.1 and Table 1.2**)**.

[1] Parties to the LRTAP Convention submit air pollution emissions and projections annually to the EMEP Centre on Emission Inventories and Projections (CEIP) and notify the LRTAP Convention secretariat thereof.

[2] Montenegro submitted its inventory for 2010 on 18 June 2012 and therefore its 2010 data cannot be included in the analysis.

[3] Methods and Procedures for the Technical Review of Air Pollutant Emission Inventories Reported under the Convention and its Protocols (EB.AIR/GE.1/2007/16).

Table 1.1: $PM_{2.5}$ emission trends (2000-2010) as reported by Parties.

Country / PM2.5 [Gg]	2000	2001	2002	2003	2004	2005	2006	2007	2008	2009	2010	Change 2009 - 10	Change 2000 - 10
Albania	8.9	9.1	9.8	12.8	14.3	13.5	13.8	13.5	13.5	11.2			26%
Armenia								0.3					
Austria	22.6	22.9	22.2	22.3	22.1	22.3	21.2	20.6	20.5	19.4	19.8	2%	-12%
Azerbaian													
Belarus			NE	NE	36.2	45.7	51.6	51.1	53.3	51.8	45.0	-13%	
Belgium	33.8	30.4	29.6	29.1	28.2	24.4	25.0	21.4	20.3	15.8	16.7	6%	-51%
Bosnia & Herzegovina													
Bulgaria	22.4	20.5	25.1	27.6	26.8	26.7	28.1	25.7	26.7	25.1	27.3	9%	22%
Canada	NR	NR	NR	NR	NR	NR	NR	NR	NR	1,105.5	1,112.6	1%	
Croatia	9.5	9.5	10.2	12.2	12.5	12.6	11.9	11.4	11.3	10.5	10.2	-3%	7%
Cyprus	3.9	3.7	3.7	3.7	3.2	2.9	2.8	2.8	2.8	2.3	2.2	-5%	-44%
Czech Republic			NE	38.4	34.9	20.9	21.5	21.2	20.9	20.4	19.6	-4%	
Denmark	22.2	22.7	22.1	23.7	24.0	25.4	26.4	29.9	27.6	25.4	25.7	1%	16%
Estonia	21.2	22.2	22.8	20.9	22.1	19.9	15.2	20.3	20.0	18.6	23.8	28%	12%
European Union	1,566	1,560	1,498	1,477	1,473	1,431	1,392	1,374	1,348	1,295	1,333	3%	-15%
Finland	38.9	39.9	40.4	40.3	39.9	36.0	36.8	34.4	38.5	38.2	40.7	7%	5%
France	368.2	357.4	332.5	333.6	321.3	304.0	287.7	273.0	267.1	251.4	254.5	1%	-31%
FYR of Macedonia				NE	NE	NE	NE	NE	NE	NE	NE		
Georgia													
Germany	143.2	140.3	133.6	129.5	126.3	121.2	119.3	114.2	109.9	105.7	110.8	5%	-23%
Greece													
Hungary	25.7	24.4	25.1	27.1	27.4	31.0	29.3	21.4	22.7	27.8	32.0	15%	24%
Iceland	NR	NR	NR	NR	NR	NR	NR	NR	NR	NR	NR		
Ireland	11.3	11.5	10.9	10.4	10.6	10.9	10.4	10.1	9.5	8.5	8.2	-4%	-28%
Italy	178.1	178.5	173.7	172.1	179.7	165.8	165.4	176.0	173.3	168.6	173.2	3%	-3%
Kazakhstan													
Kyrgyzstan													
Latvia	23.2	25.6	25.1	26.4	28.1	27.4	26.8	26.4	25.7	28.3	27.4	-3%	18%
Liechtenstein	0.03	0.03	0.03	0.03	0.03	0.03	0.03	0.03	0.03	0.03	0.04	6%	7%
Lithuania			NE	NE	8.8	8.7	8.9	9.5	9.5	8.6	9.9	15%	
Luxembourg	NR	NR	NR	NR	NR	NR	NR	NR					
Malta	1.0	1.3	1.3	1.3	1.3	1.3	1.4	1.4	1.4	1.4	0.8	-45%	-23%
Monaco		NE	NE	NE	NE	NE	NE	NE	NE	NE	NE		
Montenegro	4.3	3.7	4.9	5.2	5.1	4.6	5.0	4.5	5.5	4.0			-7%
Netherlands	24.2	23.0	21.8	21.3	19.9	19.5	18.5	18.3	17.4	15.9	15.3	-4%	-37%
Norway	59.9	59.3	61.8	58.4	55.5	51.7	48.9	48.6	46.5	44.2	47.9	8%	-20%
Poland	135.3	142.1	142.1	140.9	134.2	132.8	136.1	133.5	122.3	123.3	137.1	11%	1%
Portugal	73.9	73.0	64.6	63.1	66.0	64.6	60.7	60.6	59.4	57.2	49.2	-14%	-33%
Republic of Moldova	2.1	1.6	1.5	2.7	5.8	6.2	7.2		6.2	6.5			210%
Romania	NE	NE	NE	NE	NE	105.7	102.3	108.7	122.7	115.1	118.2	3%	
Russian Federation			376.0	341.1	383.3	350.2	408.8	347.9	316.4	311.9	417.9	34%	
Serbia	21.8	17.9	21.5	21.5	22.7	24.5	24.5	24.5	24.5	22.7	30.8	36%	41%
Slovakia	22.7	32.9	29.0	28.3	27.8	36.7	32.0	28.1	27.6	27.4	26.7	-2%	18%
Slovenia	14.5	14.4	14.1	14.1	13.9	14.0	13.8	14.1	13.4	15.9	16.8	6%	16%
Spain	100.5	99.6	99.7	99.6	98.4	97.9	94.7	96.7	87.3	80.3	79.2	-1%	-21%
Sweden	27.9	27.8	28.1	28.6	29.1	29.3	28.9	28.8	28.1	27.7	31.5	14%	13%
Switzerland	11.8	11.6	11.0	10.9	10.8	10.7	10.4	10.0	10.0	9.7	9.7	0%	-17%
Turkey													
Ukraine		NO	0.01		14.6	125.2	NE		NA	NO	40.7		
United Kingdom	100.1	96.9	86.4	84.1	82.5	81.3	79.2	76.9	73.5	67.0	66.7	-1%	-33%
United States of America	6,061	6,154	5,059	5,048	5,036	5,029	4,981	4,944	4,091	4,134			-32%

Notes: *A blank cell indicates that no data have been reported to EMEP*
Shaded cells (red) indicate increased emissions for the given period
"Differences 2009 -2010" for Albania, Montenegro, Republic of Moldova and the United States of America referrer to differences between 2000 and 2009, as 2010 was not reported
Emissions shown in the row "Russian Federation" correspond only to the "Russian Federation in the former official EMEP domain"

Table 1.2: PM_{10} emission trends (2000 - 2010) as reported by Parties.

Country / PM10 [Gg]	2000	2001	2002	2003	2004	2005	2006	2007	2008	2009	2010	Change 2009 - 10	Change 2000 - 10
Albania	12.4	12.5	13.4	16.8	18.4	17.2	17.8	17.5	17.5	15.3			24%
Armenia								0.6					
Austria	38.7	38.7	37.7	37.9	38.0	38.2	36.7	36.0	36.5	34.8	35.2	1%	-9%
Azerbaian													
Belarus			NE	NE	48.0	53.8	60.5	63.3	66.1	64.6	58.2	-10%	
Belgium	46.0	44.9	43.7	43.7	42.2	34.1	34.4	29.9	28.4	22.5	23.7	5%	-48%
Bosnia & Herzegovina													
Bulgaria	35.4	33.3	36.4	41.9	41.8	44.6	46.8	47.3	46.0	39.4	41.2	5%	16%
Canada	NR	NR	NR	NR	NR	NR	NR	NR	NR	5,824.9	5,855.4	1%	
Croatia	13.2	13.2	14.4	16.9	17.4	17.4	16.6	16.3	16.0	14.8	13.8	-7%	4%
Cyprus	5.9	5.5	5.4	5.4	4.9	4.4	4.3	4.4	4.3	3.6	3.4	-5%	-41%
Czech Republic		43.1	0.1	51.4	47.0	34.3	34.9	34.6	34.9	36.3	37.0	2%	
Denmark	28.5	29.3	28.5	30.2	30.4	31.8	32.9	36.5	33.8	31.4	31.7	1%	11%
Estonia	37.4	37.3	33.4	30.0	30.2	26.9	20.4	29.0	25.4	23.3	32.4	39%	-13%
European Union	2,292	2,290	2,217	2,181	2,180	2,133	2,080	2,048	1,989	1,912	1,969	3%	-14%
Finland	54.0	53.8	54.2	54.4	55.5	49.5	52.2	48.1	52.5	51.6	54.8	6%	1%
France	501.7	488.0	460.4	463.3	450.4	427.9	410.3	392.8	384.8	364.2	367.0	1%	-27%
FYR of Macedonia				NE	NE	NE	NE	NE	NE	NE	NE		
Georgia													
Germany	239.6	234.1	224.9	218.4	214.4	207.1	206.0	200.6	194.7	187.0	192.7	3%	-20%
Greece													
Hungary	47.0	43.4	44.3	47.7	47.4	51.6	48.0	35.6	37.8	47.8	46.1	-4%	-2%
Iceland	NR	NR	NR	NR	NR	NR	NR	NR	NR	NR	NR		
Ireland	17.4	17.9	17.1	16.2	16.4	17.1	16.1	15.6	14.7	12.9	12.5	-3%	-28%
Italy	209.0	211.0	205.6	204.0	211.9	197.3	196.6	207.4	204.1	197.6	202.1	2%	-3%
Kazakhstan													
Kyrgyzstan													
Latvia	26.6	29.3	29.0	30.5	38.9	32.6	32.1	32.7	32.1	32.9	32.6	-1%	23%
Liechtenstein	0.04	0.04	0.04	0.04	0.04	0.04	0.04	0.04	0.04	0.04	0.04	10%	8%
Lithuania		0.6	NE	NE	10.8	10.8	11.1	11.6	12.1	11.0	12.5	14%	
Luxembourg	NR	NR	NR	NR	NR	NR	NR	NR					
Malta	1.4	2.0	1.9	2.0	2.0	2.1	2.1	2.2	2.2	2.2	1.3	-41%	-9%
Monaco		NE	NE	NE	NE	NE	NE	NE	NE	NE	NE		
Montenegro	8.4	6.9	9.5	9.8	9.5	8.0	8.8	7.9	9.8	6.8			-19%
Netherlands	38.8	37.5	36.8	34.7	34.1	33.3	32.6	32.4	31.7	29.7	29.1	-2%	-25%
Norway	66.3	66.0	68.3	64.7	61.7	58.6	55.7	56.2	52.8	50.3	53.9	7%	-19%
Poland	281.9	299.6	303.2	295.7	279.7	289.2	285.5	268.7	247.1	248.6	279.5	12%	-1%
Portugal	101.1	107.4	93.0	86.6	94.5	96.9	87.9	85.1	85.1	83.0	71.3	-14%	-29%
Republic of Moldova	4.5	3.4	5.4	5.7	11.2	7.5	8.3		9.9	9.8			118%
Romania	NE	NE	NE	NE	NE	125.7	122.7	136.8	143.7	135.9	142.8	5%	
Russian Federation			561.4	575.6	646.7	590.8	613.0	521.8	474.6	483.8	622.5	29%	
Serbia	35.7	31.9	35.7	35.7	37.2	39.5	39.5	39.5	40.3	38.4	46.4	21%	30%
Slovakia	44.7	47.3	40.2	36.4	31.9	41.7	36.5	31.8	31.2	30.8	30.2	-2%	-33%
Slovenia	19.4	19.0	18.6	18.2	18.3	18.5	18.2	18.4	16.6	18.9	19.8	5%	2%
Spain	145.6	144.6	146.3	144.3	143.3	141.0	136.7	138.9	123.3	113.4	112.4	-1%	-23%
Sweden	39.6	39.5	39.8	40.6	41.3	41.4	41.3	41.2	40.3	39.2	43.8	12%	10%
Switzerland	22.4	22.0	21.4	21.2	21.1	21.1	20.9	20.6	20.6	20.4	20.5	0%	-9%
Turkey													
Ukraine		NO	2.9		118.5	131.2	NE		NA	NO	133.2		
United Kingdom	171.3	164.9	143.1	140.0	137.8	135.0	133.4	130.7	125.6	113.9	114.2	0%	-33%
United States of America	20,901	21,266	19,346	19,335	19,322	19,275	17,533	15,762	13,028	10,232			-51%

Notes: *A blank cell indicates that no data have been reported to EMEP*
Shaded cells (red) indicate increased emissions for the given period
"Differences 2009 -2010" for Albania, Montenegro, Republic of Moldova and the United States of America referrer to differences between 2000 and 2009, as 2010 was not reported
Emissions shown in the row "Russian Federation" correspond only to the "Russian Federation in the former official EMEP domain"

1.4 Contribution of key categories to total PM emissions

In order to further improve air monitoring and modelling under the Convention, it is important to identify GNFR[4] categories that have a significant influence on total emissions. Such an analysis helps to set priorities for improvement but can also highlight potential gaps in reporting.

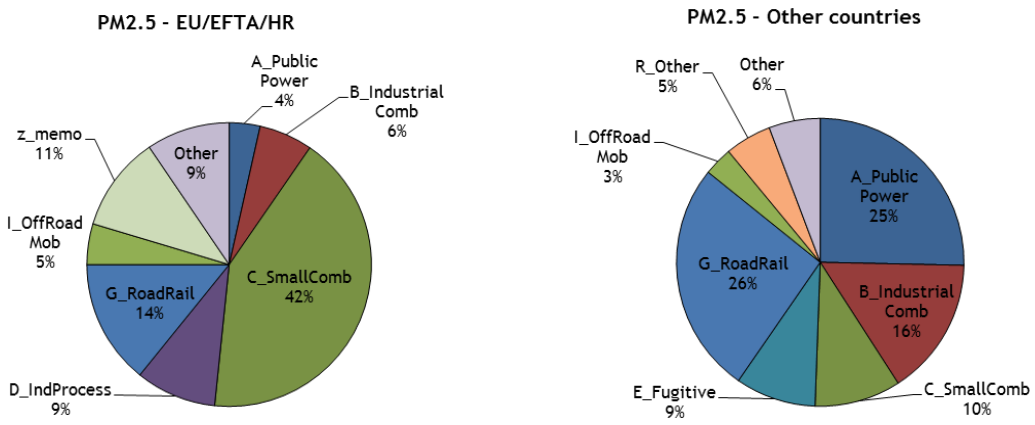

Figure 1.1: Top seven categories contributing to $PM_{2.5}$ 2010 emissions (GNFR categories).

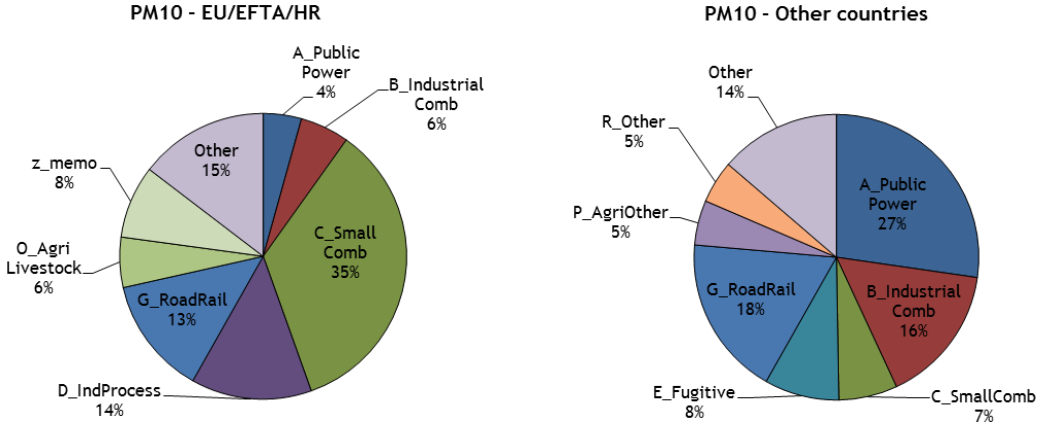

Figure 1.2: Top seven categories contributing to PM_{10} 2010 emissions (GNFR categories).

Note: *Where the total number of categories for a particular pollutant is more than seven or the contribution of a particular sector is < 2%, emissions have been summed up in the category 'Other'*
'Memo items' represent emissions reported as international maritime navigation

[4] 21 GNFR categories are aggregated NFR09 categories (see UNECE 2009 - Annex IV at http://www.ceip.at/reporting-instructions/annexes-to-the-reporting-guidelines). GNFR categories should be used for reporting of gridded emissions from 2012 onwards.

The most significant source of PM emission is the combustion of fossil fuels, contributing about 50% of PM emissions. The different distribution of GNFR sectors between EU/EFTA/HR and "Other countries[5]", and especially the relatively low contribution of "Small Combustion" to the total PM emissions of "Other countries" indicates that emissions from this sector are potentially underestimated.

Another important source of PM emissions is the transport sector with contributions of 13 to 26% to national totals (see Figure 1.1 and Figure 1.2).

1.5 Emission data prepared for modellers

Modellers use $PM_{2.5}$ and PM_{coarse}[6] ($PM_{10-2.5}$) emissions distributed in a 50 x 50 km² PS EMEP grid[7]. The extended EMEP domain comprises approximately 21 000 grid cells, but PM sectoral data is reported for less than 50% of this area. More or less complete emission data are available for Europe, except for some Balkan countries. No PM emissions were reported by a number of EECCA countries, by Turkey or for the "Russian Federation extended EMEP domain".

To make submitted emission data usable for modellers, emissions reported in NFR09 categories are converted to 10 SNAP sectors, whereas missing information (i.e. not reported by Parties) has to be added (gap filling)[8]. Emission trends in the EMEP area are significantly influenced by big countries like Ukraine, Turkey, Belarus and the Russian Federation, for which consistent time series are not available and trends are based on expert estimates.

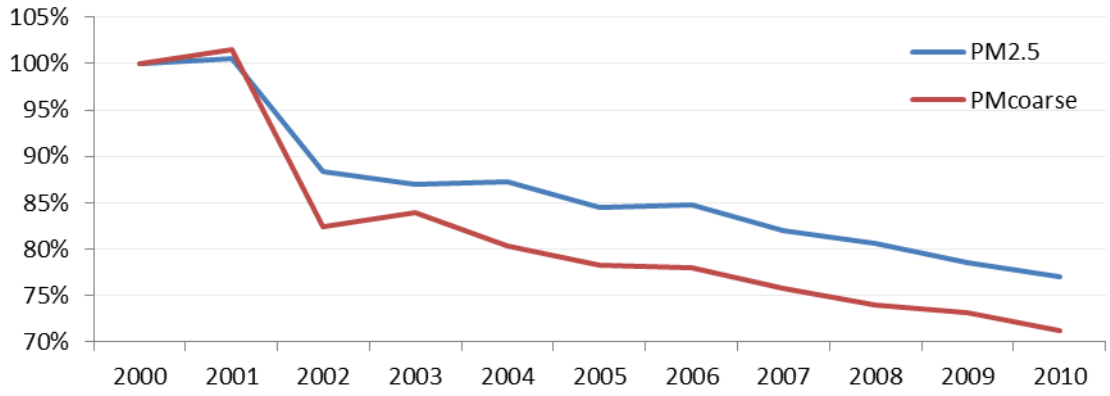

Figure 1.3: PM Emission trends in EMEP area, 2000-2010.

[5] 'Other countries ' in this chapter refer only to 5 countries, namely Belarus, FYR of Macedonia, the Russian Federation, Serbia and Ukraine. A larger number of Parties from the "Other" group did not report PM emissions at all.

[6] PM_{coarse} emissions are not reported but estimated as the difference between PM_{10} and $PM_{2.5}$

[7] Information regarding the gridding procedure can be downloaded at http://www.ceip.at/fileadmin/inhalte/emep/pdf/gridding_process.pdf

[8] Basic principles for expert estimates are described in the EEA (2009*b)* '*proposed gap-filling procedure for the European Community LRTAP Convention emission inventory'.*

In 2012 gridded emissions were reported in GNFR sectors but the modellers still requested data in SNAP sectors, and therefore CEIP converted the reported GNFR sectors to SNAP sectors using the reported NFR sector distribution for weighting. This converted grid was then used to distribute the SNAP sector emissions which had been converted from NFR09.

Gap-filled and gridded data can be accessed via the CEIP homepage at http://www.ceip.at/webdab-emission-database/emissions-as-used-in-emep-models and gridded data can also be visualized in Google Maps/Earth at http://www.ceip.at/webdab-emission-database/gridded-emissions-in-google-maps.

1.6 Update of historical gridded emissions used in EMEP models (2000 – 2009)

To provide modellers with historical data that is consistent with the latest (recalculated) data reported by Parties, CEIP has re-gridded data from previous years (from 2000 to 2009). As an example of the magnitude of the changes, see the revised data on $PM_{2.5}$ and PM_{coarse} emissions for the years 2000 and 2005. (Table 1.3). For the whole EMEP area, the differences in $PM_{2.5}$ gridded data are minimal (below 2 %). The differences in PM_{coarse} are bigger, but still less than 8%.

However, for individual countries the differences in the revised emissions are sometimes significant. For example, Belarus' updated **$PM_{2.5}$** emissions increased by 83% in 2005, whereas the revision resulted in a decrease for Bulgaria (-48%), Serbia (-33%), Portugal (-20%), Montenegro (-14%) and Italy (-10%).

Note
The years 2008 and 2009 were re-gridded using the same distribution as for 2010. For the years 1990, 2000 and 2005 new base grids were calculated for the emission distribution, based on new gridded data reported for these years. The years 2003 to 2007 were re-gridded using the new base grid for 2005 and the years 2000 to 2002 were re-gridded using the new base grid for 2000 for the emission distribution

PM_{coarse} emissions increased in Liechtenstein by 34% in the year 2005. In Serbia and Romania (-58%), Slovakia (-36%), Bulgaria (-38%), France (-29%) and Belarus (-24%) PM_{coarse} emissions decreased. In Bulgaria, France and Slovakia the revised PM_{coarse} emissions decreased significantly for the whole timeline from 2000 to 2009, whereas in Liechtenstein is the revision resulted in a significant increase. These major revisions of historical data indicate a high uncertainty of PM emissions.

Table 1.3: Total differences between PM emissions gridded in 2011 and re-gridded in 2012 for the years 2000 and 2005.

	2011 expert data	2012 expert data	Difference [Gg]	Difference [%]
$PM_{2.5}$ total 2000	3 623	3 565	-58	-1.60%
$PM_{2.5}$ total 2005	2 943	2 900	-43	-1.46%
PM_{coarse} total 2000	1 984	1 910	-74	3.73%
PM_{coarse} total 2005	1 606	1 478	-128	7.97%

A list of the differences between gridded emissions for the period 2000 - 2009 (used in models in 2011) and those re-gridded in 2012 (per country/pollutant/year and expressed both as a percentage and in Gg) can be downloaded at http://www.ceip.at/fileadmin/inhalte/emep/xls/2012/Diff_gridded_regridded_2012.xls.

2 Revision of the Gothenburg Protocol

By Zbigniew Klimont and Markus Amann

In May 2012, Parties to the Convention on Long-range Transboundary Air Pollution have reached agreement on a revision of its Gothenburg multi-pollutant/multi-effect protocol (UNECE, 2012). Inter alia, the revised protocol includes quantitative emission reduction commitments for the year 2020. For the first time in a multilateral environmental agreement, the adverse effects of particulate matter (PM) on health have been considered and include emission reduction commitments for emissions of fine primary particles ($PM_{2.5}$). Also, for the first time in an international treaty, the revised Protocol reflects upon the close linkages between regional air pollution and global climate change by including black carbon (BC), a short-lived climate pollutant.

CIAM has contributed the analysis of the baseline (current legislation) and maximum feasible reductions and discussed the scope/potential for further reductions (Amann et al., 2011a). Finally, the impacts of the committed changes in SO_2, NO_x, $PM_{2.5}$, NH_3 and VOC emissions on premature mortality from fine particulate matter and ozone and the protection of ecosystems against eutro-phication and acidification were analyzed. CIAM compared the environmental improvements that are calculated for the committed emission reductions against those estimated for the 'current legislation' baseline and the maximum technically feasible reductions (Amann et al., 2012).

The analysis employed the GAINS (Greenhouse gas – Air pollution Information and Simulation) model (Amann et al., 2011b). The cost-effectiveness analysis of the GAINS model can identify portfolios of measures that lead to cost-effective environmental improvements. Obviously, in such an optimization problem any cost-optimal solution is critically determined by the choice of environmental constraints, i.e., by the chosen ambition level of the environmental targets as well as by their spatial distribution across Europe. More stringent and more site-specific targets will result in higher costs. Targets that could usefully guide international negotiations on further emission reductions must fulfil two criteria:

- First, they must be achievable in all countries (otherwise no portfolio of measures would be available to achieve them), and
- second, they should result in internationally balanced costs and benefits, so that they could be politically acceptable by all Parties.

Ultimately, the choice of a set of environmental targets that could serve as a useful starting point for negotiations will require value judgment, and will therefore always remain a political task for negotiators. It cannot be replaced by scientific models unless they employ (implicit or explicit) quantifications of preference structures for the various parties. CIAM has contributed with the analysis of four different concepts for target setting which were discussed in an earlier (CIAM 1/2010) report and then at the 47th Session of the Working Group on Strategies. Eventually, drawing on the conclusions of that discussion, the hybrid scenarios that combine the different target setting options for individual

impacts were developed and used in the analysis (see for more details Amann et al., 2011a).

While, a complete assessment including all Gothenburg Protocol pollutants is presented in Amann et al. (2011a, 2012), here we highlight key findings focusing on particulate matter.

For the EMEP domain as a whole, the emission reduction commitments of the revised Gothenburg protocol imply a 22% decrease in primary $PM_{2.5}$ (Figure 2.1). This reduction is clearly lower than the range of future emissions that has been discussed in the cost-effectiveness analysis for the negotiations of the revised protocol (Amann et al., 2011a). For instance, compared to the 'mid' ambition level, $PM_{2.5}$ fall short by 40%. Furthermore, the agreed commitments are also lower than what has been estimated as the result from the implementation of existing emission control legislation by the GAINS model for 2020. For primary $PM_{2.5}$, the model estimated 25% larger impacts of the current legislation on emissions in 2020 than what has been agreed by Parties in the revised Gothenburg protocol (Table 2.1). These differences might be explained by a number of factors, including disagreements about the underlying projections of energy use and economic development, different assumptions about the implementation success and effectiveness of emission recent control legislation, and uncertainties in emission inventories. Furthermore, Parties might also have introduced some uncertainty margin to safeguard against unexpected developments.

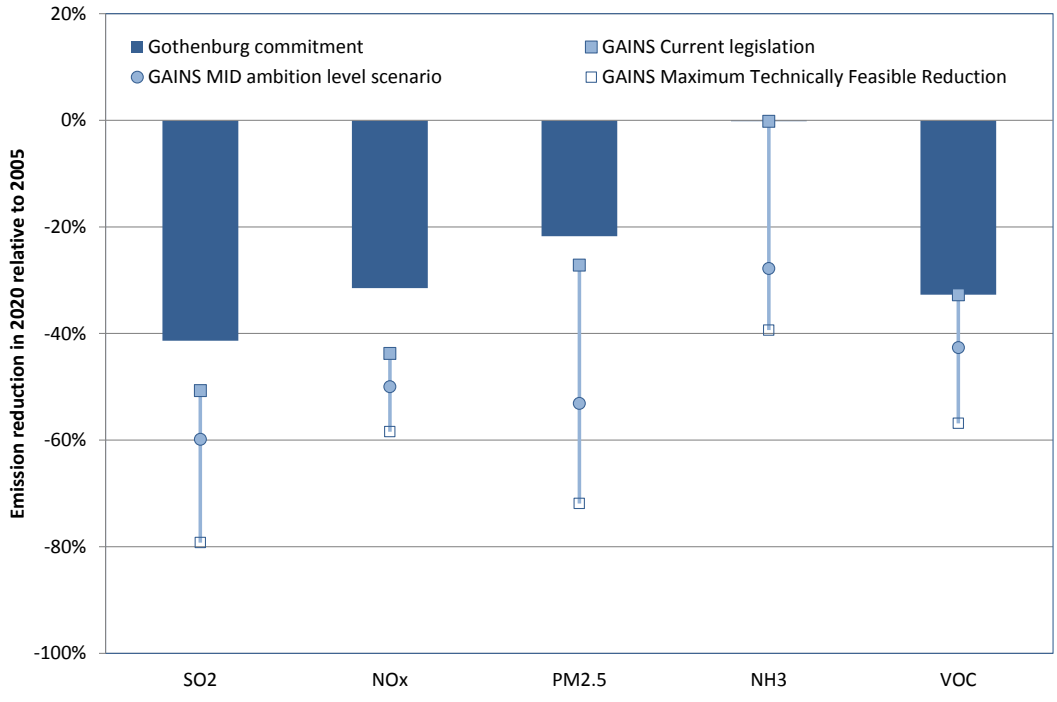

Figure 2.1: Changes in emissions in 2020 relative to 2005 over the EMEP domain. The Gothenburg commitments are indicated by the blue bars, while the lines indicate the ranges between the 'current legislation' and the 'maximum technically feasible reduction' cases estimated by the GAINS model for the PRIMES 2009 energy projection.

Table 2.1: $PM_{2.5}$ emissions.

	Emission reductions in 2020 relative to 2005				Emissions in 2005 (kilotons)	
	Gothenburg emission reduction commitment	GAINS Current legislation estimate	GAINS MID ambition level scenario	GAINS Maximum Technically Feasible Reductions	reported to EMEP in 2012	estimated by GAINS in 2011
Austria	-20%	-39%	-43%	-62%	22	22
Belgium	-20%	-27%	-32%	-47%	24	28
Bulgaria	-20%	-33%	-47%	-81%	44	51
Cyprus	-46%	-52%	-52%	-67%	3	3
Czech Rep.	-17%	-26%	-31%	-59%	22	34
Denmark	-33%	-39%	-40%	-74%	25	32
Estonia	-15%	-61%	-68%	-84%	20	20
Finland	-30%	-29%	-30%	-67%	36	31
France	-27%	-34%	-39%	-66%	304	317
Germany	-26%	-32%	-35%	-49%	121	122
Greece	-35%	-40%	-53%	-71%	56	55
Hungary	-13%	-17%	-30%	-62%	31	28
Ireland	-18%	-26%	-26%	-37%	11	10
Italy	-10%	-34%	-38%	-55%	166	151
Latvia	-16%	-18%	-25%	-83%	27	18
Lithuania	-20%	-22%	-48%	-75%	9	14
Luxembourg	-15%	-46%	-47%	-50%	3	3
Malta	-25%	-60%	-60%	-79%	1	1
Netherlands	-37%	-45%	-47%	-55%	21	25
Poland	-16%	-22%	-27%	-44%	133	125
Portugal	-15%	-44%	-67%	-85%	65	104
Romania	-28%	-30%	-52%	-86%	106	154
Slovakia	-36%	-49%	-56%	-70%	37	19
Slovenia	-25%	-38%	-46%	-71%	14	9
Spain	-15%	-33%	-45%	-61%	93	140
Sweden	-19%	-39%	-40%	-56%	29	29
United Kingdom	-30%	-42%	-44%	-54%	81	91
EU-27	-22%	-34%	-42%	-64%	1504	1634
Albania*)	0%	-16%	-34%	-77%	9	9
Belarus	-9%	-1%	-39%	-68%	53	53
Bosnia-H*)	0%	-35%	-42%	-74%	20	20
Croatia	-18%	-24%	-48%	-74%	20	19
FYR Macedonia*)	0%	-43%	-59%	-83%	13	13
R Moldova*)	0%	-9%	-59%	-74%	10	10
Norway	-30%	-38%	-39%	-69%	51	51
Russia	-3%	4%	-57%	-72%	763	763
Serbia-M*)	0%	-29%	-45%	-79%	68	68
Switzerland	-26%	-29%	-40%	-56%	10	10
Ukraine*)	0%	-4%	-59%	-81%	390	390
Non-EU	-21%	-21%	-63%	-79%	1407	1723
Total	-22%	-27%	-53%	-72%	2911	3357

For the EMEP domain as a whole, the agreed emission reductions will lead to significant reductions of the negative impacts of air pollution. Mortality from the exposure to fine particulate matter will fall by 27% in 2020 (Table 2.2). There are, however, significant regional differences across Europe and the reduction in impacts falls short of the one presented in the cost-effectiveness analysis, in fact they do not even reach the improvements estimated for the current legislation case that were estimated at over 30%.

This shortfall also applies to several targets of the Thematic Strategy on Air Pollution (TSAP) of the European Union. For the EU-27, the revised Gothenburg would reduce the years of life lost (YOLLs) from the exposure to fine particulate matter by 35%, so that additional measures would be necessary to meet the 47% target that has been established in the TSAP.

Table 2.2: Health Impacts from $PM_{2.5}$ in 2000 and 2020.

		2000	2020, with emission reduction commitments	2020, GAINS estimate for Current legislation	MFR
Health impacts from PM (million years of life lost)	Total	306.0	224.9	204.0	159.0
	EU-27	204.0	132.1	116.0	101.0
	Non-EU	102.0	92.8	88.0	58.0

3 Measurement and model assessment of particulate matter in Europe in 2010

3.1 PM mass concentrations

By Svetlana Tsyro, Karl Espen Yttri and Wenche Aas

3.1.1 Introduction

The current assessment of the concentration levels of regional background PM_{10} and $PM_{2.5}$ in 2010 has been made based on EMEP model calculations and data from EMEP monitoring network. In this chapter, we present the recent estimates of PM_{10} and $PM_{2.5}$ concentrations for 2010 and document the main changes in PM_{10} and $PM_{2.5}$ levels from 2009 to 2010. Brief information concerning PM main constituents and mass size distribution is provided based on model and observational data. Furthermore, calculated exceedances of the WHO Air Quality Guidelines by regional background PM_{10} and $PM_{2.5}$ concentrations in 2010 are presented. We also look at how well the model manages to reproduce observed exceedances of PM_{10} and $PM_{2.5}$ EU limit values and WHO Air Quality Guidelines at the individual stations.

3.1.2 The measurement network

The observed annual mean concentrations of PM_{10}, $PM_{2.5}$ and PM_1 for 2010 at European rural background sites can be found in Hjellbrekke and Fjæraa (2012). For 2010, mass concentrations of PM are reported for 69 regional or global background sites (67 for PM_{10} and 43 for $PM_{2.5}$); four more than in 2009. There are seven new sites in 2010 compared to 2009: DK0012, ES0005, ES0006, NO0039, NO0056, RO0008, SE0005; but three from 2009 have not reported data for 2010: DK0041, EE0009 and IE0031. The same number of Parties reported aerosol mass data in 2009 and 2010 (25). Romania is new, while Ireland has not reported mass data for 2010. It is worth noting that although the number of sites has increased the last years, several sites have unsatisfactory data coverage. In 2010, 56 of the 67 PM_{10} sites have data completeness higher than 75%. For $PM_{2.5}$ there are 30 of the 43 sites with satisfactory data coverage. PM_1 was reported for 6 sites in 2010, the same number as in 2009.

3.1.3 The EMEP model and runs setup

The calculations presented in this report have been performed with the EMEP/MSC-W model, version rv.4. During the past year, the EMEP/MSC-W model has been through an extensive revision and process updates with the purpose of improving model's general performance and in particular the representation of PM. As a result, several parameterisations of chemical and physical processes have been implemented or improved. The most recent developments of the EMEP MSC-W model (version rv4) are documented in EMEP Status Report 1/2012 and Simpson et al. (2012). Here, the model changes which affect model PM results the most are outlined:

- implementation of secondary Organic Aerosols (SOA);
- implementation of re-suspended road dust;

- implementation of explicit calculations of cloud water acidity (reduction of cloud pH increased sulphate formation);
- update of monthly temporal profiles of SO_x emissions;
- use of the more robust parameter "Soil Moisture Index" instead of "Soil moisture" from ECMWF-IFS data for windblown dust calculations;
- update of the rate of coarse NO_3^- formation; changing its Mass Median Diameter from 2.5 μm to 3 μm (so that 27% of coarse NO_3^- is assigned now to $PM_{2.5}$).

The meteorological data used in the model simulations for 2010 is from the ECMWF-IFS meteorological model. The national emissions of SO_x, NO_x, NH_3, NMVOC, PM_{10} and $PM_{2.5}$ for the year 2010 were prepared by EMEP/CEIP (see Chapter 1). The emissions of primary PM_{10} and $PM_{2.5}$ have been disaggregated to elemental carbon (EC), primary organic aerosol (POA) and remaining inorganic dust using the latest information from IIASA.

3.1.4 Annual PM_{10}, $PM_{2.5}$ and PM_1 concentrations in 2010

The lowest measured concentrations of PM_{10} were observed in the northern and north-western parts of Europe, i.e. the Nordic countries, British Isles, and for high altitude sites (> 800 masl) on the European mainland (Figure 1.1). The highest observed concentrations of PM_{10} are found at sites in Cyprus, the Netherlands, Hungary and Italy, while for $PM_{2.5}$ at sites in Austria, Germany, France and Italy. The regional distributions of PM_{10} and $PM_{2.5}$ are very similar.

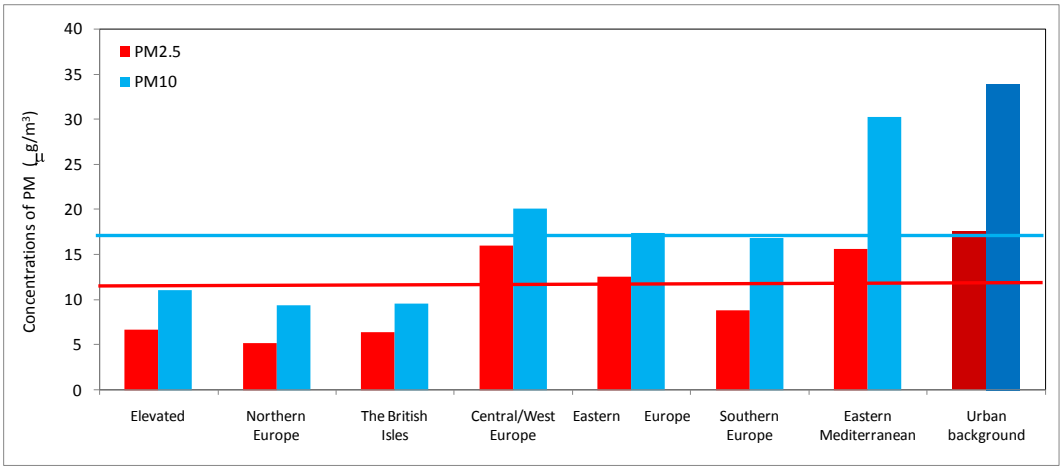

Figure 3.1: Annual mean concentrations of PM_{10} and $PM_{2.5}$ for various regions of the EMEP domain in 2010 (μg m^{-3}). Solid blue and red lines denote the average concentrations for all sites. Annual mean concentrations for European urban background sites (from AirBase) are included for comparison.

Annual mean concentration fields of regional background PM_{10} and $PM_{2.5}$ in 2010, based on EMEP/MSC-W model calculations and measurements from the EMEP monitoring network, are presented in Figure 3.2. The modelled PM_{10} and $PM_{2.5}$ concentrations include secondary inorganic aerosols (SIA= SO_4^{2-}+NO_3^-+ NH_4^+), organic aerosols (OA=POA+SOA), elemental carbon, sea-salt, mineral

dust and water. The aerosol water content is calculated for a temperature of 20 °C and a relative humidity of 50%, which corresponds to required standardized conditions for equilibration of PM samples.

The following procedure has been used to generate the combined maps. For each measurement site with PM data in 2010, the difference between the measured value and the modelled value in the corresponding grid cell has been calculated. The differences for all sites have been interpolated spatially using radial base functions, which provide a continuous 2-dimentional function describing the difference in any cell within the modelled grid. The combined maps have been constructed by adjusting the model results with the interpolated differences, giving larger weight to the observed values close to the measurement site, and using the model values in areas with no observations. The range of influence of the measured values has been set to 500 km.

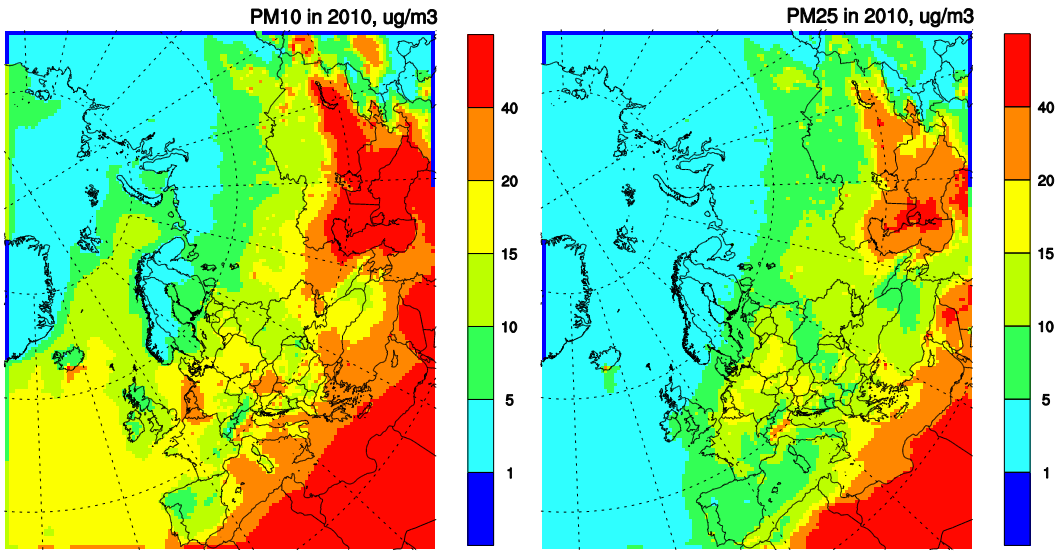

Figure 3.2: Annual mean concentrations of PM_{10} (left) and $PM_{2.5}$ (right) in 2010 based on EMEP/MSC-W model calculations and EMEP observation data.

The concentration maps constructed from EMEP model and observational data (Figure 3.2) show a typical north to south gradient, with the annual mean PM_{10} decreasing from 1-5 μg/m^3 in Northern Europe to 15-25 μg/m^3 in Southern Europe. The annual mean concentrations of $PM_{2.5}$ decrease from 1-3 μg/m^3 in Northern Europe to 5-20 μg/m^3 in Southern Europe. On the top of this zonal PM distribution, there are areas with enhanced $PM_{2.5}$ and PM_{10} levels associated with large emissions in major cities and industrial and agricultural regions.

The average observed annual mean PM_{10} concentration for all sites (average between regions) was 15.5 μg/m^3, the lowest annual mean was recorded at the high altitude global site Jungfraujoch in Switzerland (2.2 μg/m^3) and the Swedish site Bredkälen (3.6 μg/m^3), whereas the highest levels were recorded at Ayia Marina in Cyprus (30.4 μg/m^3) and at the Hungarian site K-puszta (27.8 μg/m^3). The mean European urban background concentration of PM_{10} has been included

in Figure 3.1 to give an idea of the rural background influence. Somewhat less than 50% of the urban background concentration is likely to be attributed to the mean rural background concentration. Close to 60% of the urban background concentration is likely to be attributed to the mean rural background concentration of $PM_{2.5}$ (Figure 3.1).

3.1.5 PM_{10} and $PM_{2.5}$ in 2010 compared to 2009

Close to 50% of the sites which reported concentrations of PM_{10} both for 2009 and 2010 had lower annual means in 2010 compared to the previous year, meaning that the levels in 2010 and 2009 are quite comparable. On average there was a small decrease of 3%, however, there are large variations between sites, and the largest relative decrease was at the Moldavian site Leova (MD0013), where the annual mean went from 15.6 $\mu g/m^3$ in 2009 to 4.7 $\mu g/m^3$ in 2010 (230% decrease). The largest relative increase of 23% (from 23.4 to 30.3 $\mu g/m^3$) was seen at Ayia Marina in Cyprus (CY0002).

For $PM_{2.5}$ there is an average increase of 4% for all sites, but it was the same number of sites with decrease or increase. The highest relative decrease was seen at the Latvian site Rucava (LV0010), with a change from 18.8 $\mu g/m^3$ in 2009 to 14.6 $\mu g/m^3$ in 2010 (40% decrease) , and the highest relative increase of 42% was found at Hyytiälä (FI0050) (from 4.5 to 5.5 $\mu g/m^3$). For PM_1, there was a general increase in concentration at the six sites with measurements both years, on average 22%.

When comparing the calculated PM_{10} and $PM_{2.5}$ concentrations from the EMEP/ MSC-W model, there is a general increase in PM_{10} and $PM_{2.5}$ levels calculated with the model for 2010 compared to those for 2009 produced last year. As briefed above, an extensive revision of a number of chemical and physical processes in the EMEP/MSC-W model has been made since last year reporting. Thus, the differences in PM concentrations for 2010 and 2009 in EMEP Report 4/2011 are partly due to the model modification. When calculated with the same model version (rv.4), PM_{10} and $PM_{2.5}$ concentrations in 2010 are respectively 0.5-5 $\mu g/m^3$ and 0.5-3 $\mu g/m^3$ higher than in 2009 in most of EMEP area. In arid areas in southern/south-eastern parts of the domain, PM_{10} and $PM_{2.5}$ in 2010 exceed by 5-7 $\mu g/m^3$ those in 2009, which is due to windblown dust (see below). Only in Mediterranean region and Norway, calculated 2010 concentrations are 0.5-2 $\mu g/m^3$ lower than those in 2009.

Component-wise analysis shows that the differences between 2010 and 2009 concentrations have the same pattern for both primary PM and SIA. The belt of higher 2010 concentrations stretches from north-eastern France east, crossing Germany, Poland, the Baltic Countries, Belarus, north-western Russia and Finland. Also in Turkey, Malta, and the Caucasus PM concentrations in 2010 are calculated to be higher in 2009. Comparison of meteorological conditions (based on fields from ECMWF-IFS model) shows some spatial correspondence between the areas with higher PM concentrations and the areas with less precipitation in 2010 compared to 2009. On the other hand, southern/south-eastern Europe received in 2010 more precipitation than in 2009, which led to efficient scavenging of pollutants.

Calculated dust concentrations in 2010 are higher than in 2009 in many of arid/semi-arid areas in south-eastern EECCA regions, Turkey and North Africa. This is due to more favourable meteorological conditions for dust generation and transport, i.e. higher temperatures and less precipitation yielded drier soil, while larger surface stress facilitated soil particle uplift in 2010. At the same time, a recent correction of dust boundary conditions resulted in reduced levels of Saharan dust calculated for 2010.

Furthermore, there are two locations with markedly enhanced PM concentrations in 2010 compared to 2009. The first one, centred in the southern coast of Iceland, is due to Eyjafjallajökull volcano eruption (mid-April to mid-May 2010). The second one, over central Russia, is due to severe forest fires during July-August 2010. The Eyjafjallajökull eruption emissions contained large amount of ash and some SO_2, thus contributing with primary PM. See further discussions of the Eyjafjallajökull eruption in Chapter 5. The Russian fires emitted large amounts of CO and NO_2, leading to large ozone production and enhancing the formation of SOA.

3.1.6 PM_{10} and $PM_{2.5}$ seasonality in 2010

One of the most pronounced features of PM seasonal variation in 2010 are elevated PM_{10} and $PM_{2.5}$ concentrations reported for January and February at the sites in central Europe. Figure A1 in Appendix shows measured and calculated monthly variations of PM_{10} and $PM_{2.5}$ averaged over sites in the individual countries. Enhanced PM_{10}, and especially $PM_{2.5}$ levels, are indeed seen at German, Austrian, Swiss, Czech, Dutch, British and Swedish sites, and elevated $PM_{2.5}$ levels at Norwegian and French sites. Meteorological maps reveal that those winter months were characterised by low temperatures and low surface winds, causing stagnant pollution situation in Central Europe. Monthly mean trajectories, calculated from ECMWF-IFS 925 hPa winds (http://www.emep.int) indicate frequent easterly and south-easterly transport in January-February 2010.

At Spanish sites, monthly PM_{10} and $PM_{2.5}$ concentrations peaked in March, June and July 2010. The model calculations suggest that the elevated PM levels in March are due to mineral dust episodes at some of the sites.

3.1.7 Trends in PM_{10} and $PM_{2.5}$

The longest time series of PM data reported to EMEP goes back to 1996-1997; i.e. for four Swiss sites, one Czech and one British. Significant inter-annual variations in the PM concentrations are observed, of which those associated with the peak in 2003 is the most pronounced (Figure 3.3). However, despite large inter-annual variations, there is a relatively clear general decrease in the observed mass concentration in Europe the last decade (Tørseth et al., 2012; Barmpadimos et al., 2012). Trend analysis, using the Mann Kendall test, of PM_{10} mass measurements from twenty four sites, with measurements from 2000 (or 2001) to 2010 show an average decrease of 21% ±13%, which corresponds to an annual loss in average mass of 0.33 $\mu g/m^3$ pr year. 54% of the sites show a significant decrease, non with significant increase. Similar numbers are observed for $PM_{2.5}$; an average decrease of 27 ±14%, at 13 sites with measurements from 2000 or 2001. 38% of the sites have a significant downward trend, non with positive trend. The downward

tendency in the observed annual mean concentration of PM, corresponds to a rather broad reduction in the emissions of primary PM and secondary PM precursors in Europe in the actual period (Tørseth et al., 2012; Barmpadimos et al., 2012; EMEP/CEIP, 2011).

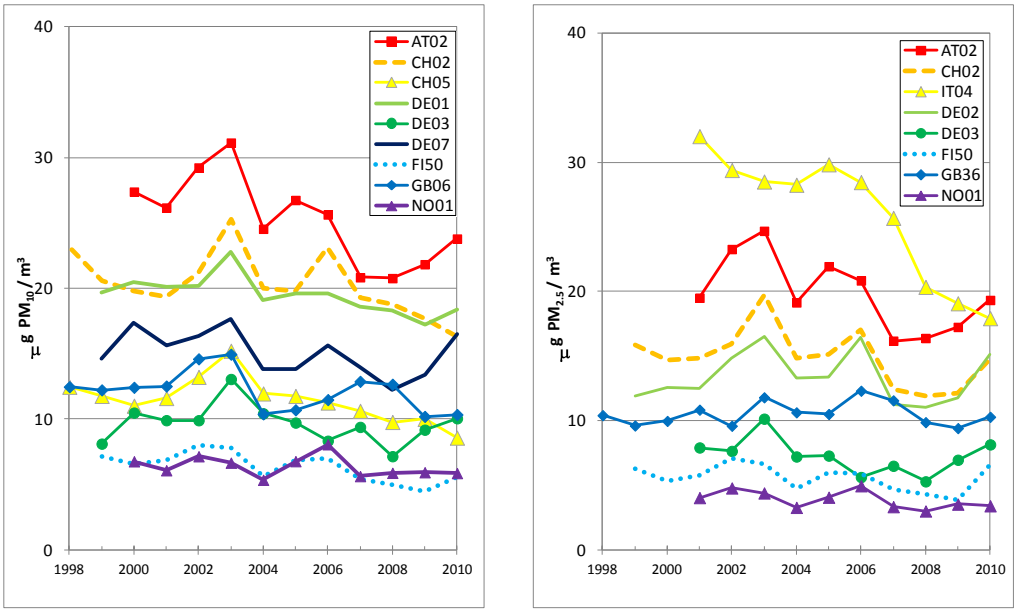

Figure 3.3: Time series from 1998 to 2010 of PM_{10} (left) and $PM_{2.5}$ (right) at selected EMEP sites.

Figure 3.4 shows model calculated and observed 11-year trends of annual mean PM_{10} and $PM_{2.5}$ concentrations in the period 2000-2010. Only the sites with measurements in all these eleven years are included in the trend plots. Here, the concentrations are averaged over all EMEP sites with at least 75% data for each of the years. Only eleven sites for PM_{10} and four sites for $PM_{2.5}$ satisfy the criteria. Those sites are located in Germany, Switzerland and Austria and thus the trends are representative for Central Europe. As was also seen for the somewhat larger dataset presented above, there is a slight downward trend in annual mean PM_{10} and $PM_{2.5}$ levels from 2000 to 2010. In both observational and model data, elevated PM levels occurred in 2003 and less so in 2006. Furthermore, observations indicate that PM_{10} and $PM_{2.5}$ increased from 2008 to 2009 and further to 2010, whereas the model calculates rather flat average concentration level for both PM_{10} and $PM_{2.5}$ for the same period. The measured PM_{10} and $PM_{2.5}$ increase is due to concentration increase at German and Austrian sites, while at Swiss sites they went down from 2008 to 2010. Probably, the recorded increase in annual mean PM levels is due to enhanced PM pollution in German and Austrian sites in January-February 2010 (see 3.1.6). If we zoom in at the period 2008-2010, for which observations from as many as 35 stations for PM_{10} and 23 stations for $PM_{2.5}$ are available, the data indicate a very slight (about 1 $\mu g/m^3$) decrease for PM_{10} and flat concentration level for $PM_{2.5}$. Model results agree well with these observed PM changes.

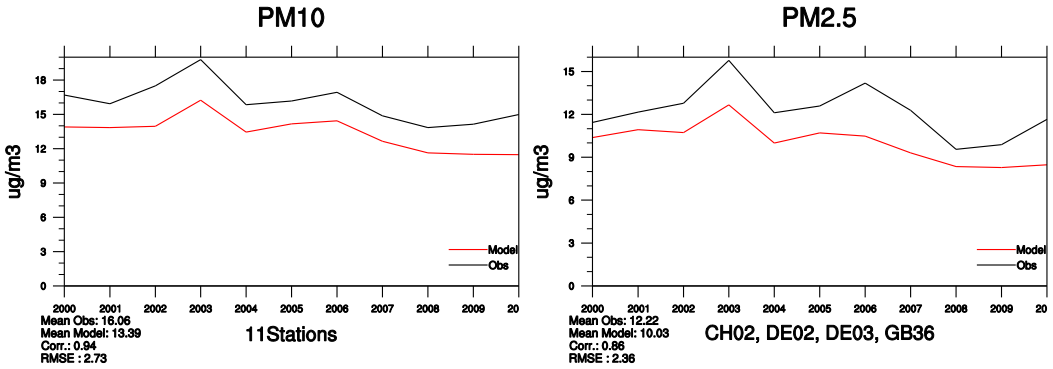

Figure 3.4: Calculated and observed changes in annual mean PM_{10} and $PM_{2.5}$ concentrations between 2000 and 2010.

3.1.8 PM size fractions

Table 3.1 shows annual mean $PM_{2.5}$ to PM_{10} ratio at EMEP sites based on observational data and model calculations for 2010. The ratios have been calculated for common days, i.e. when both observational and modelled concentrations of $PM_{2.5}$ and PM_{10} were available. Further, only sites with similar methods for both size fractions are used, i.e. sites with TEOM for one size fraction and gravimetric for the other has not been included in order to avoid inconsistencies due to different methodologies. Only sites with measurements over the whole year are included. Notice that some of the sites have data capture with less than 75% coverage. These are denoted in the table.

In general, there is a fairly good agreement between model calculations and measured data regarding the fraction of $PM_{2.5}$ in PM_{10}. However, the model calculates somewhat larger $PM_{2.5}$ to PM_{10} ratios compared to measurements. Averaged over all sites, the observed $PM_{2.5}$ to PM_{10} ratio is 0.63, while it is 0.71 calculated by the model. Considering geographical differences, mean observed ratios for Northern, Central/Western and Southern Europe are 0.54, 0.70 and 0.59 respectively. The correspondent numbers from the model results are 0.71, 0.75 and 0.69. The observational and model data agree that fine fraction in PM_{10} is larger in central Europe (0.6-0.8), where anthropogenic emissions dominate, compared to southern Europe (0.5-0.7), where windblown dust has a large influence. Lower $PM_{2.5}$ to PM_{10} ratios (0.5-0.7) are derived from model and observational data for French, British and Dutch sites located relatively close to the coast and thus influenced by sea salt aerosols. For Scandinavian (Norwegian and Swedish) sites, the model and measurements show a larger disagreement. Compared to observations, the model allocates a larger portion of aerosol mass to $PM_{2.5}$ fraction. Tables A1 and A2 in Appendix show that the model negative biases are somewhat larger for PM_{10} than for $PM_{2.5}$ compared to observations at those sites, indicating that the model tends to underestimate measured coarse PM mass. This could partly be due to too little road dust in model calculations, which contribution to coarse mass can be significant due to the use of studded tires in north-European countries. Also primary biogenic aerosol particles (PBAP), which can have large influence at some sites, are not presently incorporated in the model. PBAP may contribute significantly at the Nordic sites, especially during summer (Yttri et al., 2007; 2011a,b; Genberg et al., 2011).

Table 3.1: Observed and model calculated annual mean PM ratios at EMEP sites in 2010.

		Site	$PM_{2.5}/PM_{10}$		PM_1/PM_{10}	$PM_1/PM_{2.5}$
			Obs	Mod	Obs	Obs
Northern Europe	Norway	NO02[1)]	0.60	0.73		
	Sweden	SE05	0.57	0.78		
		SE14	0.54	0.62		
		SE11[2)]	0.45	0.72		
	Finland	*FI50*	*0.85*	*missing*	0.82	0.71
The British isles	Great Britain	GB36	0.62	0.61		
		GB48[3]	0.52	0.60		
Central/Western Europe	Austria	AT02	0.78	0.83	0.82	0.79
	Switzerland	CH02[3)]	0.68	0.79	0.51	0.77
		CH05[3)]	0.77	0.80	0.69	0.81
	Czech Rep.	CZ03[3)]	0.82	0.81		
	The Netherlands	NL09	0.56	0.64		
		NL10	0.60	0.71		
	Germany	DE02	0.74	0.73	0.50	0.67
		DE03[3)]	0.76	0.80		
		DE44	0.77	0.78		
	France	FR09[2)]	0.65	0.76		
		FR13[2)]	0.61	0.68		
		FR15[2)]	0.72	0.70		
		FR18[2,3)]	0.68	0.66		
Eastern Europe	Latvia	LV10[3]	0.59	0.74		
		LV16	0.65	0.82		
	Poland	PL05	0.77	0.81		
Southern Europe	Spain	ES01	0.57	0.65		
		ES07	0.59	0.56		
		ES09	0.54	0.71		
		ES10	0.50	0.57		
		ES11	0.50	0.61		
		ES12	0.49	0.71		
		ES13	0.56	0.70		
		ES14	0.58	0.72		
		ES16[3)]	0.67	0.69		
		ES1778[3)]	0.71	0.80		
	Slovenia	SI08	0.77	0.83		
Eastern Mediterranean	Cyprus	CY02	0.52	0.60		
Average			0.63	0.71	0.67	0.75

1) Estimated based on weekly data; 2) Based on hourly data; 3)less than 75% data coverage

3.1.9 Exceedances of EU limit values and WHO Air Quality Guidelines in the regional background environment in 2010

The EU limit values for PM_{10} (Council Directive 1999/30/EC) are 40 μg/m^3 for the annual mean and 50 μg/m^3 for the daily mean. The daily mean should not be exceeded more than 35 times per calendar year.

The WHO AQGs (WHO, 2005) are:
for PM_{10}: < 20 μg/m^3 annually, 50 μg/m^3 24-hour (99th perc. or 3 days per year)
for $PM_{2.5}$: < 10 μg/m^3 annually, 25 μg/m^3 24-hour (99th perc. or 3 days per year).

EU limit values for PM for protection of human health and WHO Air Quality Guidelines (AQGs) for PM apply to PM concentrations for so-called zones, or agglomerations, in rural and urban areas, which are representative of the exposure of the general population. The EMEP model is designed to calculate regional background PM concentrations. Clearly, the rural and urban PM levels are higher than those at the background due to the influence of local sources. However, comparison of model calculated PM_{10} and $PM_{2.5}$ with EU limit values and WHO AQGs can provide an initial assessment of air quality with respect to PM pollution, flagging the regions where already the regional background PM is in excess of the critical values.

The combined model and observation maps show that the annual mean regional background PM_{10} concentrations were below the EU limit value of 40 μg/m^3 over all of Europe in 2010, with the exception of the south most areas in Europe and the EECCA countries affected by desert dust outbreaks (Figure 3.2). However, the annual mean PM_{10} concentrations calculated by the model exceed the WHO recommended AQG of 20 μg/m^3 in Benelux, Hungary and the Po Valley. Calculated PM_{10} concentrations were also found to be in excess of 20 μg/m^3 in the southern and south-eastern parts of the Mediterranean basin, in the Caucasus and in the EECCA countries due to the influence of windblown dust from deserts and semi-arid soils. The regional background annual mean $PM_{2.5}$ concentrations were above the WHO recommended AQG value of 10 μg/m^3 in many parts of Central, Eastern and South-Eastern Europe, in the Po Valley and EECCA area.

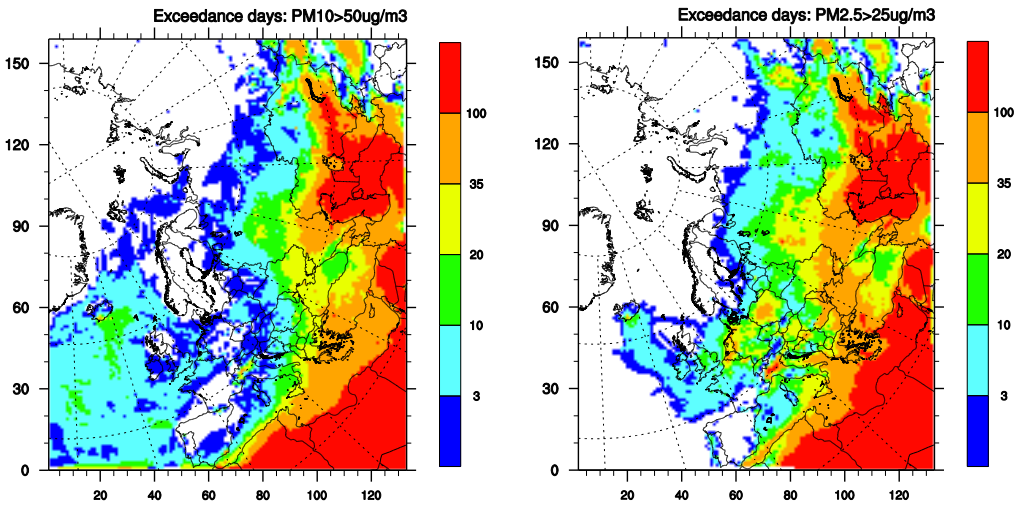

Figure 3.5: Calculated number of days with WHO AQG exceedances in 2010: PM_{10} exceeding 50 μg/m^3 (left) and $PM_{2.5}$ exceeding 25 μg/m^3 (right). Note: EU Directive requires that no more than 35 days exceed the limit value, while the WHO AQG recommendation is not to be exceeded more than 3 days.

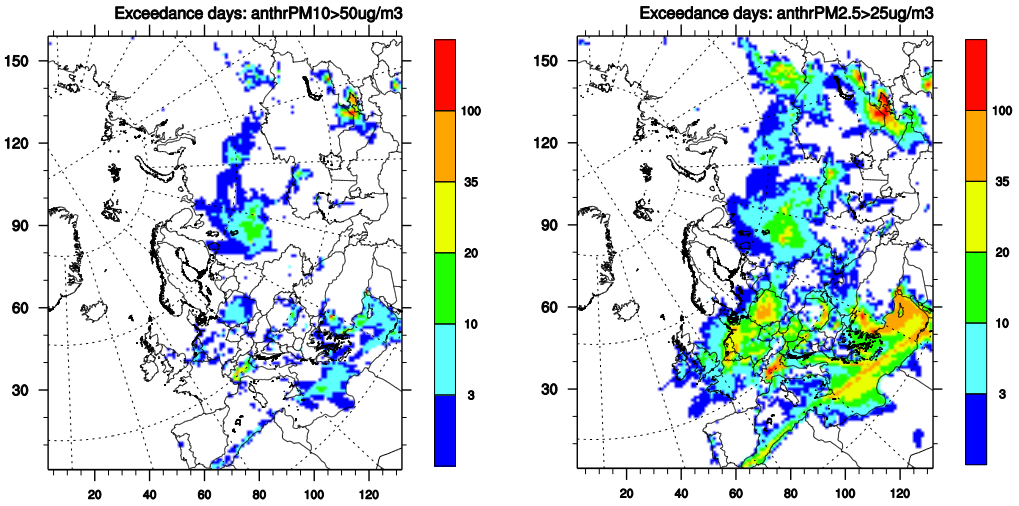

Figure 3.6: Calculated number of days with WHO AQG exceedances in 2010: same as Figure 3.5 but for anthropogenic PM_{10} (left) and anthropogenic $PM_{2.5}$ (right).

The maps in Figure 3.5 show the model calculated number of days with exceedances of 50 μg/m^3 for PM_{10} and 25 μg/m^3 for $PM_{2.5}$ in 2010. To illustrate the relative importance of man-made and natural particulates in the deterioration of air quality, Figure 3.6 shows the correspondent exceedance maps for anthropogenic PM_{10} and $PM_{2.5}$. Compared to the estimate of exceedance days for 2009 presented last year, calculated number of days with exceedances of PM_{10} and $PM_{2.5}$ limits is somewhat greater for 2010. This is partly a reflection of the pollution situation in 2010, and partly due to improved model ability to reproduce observed PM (as shown below, model negative bias with respect to measured PM has been considerably reduced). Thus, the model now is capable of reproducing more of measured exceedances.

In most of Europe, except from southern parts of Greece, Malta, much of Turkey and EECCA countries, PM_{10} did not exceed 50 μg/m^3 more than 35 days in the rural background (i.e. the EU limit value) in 2010. However over large areas in the south of the EMEP territory, PM_{10} exceeded 50 μg/m^3 more than 3 days recommended by WHO. Furthermore, the WHO AQG for $PM_{2.5}$ was exceeded by regional background concentrations in more than 3 days in most EMEP countries, except from Northern Europe and southern and eastern parts of Russia.

In areas distant from the main sources of anthropogenic pollution in Europe, exceedances occur due to either advection episodes or due to influence of natural aerosols. Model calculations indicate that regional background PM_{10} of anthropogenic origin exceeded the EU limit value in just some small areas and mostly in less than 5-10 days (Figure 3.6, left). However for anthropogenic $PM_{2.5}$, we have calculated between 3 and 20 days with exceedances on a rather large territory, and even 20-40 days (up to 100) in the Po Valley and in the grid cells in Poland, Benelux and adjacent areas, in some south-eastern countries, Turkey, Central Russia and on the Uzbekistan-Kyrgyzstan/Tajikistan border.

Based on model and measurements data, a number of days with exceedances of the WHO AQGs at EMEP sites have been calculated for 2010. The observed and calculated numbers of exceedance days, as well as the number of common exceedance days, i.e. the days for which observed PM exceedances are also predicted by the model, are presented in Table 3.2.

For most of the sites, where PM_{10} and $PM_{2.5}$ concentrations exceeded the WHO recommended limits in 2010, also the model calculated exceedances. However, the model tends to under-predicts registered number of exceedance days for PM_{10} and $PM_{2.5}$ for most of the sites. The largest under-prediction of the occurrence of PM_{10} and $PM_{2.5}$ exceedance days is found for AT02, HU02, at Dutch and Italian sites, several of the German sites, and also for Latvian sites, CH02 and PL05 for $PM_{2.5}$. At several sites in southern/south-eastern Europe (CY02, ES07, ES17, GR02 and MK07), the model calculates more than observed days with exceedances of EU limit values for PM_{10} and/or $PM_{2.5}$. Most of calculated PM episodes at those sites appear to be due to overestimated concentrations of dust from Sahara coming from boundary conditions.

The "Hit ratio" in Table 3.2 shows the percentage of observed exceedance days correctly predicted by the model. The hit ratios vary between the sites all from 0 to 100%, and more non-zero hit ratios are achieved for $PM_{2.5}$ than for PM_{10}.

Table 3.2: Number calculated and observed days exceeding the WHO AQGs (50 μg m^{-3} for PM_{10} and 25 μg m^{-3} for $PM_{2.5}$) at EMEP sites.

	PM_{10}				PM_{25}			
Site	Obs	Model	Common	Hit ratio,%	Obs	Model	Common	Hit ratio,%
AT02	37	2		0	90	14	11	12
AT05	2	2		0				
AT48	0	1						
CH01	1	0		0				
CH02	4	1		0	31	7	5	16
CH03	7	0						
CH04	0	1						
CH05	0	0			8	9	4	50
CY02	37	75	21	57	33	95	17	52
CZ01	0	0						
CZ03	2	0			17	7	5	29
DE01	9	2	1	11				
DE02	12	0		0	44	14	13	30
DE03	2	1	1	50	9	2		0
DE07	11	0		0	12	4	3	25
DE08	4	0		0	1	3	1	100
DE09	10	1		0				
DE44	22	3		0	72	27	24	33
DK05	6	1		0				
DK12	2	0		0				
ES01	6	1	1	17	3	0		0
ES06	9	2	1	11				
ES07	6	5	2	33	4	0		0
ES09	4	0		0	0	0		
ES10	3	0			2	0		0
ES11	5	0			3	0		0
ES12	3	1	1	33	0	0		
ES13	3	0		0	2	0		0
ES14	1	0			4	0		0
ES16	0	0			1	0		0
ES17	1	2		0				
ES1778	2	0		0	3	5	1	33
FR09	*6*	*0*		0	*61*	*12*	*9*	*15*
FR13	*1*	*1*		0	*29*	*8*	*1*	*3*
FR15	*3*	*4*		0	*40*	*14*	*8*	*20*
FR18	*1*	*4*		0	*19*	*7*	*4*	*21*
GB06	*0*	*1*						
GB36	0	4			14	10	3	21
GB48	0	0			1	0		
GB43	*0*	*0*						
GR02	*16*	*40*	*14*	*88*				
HU02	*46*	*2*	*1*	2				
IT01	15	2		0				
IT04					85	42	17	20
LV10	1	0		0	21	3		
LV16	5	0		0	16	3	1	6
MD13	1	7		0				
MK07	*8*	*12*	*4*	**50**				
NL07	26	3	3	12				
NL09	16	2	1	6	38	28	21	55
NL10	14	3	3	21	58	35	29	50
NL11					37	21	18	49
NL91	15	4	2	13				
PL05	9	0		0	61	21	11	18
RO08	0	5						
SE05	0	0			0	0		
SE11	*1*	*0*		0	*12*	*1*	*1*	*8*
SE12	0	0						
SE14	1	0		0	2	2		
SI08	5	2		0	24	7	2	8

Hit ratio (%) shows the percentage of observed exceedance days correctly predicted by the model (common_days/obs_days x100%). Cursive font is used for sites for which hourly measured PM concentrations were averaged to obtain daily values. Cell in grey are sites with less than 75% data coverage.

3.1.10 Evaluation of the model performance for PM in 2010

The ability of the EMEP model to reproduce PM concentrations measured at EMEP monitoring sites in 2010 has been evaluated. The model performance has been evaluated for PM_{10}, $PM_{2.5}$ and also individual aerosol components and the main result are summarised in this section and in Appendix.

Overall statistical analysis. Table 3.3 provides a summary of annual and seasonal statistical analysis of model results versus EMEP monitoring data for 2010. Note that only measurement data, obtained from 24-hourly sampling, have been included here. Shown statistical parameters are the Mean observed and modelled values, the Relative Bias, the Root Mean Square Error, the Correlation coefficient and the Index of Agreement (IOA). The IOA quantifies the degree to which the model predictions are error free and varies from 0.0 (theoretical minimum) to 1.0 (perfect agreement).

As a result of recent endeavours at the MSC-W (Simpson et al., 2012), model performance for PM has been significantly improved. On the annual basis, calculated PM_{10} and $PM_{2.5}$ are 23% and 21% respectively lower than measured concentrations. The PM_{10} underestimation of observations is relatively flat for all seasons, while negative bias for $PM_{2.5}$ is somewhat larger in winter compared to the summer-autumn period. This is thought to be related to underestimation of emissions from residential and commercial heating in winter. The annual mean spatial correlation between calculations and measurements is 0.71 for PM_{10} and 0.79 for $PM_{2.5}$.

The calculated concentrations of secondary inorganic aerosols are lower than the measured ones by between 8% for NO_3^- and 27% for SO_4^{2-} on average in 2010. Note that when SO_4^{2-} is corrected for sea salt sulphate (assumed 7.7% of sea salt), calculations are only 20% lower than measurements. Modelled NH_4^+ is 16% lower than measured value on the annual basis. The annual mean spatial correlations are 0.80, 0.86 and 0.74 for SO_4^{2-}, NO_3^- and NH_4^+ respectively. Modelled sodium from sea spray compares quite well with measured Na^+ concentrations, showing just a slight overestimation of the latter by 6% and correlation of 0.85.

Measurements of EC and OC were performed at fewer sites and with rather variable regularity in 2010 (Chapter 3.2.3). Therefore they are not included in Table 3.3, but are presented for individual sites in Table A3 (Appendix). Since measurements of total carbon (TC) are more robust (less artefact prone) than EC and OC separated, model comparison with observations for TC is also provided. Model calculated OC is 35-60% lower than measurements at all of the sites, except Montseny and Birkenes II. For EC, the model both under- and overestimates the measured concentrations. The largest overestimation is at Montseny. Also at Schauinsland (DE03) and Schmücke (DE08), which are elevated sites, calculated EC in $PM_{2.5}$ is higher than observations. The results for TC are quite similar to those for OC, with the model tending to calculate TC concentrations 30-60% lower than observed for all but Montseny and Birkenes II sites. The differences between model and measured EC/OC are due to uncertainties in both modelled and measured estimates, the latter is further discussed in Chapter 3.2.3.

Table 3.3: Annual and seasonal comparison statistics between EMEP model calculated and EMEP observed concentrations of PM_{10}, $PM_{2.5}$, SIA, SO_4^{2-}, NO_3^- and NH_4^+ for 2010.

Period	N sites	Obs (μg/m^3)	Mod (μg/m^3)	Rel.Bias, %	RMSE	R	IOA
PM_{10}							
Annual mean	48	15.23	11.68	-23	5.67	0.71	0.75
Daily mean	48	15.21	11.66	-23	11.54	0.56	0.71
Jan-Feb	47	18.41	13.19	-28	8.88	0.81	0.75
Spring	47	15.36	11.71	-24	5.28	0.73	0.75
Summer	48	14.95	11.14	-25	5.63	0.73	0.77
Autumn	48	13.17	11.02	-16	5.25	0.63	0.74
PM_{25}							
Annual mean	32	10.70	8.45	-21	3.70	0.79	0.79
Daily mean	32	10.69	8.34	-22	8.51	0.63	0.74
Jan-Feb	30	14.97	9.8	-35	8.59	0.91	0.76
Spring	30	10.54	7.9	-25	3.52	0.77	0.76
Summer	32	9.17	8.03	-12	2.72	0.79	0.86
Autumn	32	8.59	7.99	-7	2.61	0.76	0.85
SO_4^{2-}							
Annual mean	43	1 .74	1 .26	-27	0 .77	0 .78	0 .80
Daily mean	43	1 .75	1 .29	-27	1 .55	0 .61	0 .75
Jan-Feb	42	2 .55	2 .12	-17	1 .20	0 .74	0 .84
Spring	41	1 .67	0 .96	-42	0 .97	0 .65	0 .61
Summer	41	1 .63	1 .04	-36	0 .82	0 .72	0 .73
Autumn	41	1 .40	1 .09	-22	0 .63	0 .78	0 .84
SO_4^{2-} SScorr							
Annual mean	43	1.74	1.40	-20	0.68	0.80	0.84
Daily mean	43	1.75	1.42	-19	1.50	0.61	0.76
Jan-Feb	42	2.55	2.21	-13	1.17	0.74	0.84
Spring	41	1.67	1.12	-33	0.85	0.66	0.66
Summer	41	1.63	1.18	-28	0.71	0.74	0.77
Autumn	41	1.40	1.24	-11	0.54	0.81	0.88
NO_3^-							
Annual mean	20	1.76	1.62	-8	0.95	0.86	0.88
Daily mean	20	1.86	1.70	-8	2.12	0.67	0.80
Jan-Feb	20	2.80	2.26	-19	1.91	0.85	0.84
Spring	19	1.92	1.64	-15	1.12	0.82	0.82
Summer	18	1.16	1.08	-8	0.59	0.82	0.90
Autumn	19	1.53	1.83	19	0.90	0.80	0.88
NH_4^+							
Annual mean	22	1.09	0.91	-16	0.45	0.74	0.79
Daily mean	22	1.06	0.92	-14	0.98	0.68	0.80
Jan-Feb	21	1.73	1.43	-17	0.85	0.80	0.82
Spring	21	1.04	0.80	-23	0.48	0.66	0.70
Summer	22	0.74	0.59	-21	0.43	0.37	0.61
Autumn	21	0.87	0.88	1	0.41	0.64	0.8
Na^+							
Annual mean	26	0.60	0.63	6	0.39	0.85	0.92
Daily mean	26	0.62	0.68	10	0.86	0.72	0.84
Jan-Feb	24	0.54	0.50	-6	0.47	0.79	0.87
Spring	22	0.67	0.79	18	0.40	0.89	0.93
Summer	23	0.60	0.66	9	0.38	0.86	0.91
Autumn	23	0.69	0.71	3	0.50	0.83	0.91

Here, Ns – the number of stations, Obs – the measured mean, Mod – the calculated mean, Bias is calculated as Σ(Mod-Obs)/Obs x 100%, RMSE – the Root mean Square Error= $[1/Ns\Sigma(Mod-Obs)^2]^{1/2}$, R – the tempo-spatial correlation coefficient between modelled and measured daily concentrations and spatial correlation for seasonal mean concentrations. IOA=1-($\Sigma(Mod-Obs)^2$ / $\Sigma(|Mod-<Obs>|+\Sigma|Obs-<Obs>|)^2$)

The parameter IOA for PM_{10}, $PM_{2.5}$ and the individual components varies between 0.75 and 0.92, which is considered to be fairly good results (Elbir, 2003). Furthermore, Table 3.3 shows that model is in general equally good in reproducing observed PM_{10}, $PM_{2.5}$ and the individual aerosols for different seasons. The only somewhat larger disagreement between model and measurements is for SO_4^{2-} in spring/summer. It could be that despite the recent update of temporal profile in the model, SO_x emissions are still too low in warm seasons.

Individual stations. Statistical analysis of model calculated PM_{10} and $PM_{2.5}$ versus daily observations at individual sites are summarised in Tables A.1 and A.2 in the Appendix. All measurements of PM_{10} and $PM_{2.5}$ from EMEP monitoring network in 2010, available to MSC-W by June 2012, have been made use of, e.g. daily, hourly and weekly. The hourly concentrations have been averaged to 24-hourly concentrations.

Averaged over all sites with daily and hourly data, the model bias is -17% for $PM_{2.5}$ and -16% for PM_{10}, and the temporal correlations between calculated and measured concentrations are 0.61 and 0.57 respectively. Compared to weekly data, reported from four Norwegian and three Slovakian sites, the correlation between calculations and measurements appears worse: 0.23 for $PM_{2.5}$ and 0.33 for PM_{10}.

Model performance is fairly robust for most of the sites. However, some outliers are found. PM_{10} is typically overestimated at the high-mountain Jungfraujoch due model's coarse description of orography. Also at Finokalia (GR02), calculated PM_{10} is 94% higher than observed (only first half of 2010 data available) due to overestimated concentrations of African dust. Another outlier is the Leova II site (MD13). All in all, model calculated PM_{10} is within 35% of observed value at 87% of the sites and within 50% of it at 96% of the sites on the annual basis. For $PM_{2.5}$, all calculated annual concentrations are within 50% on measurements and only at 18% sites the calculations differ by more than 35% from measurements.

3.2 Contribution of individual components to PM_{10} mass

3.2.1 Modelled chemical composition of PM_{10}

By Svetlana Tsyro

The modelled PM_{10} and $PM_{2.5}$ concentrations include primary PM and secondary inorganic aerosols (SIA) from anthropogenic particulate and gaseous precursor emissions, secondary organic aerosols formed from both anthropogenic and biogenic VOCs, sea-salt and windblown dust from natural sources and particulate water. Figure 3.7 presents model calculated annual mean relative contributions of individual aerosols to PM_{10} concentrations in 2010. The concentration fields of the respective aerosols can be found in Appendix in Figure A3.

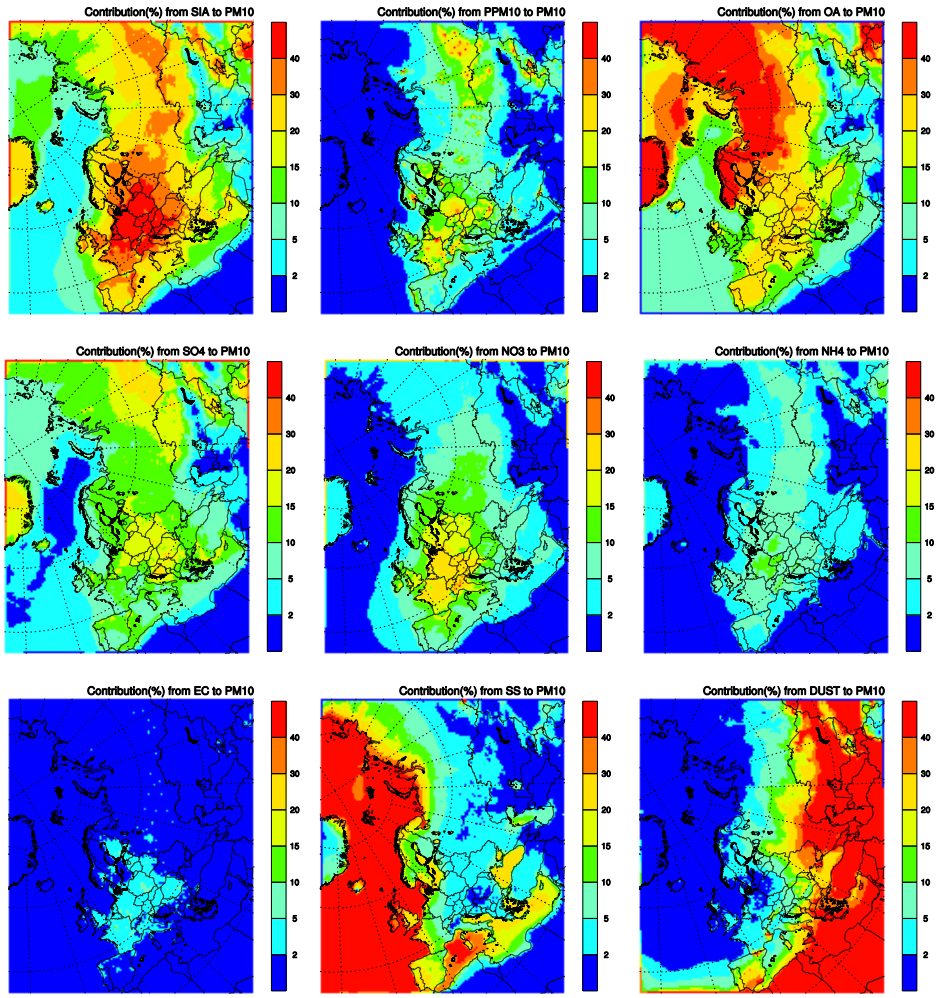

Figure 3.7: Annual mean relative contribution (in %) of SIA, primary PM_{10}, OA (upper panel); SO_4^{2-}, NO_3^-, NH_4^+ (middle panel); EC, sea salt and mineral dust (lower panel) to PM_{10} in 2010, calculated using the EMEP/MSC- model. Note: 1) OA (organic aerosol) is the sum of primary OM and SOA; 2) EC and primary OM are components of primary PM.

There are clear geographical differences in the importance of different components in PM_{10} concentrations. SIA dominates in Central Europe, comprising 40-50% of PM_{10}, while organic aerosols (OA) prevail in Northern Europe and northern/mid-latitude part of Russia (30-55% of PM_{10}) and particularly in Siberian areas of Russia (up to 60% of PM_{10}). The contribution of primary emitted anthropogenic aerosols to PM_{10} is in general smaller than those of SIA and OA (mostly in a range of 5 to 20%) and has a rather local character, reaching as much as 40-50% of PM_{10} in the vicinity of major urban agglomerates due to large emissions from traffic and residential heating and also in industrial areas.

Among SIA components, NO_3^- contributes the most to PM_{10} in Western/Central Europe (20-30%), whereas largest SO_4^{2-} contribution is found in South-Eastern/ Eastern Europe and in the south-east of Russia. NH_4^+ contributes at the most with 10-15% in Central Europe, 5-10% in most of remaining Europe and mid-latitude Russia, and below 5% in northern and southern parts of the domain.

Elemental carbon is a part of primary PM. EC's contribution PM_{10} is between 3 and 6% in most parts of Central Europe, reaching 7-10% in large cities, whereas beyond the main source areas its contribution is below 2%.

3.2.2 Measurements of secondary inorganic aerosols (SIA)

By Wenche Aas

In the EMEP measurement programme, speciation of PM has historically been focused on the secondary inorganic constituent (SIA), which are known to have a long range transport potential; i.e. sulphate, ammonium and nitrate. Thus, the majority of the EMEP Parties have measured these ions for decades. In 2010, concurrent measurement of sulphate and PM_{10} is performed at a total of 39 sites. At the majority of these sites, SO_4^{2-} is collected using a sampler with an undefined cut-off, whereas at a few sites a sampler with a PM_{10} inlet is applied. The sampling conditions are similar for nitrate and ammonium, but these variables are collected at somewhat fewer sites; i.e. 28 for NO_3^- and 15 for NH_4^+. However, this doesn't reflect the total picture of the number of sites performing reactive nitrogen measurements, as there are 54 sites measuring nitrate as the sum of NO_3^- and HNO_3 and 52 measuring ammonium as the sum of NH_4^+ and NH_3; though not all of these sites do have concurrent PM measurements. For details see the EMEP/CCC data report (Hjellbrekke and Fjæraa, 2012). It should be noted that only IT01 and Netherlands measure NO_3^- and NH_4^+ using the recommended denuder method. In addition, DE44 and GB48 have an online IC system (Marga instrument) with hourly ammonium measurements. It is expected that these are without systematic artefacts. The method used at the other sites however may give a positive artefact due to absorption of NH_3 or HNO_3 or a negative artefact due to evaporation of NH_4NO_3. Also base cations, sea salt ions and mineral dust are part of the monitoring programme, but only a few countries are currently reporting data. 13 sites measure one or all three major sea salt ions (Na^+, Cl^- and Mg^{2+}). Mineral dust is mainly measured during intensive measurement periods and typically at sites in southern Europe.

The relative contribution of SIA to PM_{10} mass as calculated from the measured data are comparable to the modelled estimates described above. The average contribution of SIA from the 15 sites with concurrent measurements of SO_4^{2-}, NO_3^- and NH_4^+ is 35±12%, where Central Europe had the highest SIA contribution with around 50%. The average relative contribution of SO_4^{2-}, NO_3^- and NH_4^+ to PM_{10} were 12±2%, 13±7% and 8±3%, respectively. For sea salt the relative contribution to PM_{10} based on observations was 7±3%. The contribution of sea salt is very dependent on distance to the sea, i.e. 1% at the continental site in Slovakia (SK06) and 20% at a more coastal site in UK (GB48). The discussion of the relative contribution of the carbonaceous fraction based on measurements is described in the next chapter (Chapter 3.2.3).

There are only eight sites with chemical speciation in the fine fraction, though only three site with measurement in both size fractions (DE44, ES1778 and GB48). The relative contribution of SIA is somewhat lower for PM_{10} than for $PM_{2.5}$. This is to be expected as most of these ions reside in the fine fraction of $PM_{10.}$ On average for the eight sites, SIA contributes with 41% to the $PM_{2.5}$ mass.

3.2.3 Measurements of carbonaceous matter

By Karl Espen Yttri

3.2.3.1 Status of sampling and measurement, and quality of observation data

The lack of comparable EC/OC data in Europe has hampered the possibility to address the spatial and temporal variation of these variables on the regional scale. Exceptions are the EMEP EC/OC campaign (Yttri et al., 2007), and the CARBOSOL project (Pio et al., 2007), with data for the period 2002–2004, which can be used for such a purpose. More recent measurements are needed to get an overview of the current situation, and to validate the progress made with respect to model development.

An increased number of countries and sites have started reporting levels of EC and OC following from the development of the EUSAAR protocol. Twelve sites reported measurements of EC and OC for 2010, which are two more than for 2009. Measurements performed at the two Norwegian sites Hurdal (NO0056R) and Kårvatn (NO0038R) are reported for the first time for 2010. See Table 3.4 for all sites reporting levels of EC and OC for 2010. In addition, total carbon (TC) was reported for the Hungarian site K-puszta.

We recognise that the quality of the EC/OC data reported to EMEP has improved with respect to variables such as sampling time and sampling frequency; i.e. these variables are the same for consecutive years, which substantially reduces the uncertainties when comparing data from one year to the other. Also the data capture has improved, as well as the datasets includes year-round measurements, making it possible to study seasonal variability.

Eleven of the twelve sites listed in Table 3.4 quantified EC and OC according to a thermal-optical method protocol. Further, ten of these twelve sites followed the recommended EUSAAR-2 analytical protocol, being an important step towards

harmonized and comparable data for EC and OC within EMEP. A detailed description of the EUSAAR-2 protocol and its performance can be found in Cavalli et al. (2010). Work is currently in progress to finalize the standard operating procedure (SOP) for subsequent inclusion to the EMEP manual. Effort concerning how to handle samples which are impacted by carbonate carbon are currently undertaken within the EU-funded project ACTRIS (Chapter 4). Guidelines for how to deal with such samples will be developed based on the results obtained in ACTRIS and will subsequently be added to the SOP for EC/OC.

Table 3.4: Sites reporting EC and OC for 2010, including size fractions and sampling period.

Site (Country)	EC	OC	PM_1	$PM_{2.5}$	PM_{10}	Period
Aspvreten (Sweden)	x	x			x	2008, 2009, 2010
Birkenes (Norway)	x	x		x	x	2001, 2002, 2003, 2004, 2005, 2006, 2007, 2008, 2009, 2010
Finokalia (Greece)	x	x			x	2008, 2009, 2010
Harwell (UK)	x	x			x	2009, 2010
Hurdal (Norway)	x	x		x	x	2010,
Ispra (Italy)	x	x		x		2002[1)], 2003[2)], 2004[2)], 2005[2)], 2006, 2007, 2008, 2009, 2010
Košetice (Czech Rep.)	x	x		x		2009, 2010
Kårvatn (Norway)	x	x		x	x	2010
Melpitz (Germany)	x	x		x	x	2006, 2007, 2008, 2009, 2010
Montseny (Spain)	x	x		x	x	2007, 2008, 2009, 2010
Pay de Dome (France)	x	x		x		2008, 2009, 2010
Vavihill (Sweden)	x	x			x	2008, 2009, 2010

1. EMEP EC/OC campaign
2. Both $PM_{2.5}$ and PM_{10}.

The EUSAAR-2 protocol has already been used for other site categories than rural background, and is one of the candidate methods to be tested for a standardized method for EC/OC measurements within CEN. With EMEP adapting the EUSAAR-2 protocol, we hope the EMEP community's, and others, can be in favour of the choice of this protocol also within CEN, thus providing comparable EC/OC data for a wider range of site categories.

Particular concern should be made regarding EC/OC data obtained by other than thermal-optical analysis methodology, which do not account for charring of OC during analysis. For 2010, this concerns the German site Melpitz, only, for which the EC concentration is grossly overestimated. However, thermal-optical analysis is planned from July 2012 on.

Only the analytical part of the EUSAAR unified protocol is considered finalized at present, as some final tests still remain concerning the design of the "artefact-free" sampling train. Comparable data, in particular for OC, require that both the analytical and the sampling protocol are harmonized, which currently is not the

case. The final tests of the EUSAAR best affordable, "artefact-free" sampling train is currently taking place within the EU-funded project ACTRIS. The variability amongst the various sampling approaches used is apparent from the variables listed in Table 3.5. Most sites sample for 24 hours, whereas the sampling time range from 48 hours to one week for low loading sites such as Birkenes and Pay De Dome. Three sites (Aspvreten, Ispra and Vavihill) attempted to account for both positive and negative sampling artefacts, whereas one (Košetice) used the QBQ-approach (Quartz-behind-Quartz) to account for positive artefacts. Eight of the twelve sites did not address sampling artefacts on a regular basis, but some addressed the positive sampling artefacts based on results from intensive measurements periods.

Table 3.5: Sampling equipment and analytical approach used at the sites reporting EC and OC to EMEP for 2010.

Site (Country)	Sampling time/frequency	Filter face velocity	Sampling equipment	Analytical approach
Aspvreten (Sweden)	24 hr, every 3rd day	55 cm s^{-1}	Denuder/Backup filter pos/neg artifact	Sunset TOT (EUSAAR-2)
Birkenes (Norway)	168 hr, every 7th day	54 cm s^{-1}	Single filter (no correction)	Sunset TOT (EUSAAR-2)
Finokalia (Greece)	24 hr, every 2nd day	26 cm s^{-1}	Single filter (no correction)	Sunset TOT (EUSAAR-2)
Harwell (UK)	24 hr, daily	20 cm s^{-1}	Single filter (no correction)	Sunset TOT (Quartz)
Hurdal (Norway)	168 hr, every 7th day	54 cm s^{-1}	Single filter (no correction)	Sunset TOT (EUSAAR-2)
Ispra (Italy)	24 hr, daily	20 cm s^{-1}	Denuder/Backup filter Pos/neg artifact	Sunset TOT (EUSAAR-2)
Košetice (The Czech Rep.)	24 hours, every 6th day	20 cm s^{-1}	QBQ (pos. artifact)	Sunset TOT (EUSAAR-2)
Kårvatn (Norway)	168 hr, every 7th day	54 cm s^{-1}	Single filter (no correction)	Sunset TOT (EUSAAR-2)
Melpitz (Germany)	24 hr, daily	50 cm s^{-1}	Single filter (no correction)	VDI 2465 Part 2
Montseny (Spain)	24 hr, every 4th day	74 cm s^{-1}	Single filter (pos. artefact/camp)	Sunset TOT (EUSAAR-2)
Pay de Dome (France)	48 hr, every 7th day	69 cm s^{-1}	Single filter (pos. artifact/camp)	Sunset TOT (EUSAAR-2)
Vavihill (Sweden)	72 hr, every 3rd day	55 cm s^{-1}	Denuder/Backup filter pos/neg artifact	DRI (EUSAAR-2)

Five of the twelve sites performed measurements of EC and OC in PM_{10} and $PM_{2.5}$, hence providing valuable information on the size distribution of these variables, which also add to the understanding of sources and atmospheric processes. An overview of the annual mean EC/OC/TC concentration reported for 2010 are shown in Table 3.6.

Since 2008, i.e. data from 2007, EC/OC data are reported to EBAS according to the EUSAAR format.

In last year's EMEP PM report we pointed out that reporting EC/OC data to EBAS according to the EUSAAR format appeared to be somewhat challenging

given its complexity. Although the situation improves year by year there is still room for improvement. The requested meta-data is an absolute prerequisite needed to understand the individual datasets as well as to evaluate upon the comparability of various dataset.

Table 3.6: Annual mean concentrations of EC, OC and TC for 2010. Only sites which reported for more than 6 months have been included.

	EC PM_{10} (µg C/m^3)	OC PM_{10} [1] (µg C/m^3)	TC [1] PM_{10} (µg C/m^3)	EC/TC (%)	EC $PM_{2.5}$ (µg C/m^3)	OC $PM_{2.5}$ [1] (µg C/m^3)	TC $PM_{2.5}$ [1] (µg C/m^3)	EC/TC (%)
Aspvreten (Sweden)	0.30	1.7	2.0	16				
Birkenes (Norway)	0.11	0.90	1.0	11	0.10	0.67	0.78	13
Finokalia (Greece)	0.36	2.0	2.3	14				
Harwell (UK)	0.53	1.8	2.2	21				
Hurdal [2] (Norway)	0.16	1.3	1.4	12	0.15	0.87	1.0	16
Ispra (Italy)					1.3	5.9	7.2	22
Košetice (Czech Rep.)					0.49	2.6	3.1	21
Kårvatn [3] (Norway)	0.06	0.98	1.0	7.0	0.07	0.85	0.92	9.1
Melpitz (Germany)	1.6	3.1	4.7	30	1.3	2.6	3.9	31
Pay de Dome (France)					0.1	1.0	1.0	12
Montseny (Spain)	0.23	1.7	2.0	12	0.23	1.5	1.8	14
Vavihill [4] (Sweden)	0.18	1.7	1.8	9.7				

1) Both sampling-artefact-corrected and uncorrected concentrations of OC and TC are here denoted "OC" and "TC"
2) Not full year of sampling. Sampling started in May 2010
3) Not full year of sampling. Sampling started in June 2010
4) Not full year of sampling. Sampling ended in September 2010

3.2.3.2 Observed levels of EC and OC in 2010

EC

Annual mean concentrations of EC

The levels of EC (here: both in PM_{10} and $PM_{2.5}$) obtained by thermal-optical analysis varied by a factor of 19 between the site reporting the lowest (0.06 µg C/m^3 at Kårvatn, Norway) and the highest annual mean concentration of EC (1.3 µg C/m^3 at Ispra, Italy) (see Figure 3.8). The lowest concentrations were observed in Scandinavia (0.06–0.30 µg C/m^3), at certain high altitude European continental sites in western/south-western Europe (0.10–0.23 µg C/m^3). The annual mean EC concentrations observed at Košetice and Melpitz in Eastern Europe, Harwell in the UK, and Ispra in northern Italy (0.49–1.3 µg C/m^3), were noticeably higher than for the Scandinavian and the continental sites in

western/south-western Europe, whereas the level observed at Finokalia (0.36 µg C/m^3) in the Eastern Mediterranean should be considered in-between. Note though that the EC levels at the Melpitz site are overestimated due to the analytical method used (VDI 2465 part 2), however it is more likely that the "true" EC level at this site falls within the upper rather than the lower range reported in Table 3.6.

The Norwegian site Birkenes has typically reported the lowest annual mean concentration of EC (approximately 0.1 µg C/m^3) within EMEP since 2001 and that by a fair margin. By inclusion of measurements at the Norwegian sites Kårvatn in 2010, we find that the EC level at this site is no more than 0.06 µg C/m^3, i.e. no more than 60% of at observed at Birkenes, indicating substantial spatial variability even within the Southern parts of Norway.

Seasonality of EC

For nine out of twelve sites the EC loading was increased by a factor 1.3–2.9 during winter compared to summer (Figure 3.8). The EC level increased by a factor of two or more at the four sites reporting the highest annual mean concentrations of EC; i.e. Ispra (2.9), Košetice (2.7), Melpitz (2.3–2.8, including both EC in PM_{10} and $PM_{2.5}$), and Harwell (2.0). There was also as substantial 2.1 times increase during winter at Puy de Dome, whereas for four out of five Scandinavian sites the EC level increased by a factor 1.3–2.0. For the sites Finokalia and Kårvatn there was a modest increase in the EC concentration during summer corresponding to less than a factor of 1.1. For Montseny, no consistent conclusion can be draw as measurements of EC in PM_{10} and $PM_{2.5}$ diverge; i.e. EC in $PM_{2.5}$ increased during winter, whereas EC in PM_{10} decreased during winter. The increased levels observed during winter likely reflects both increased emissions, e.g. results from the EMEP intensive measured periods 2008/2009 show a substantial influence of wood burning emissions in winter based on measurements of levoglucosan, as well as meteorological conditions preventing dispersion of the air pollution; i.e. inversion.

Size distribution of EC

Five sites performed concurrent measurements of EC and OC in two size fractions (here: PM_{10} and $PM_{2.5}$) which is two more than for 2009. At the three Norwegian sites, 88–94%% of EC in PM_{10} could be attributed to EC in $PM_{2.5}$. For Melpitz the corresponding percentage was 78%, whereas it was 73% for Montseny. Note that for Montseny, concurrent sampling of PM_{10} and $PM_{2.5}$ filter samples only took place for a certain fraction of the days. These percentages underlines that EC is associated mainly with fine particles, resulting from incomplete combustion of fossil fuels and biomass. It should be noted that the mean percentages are based on the EC in $PM_{2.5}$/EC in PM_{10} ratios for individual samples and not the ratio of the annual mean of EC in $PM_{2.5}$ and EC in PM_{10}. Selection criteria have excluded ratios exceeding 105%.

Annual mean EC/TC ratio

The annual mean EC/TC ratio varied from 7–22%; i.e. for the sites analysing according to a thermal-optical protocol (here: EUSAAR2 and Quartz.par). This range corresponds with that reported by Yttri et al. (2007) (12–24%) for the EMEP EC/OC campaign, using Quartz.par. The extension of the lower range of

the EC/TC ratio seen for 2010 (7%) compared to 2009 (10%) is attributed to the inclusion of the Norwegian site Kårvatn. For Melpitz, using the VDI (2465 part 2) protocol, EC accounted for 32% (PM_{10}) and 37% ($PM_{2.5}$), however as stated above, the VDI protocol does not account for charring of OC during analysis and thus overestimates the samples EC content. The EC/TC ratio for the Scandinavian sites and the western/south-western European high altitude sites were all <16% (Mean±SD = 12±2.5), whereas it ranged from 21–22% for Harwell, Košetice, and Ispra. EC was found to be a more pronounced fraction of TC in winter compared to summer, except for the sites Finokalia, Ispra and Košetice. The increased fraction of TC attributed to EC in winter is in accordance with that observed during the EMEP EC/OC campaign (Yttri et al., 2007).

Changes in annual mean concentration of EC from 2009 to 2010

10 out of 12 sites reporting annual mean concentrations of EC for 2010 did also report this variable for 2009. In cases where sampling is performed once a week for a period of e.g. 24 hours, the data coverage is no more than 14% per year. Consequently, the variability of the annual mean is increased and the comparability of the annual mean from one year to the other correspondingly reduced. Further, irregular sampling frequency, e.g. covering the entire heating season but only a minor part of the non-heating season and vice versa the consecutive year, is another potential bias, hampering the comparability on an annual basis. For 2009 we found that only three sites had a sufficient data consistency suitable for comparison with the previous year; i.e. Birkenes, Ispra and Melpitz, which had a sampling time and frequency covering the entire year. For 2010, we find that such a comparison can be made for seven of the sites, which is a noticeable improvement from the previous year. Note though that for three of these sites the sampling time and frequency do not cover the entire year, however, they do have a sampling time and frequency which is consistent with the previous year.

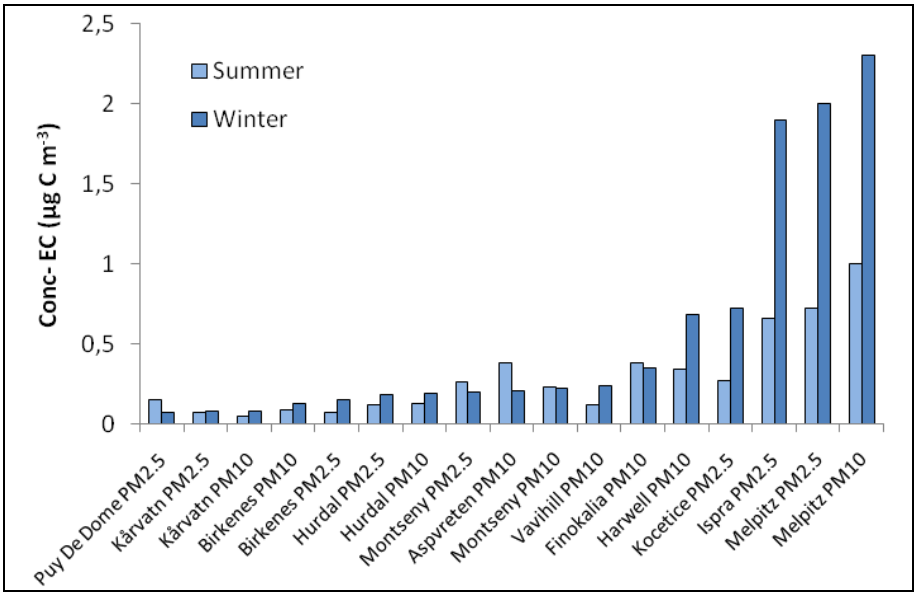

Figure 3.8: Mean summer and winter time concentrations of EC in PM_{10} and $PM_{2.5}$ at EMEP sites in 2010. The sites are ranked according to increasing winter time concentration of EC.

For Birkenes and Harwell a < 10% increase was observed going from 2009 to 2010, including EC in both PM_{10} and $PM_{2.5}$ for the Norwegian site, whereas a 14 – 18% increase was observed for Melpitz (including both EC in PM_{10} and $PM_{2.5}$). For Ispra the EC level was reduced by 7% going from 2009 to 2010, whereas an 18% reduction was observed for Košetice. For Montseny the results for PM_{10} and $PM_{2.5}$ diverge, as no change is observed for EC in $PM_{2.5}$ going from 2009 to 2010, whereas there is a substantial 28% reduction for EC in PM_{10}. At Puy de Dome no change in the annual mean EC concentrations was observed going from 2009 to 2010.

OC

For the sake of simplicity sampling-artefact-corrected OC (OC_p) and uncorrected levels of OC have been denoted as "OC" in Table 3.6, and subsequently discussed and compared in the following section as OC.

Annual mean concentrations of OC

For the sites using thermal-optical analysis for EC/OC analysis the annual mean concentration of OC in PM_{10} ranged from 0.9 µg C/m^3 at the Norwegian site Birkenes to 2.0 µg C/m^3 at the Greek site Finokalia. For $PM_{2.5}$, the corresponding range was 0.67 µg C/m^3 (Birkenes) to 5.9 µg/m^3 (Ispra in Italy). The VDI 2465 part 2 method used to quantify EC and OC at the Melpitz site underestimates the samples level of OC by not accounting for charring of OC to EC, thus the level of 3.1 µg C/m^3 of OC observed for PM_{10} and 2.6 µg C/m^3 of OC observed for $PM_{2.5}$ at this site should most likely be higher.

As observed for EC, the lowest levels of OC (here: considering OC in both PM_{10} and $PM_{2.5}$) were observed in Scandinavia (0.67–1.7 µg C/m^3) and at certain high altitude European continental sites in western/south-western Europe (1.0–1.8 µg C/m^3). The annual mean OC concentration observed at Harwell (1.8 µg C/m^3) was in the upper range of that observed for the sites in Scandinavia and western/south-western Europe, whereas the annual mean OC concentration at Finokalia (2.0 µg C/m^3) just exceeded the level observed at Harwell. For Košetice and Melpitz in Eastern Europe, and Ispra in northern Italy, the annual mean OC concentration ranged from 2.6–5.9 µg C/m^3, thus being substantially higher than for the other sites. As observed for previous years the annual mean OC concentration observed at Ispra far exceeded that observed for the other sites also in 2010; e.g the annual mean OC concentration at Ispra was more than twice that observed at Košetice, which observed the second highest annual mean OC concentration for 2010.

Seasonality of OC

The sites reporting the three highest annual mean concentrations of OC all experienced substantially elevated OC concentrations in winter (Figure 3.9). The difference was most pronounced at Košetice (Factor 3.6 higher in winter compared to summer), followed by Ispra (3.3) and Melpitz (2.3 for $PM_{2.5}$ and 1.7 for PM_{10}). Also at Harwell the OC concentration was higher in winter compared to summer (1.3 times higher in winter), although not that pronounced as seen for the three high loading sites. High OC loadings in winter can be explained by the same reasons as described for EC, i.e. a combination of increased emissions and meteorological conditions preventing dispersion of the air pollution (inversion). In particular, wood burning emissions increase during winter and with a high OC/TC

ratio for such emissions this could contribute to the winter time increase of OC. One should not exclude the possibility that sampling artefacts change according to season, thus having an influence on the observed seasonal variation of OC. This ought to be examined in further detail.

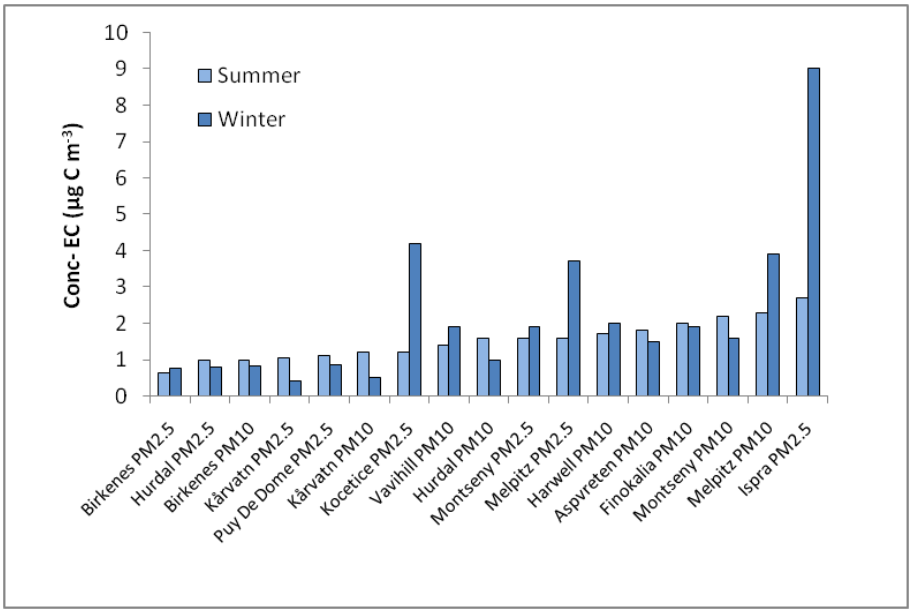

Figure 3.9: Mean summer and winter time concentrations of OC in PM_{10} and $PM_{2.5}$ at EMEP sites in 2010. The sites are ranked according to increasing summer time concentration of OC.

At Aspvreten and Puy de Dome the summer time concentrations of OC was slightly higher in summer compared to winter by a factor 1.2 and 1.3 respectively, whereas for Finokalia no change between summer and winter were observed (Figure 3.9). At Birkenes and Montseny, the seasonality of OC was dependent upon the PM cut off size. OC in PM_{10} was found to be increased in summer compared to winter by a factor 1.2 for Birkenes and a factor of 1.4 for Montseny, whereas for $PM_{2.5}$, OC was found to be increased by a factor 1.2 during winter compared to summer for both Birkenes and Montseny. Increased summer time concentrations of OC have typically been associated with formation of secondary aerosol, both from anthropogenic and natural precursors. It has also been shown that primary biological aerosol particles (PBAP) could contribute to increased levels of OC in summer, at least for certain regions. Typically, increased summer time OC concentrations was observed for the sites experiencing the lowest carbonaceous aerosol loading, suggesting they are situated in areas less perturbed by anthropogenic sources. The observed summer time increase for OC in PM_{10} at Birkenes and Montseny, and which was not observed for OC in $PM_{2.5}$, demonstrates an increase of coarse OC in summer of which PBAP most likely is the major contributor. As previously stated, concurrent collection of PM_{10} and $PM_{2.5}$ filter samples at the Montseny site was only performed for a certain fraction of the days, making this finding less robust than for the Birkenes site. Further insight into the contribution of PBAP to OC in the Nordic environment can be found in Yttri et al. (2011a, b) and Genberg et al. (2011).

Size distribution of OC

Concurrent measurements of EC and OC in two size fractions (here: PM_{10} and $PM_{2.5}$), were performed at three sites. At Birkenes, 70% of OC in PM_{10} could be attributed to OC in $PM_{2.5}$ on an annual basis, the corresponding percentage for Melpitz was 76%. As previously stated, collection of PM_{10} and $PM_{2.5}$ filter samples for subsequent analyses of EC and OC was only to a certain degree performed on the same days at the Montseny site, thus complicating the calculation of a similar percentage. The results show that 73% of OC in PM_{10} could be attributed to OC in $PM_{2.5}$. By assuming that the annual averages of OC in PM_{10} and $PM_{2.5}$ at Montseny are representative for the entire year, 89% of OC in PM_{10} could be attributed to $PM_{2.5}$. As a conclusion, the size distribution of OC at Montseny must be regarded as highly uncertain and indicative only.

At all three sites, levels of OC in $PM_{10-2.5}$ were found to be increased in summer. This was particularly pronounced at Birkenes and Montseny, at which the summer time concentration was in excess of two times higher than that observed in winter. Note though that the estimates made for Montseny are highly uncertain for reasons already mentioned. For Melpitz, the concentration of OC in summer was no more than 1.2 times higher in summer compared to winter. For Montseny the calculations suggest a twofold increase in the relative contribution of OC in $PM_{10-2.5}$ to OC in PM_{10} going from winter (17%) to summer (31%). A similar increase was observed going from winter to summer for the sites Birkenes and Melpitz, at which OC in $PM_{10-2.5}$ accounted for 32-33% of OC in PM_{10} during summer.

Changes in annual mean concentration of EC from 2009 to 2010

For more information regarding selection criteria of sites subject to comparison with respect to OC levels in 2009 versus 2010 see subchapter "Changes in annual mean concentration of EC from 2009 to 2010" above.

For Birkenes (including OC in both PM_{10} and $PM_{2.5}$) a <10% increase was observed going from 2009 to 2010, whereas a 15% (OC in PM_{10}) – 30% (OC in $PM_{2.5}$) increase was observed for Melpitz. For Ispra the OC level was reduced by 13% going from 2009 to 2010, whereas a 10% reduction was observed for Košetice. For the sites Harwell and Puy de Dome a substantial 22–23% reduction was observed. It is worth notifying the quite substantial reduction (10–22%) observed for the three high/medium OC loading sites Ispra, Košetice and Harwell, going from 2009 to 2010. For Montseny the results for PM_{10} and $PM_{2.5}$ diverge, as a <10% reduction was observed for OC in PM_{10} going from 2009 to 2010, whereas there was a substantial 25% increase for OC in $PM_{2.5}$.

3.2.3.3 Levels of EC and OC at sites reporting for the first time in 2010

In the 2010 EMEP status report on PM, a brief description of EC and OC, including levels, size distribution, and seasonality, was provided for each site reporting these two variables. In the 2011 EMEP status report on PM (EMEP, 2011), a similar description was provided for the sites reporting levels of EC and OC for the first time in 2009 (i.e. Košetice (Czech Republic), Harwell (UK) and Finokalia (Greece).

For 2010, two sites reported concentrations of EC and OC to EMEP, being the Norwegian sites Hurdal and Kårvatn (Chapter 3.2.3.4). In addition, the Greek site Finokalia has reported EC/OC in PM_{10} for the first time (Chapter 3.2.3.5).

3.2.3.4 EC and OC levels at the two Norwegian sites Hurdal (NO0056R) and Kårvatn (NO0038)

The Hurdal site (60°22'N, 11°04'E, 300 m.a.s.l.) is located 70 km north east of Oslo, and is situated in the Boreal forest with mixed conifer and deciduous trees, which together with the Hurdal Lake (32 km^2) account for the majority of the surrounding land use. The Kårvatn site (62º47'N, 8º53'E) is situated far from major sources of air pollution, with the local community of Surnadal (2275 inhabitants), located 30 km to the north, being the nearest local emission source. The site is situated in the boreal forest region with mixed conifer and deciduous trees and surrounded by farmland.

There are EC/OC measurements for only in excess of half a year at the sites Hurdal and Kårvatn for 2010, thus we will only briefly outline the concentrations presented in Table 3.6 and come back with a more detailed description for the 2012 EMEP report on PM.

Mean concentrations of EC (0.16 µg C/m^3) and OC (1.3 µg C/m^3) in PM_{10} was approximately 50% higher at the Hurdal site compared to what has been observed at Birkenes and is within the range observed for the Scandinavian sites (see Table 3.6). The elevated EC concentrations at Hurdal compared to Birkenes could indicate that the site is somewhat more influenced by anthropogenic sources, which could be explained by the fact that Hurdal is situated in the more densely populated South- Eastern region of Norway. On the other hand, OC in $PM_{10-2.5}$ accounted for more than 30% of OC in PM_{10}, suggesting a sizeable contribution of primary biological aerosol particles (PBAP), which typically should be considered a natural source. With the first four months of the year not accounted for, the relative contribution of OC in $PM_{10-2.5}$ to OC in PM_{10} for Hurdal is likely overestimated, as PBAP in Norway do not appear to be an important source until after the onset of the vegetative season.

The mean EC concentration (0.06 µg C m^{-3}) at Kårvatn was no more than 40% of that observed at Hurdal and 55% of that observed at Birkenes, suggesting very low influence of anthropogenic sources. Note that Birkenes reported the lowest annual mean concentrations of EC in Europe for the period 2001–2010 until measurements started at Kårvatn. The mean PM_{10} OC concentration at Kårvatn (0.98 µg C/m^3) was only slightly higher than OC in PM_{10} observed at Birkenes (0.90 µg C/m^3). OC in $PM_{10-2.5}$ was not as abundant at the Kårvatn site as for Birkenes and Hurdal, accounting for no more than 13% of OC in PM_{10}.

The mean $PM_{2.5}$ OC concentration at Hurdal (0.87 µg C/m^3) and at Kårvatn (0.85 µg C/m^3) equaled each other and was 20 – 25% higher compared to OC in $PM_{2.5}$ observed at Birkenes. All EC was confined within the $PM_{2.5}$ fraction at the Hurdal and Kårvatn sites, corresponding to what has previously been reported for Birkenes.

Three sites reporting EC/OC levels for various site categories within the rural background environment category in southern Norway provides a great possibility to explore the spatial variation for these variables with respect to e.g. concentration, seasonality, size distribution, and to some extent sources. E.g. the very low EC levels observed at Kårvatn compared to e.g. Birkenes and the fact that OC in $PM_{2.5}$ is noticeably higher at Kårvatn compared to Birkenes ought to be subject to further investigation, given that this finding is observed also for a full year of data for EC/OC at Kårvatn.

3.2.3.5 EC and OC levels at the Greek site Finokalia (GR0002R)

By Giorgos N. Kouvarakis

Measurements of EC and OC in PM_1 has previously been reported for the Greek site Finokalia (GR0002R) (150 m asl) located at the island of Crete. However, 2010 was the first year EC and OC was reported in PM_{10}.

Carbonaceous compounds were measured in 100 daily samples collected all year round at Finokalia and analysed using the EUSAAR 2 method. The median organic carbon (OC) and elemental carbon (EC) concentrations for the whole sampling period (1/1-31/12/2010) were equal to 1.68 μg/m^3 and 0.27 μg/m^3, respectively.

The monthly average distributions of OC and EC showed a bimodal distribution with maxima during late winter (February-March) and summer (July-August, Figure 3.10). The summer peak was associated with photochemical activities that favor secondary aerosol formation in the area (Mihalopoulos et al., 2007), in conjunction with the absence of precipitation. During winter additional sources associated with air masses coming from Central-Eastern Europe contribute to the total carbon loadings (Sciare et al., 2008).

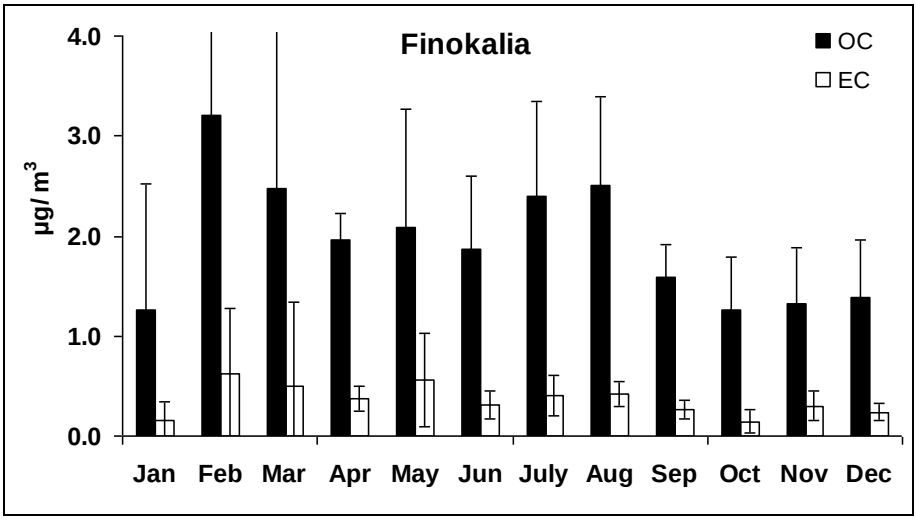

Figure 3.10: Monthly mean values of OC and EC (μg/m^3) in the PM_{10} samples at Finokalia Station. Error bars represent the standard deviation of the OC, EC concentrations.

A significant correlation was observed between OC and EC with slope close to 3, being strong indicator of secondary organic aerosol (SOA) formation (Figure 3.11). If the median of all individual OC/EC samples is examined the value becomes even higher (6.1), indicating that organic aerosols in the area are mostly secondary and aged (processed) after long-range transport.

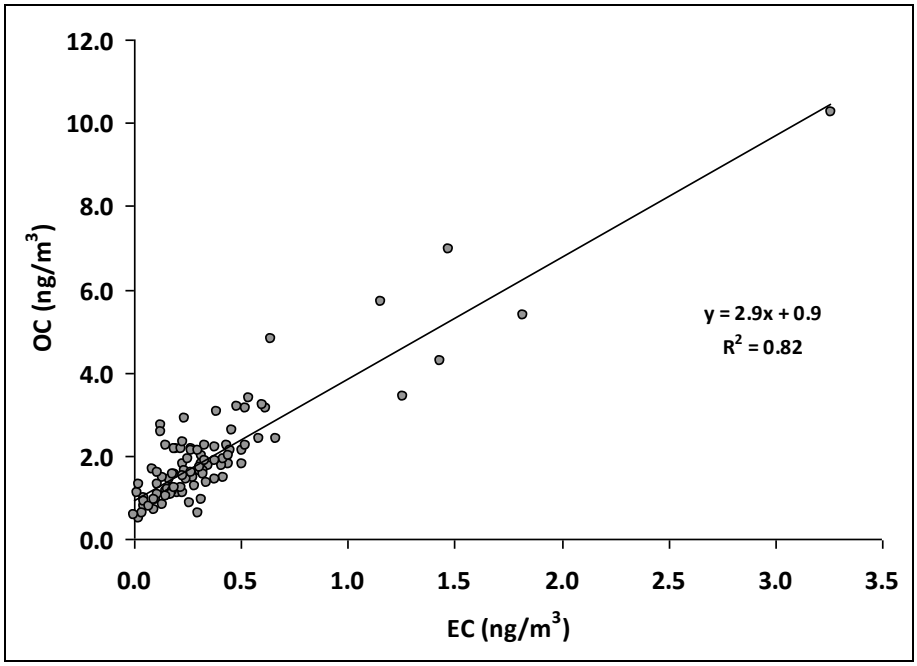

Figure 3.11: Regression between OC and EC ($\mu g/m^3$) in the PM_{10} samples at Finokalia.

3.2.4 Time series of EC and OC

The sites Birkenes, Ispra and Melpitz all have time series of EC and OC extending five years. At Birkenes, measurements go back to 2001, at Ispra measurements started in 2003, whereas at Melpitz measurements have been reported since 2006. Birkenes has a continuous time series of EC and OC for both PM_{10} and $PM_{2.5}$, and thermal-optical analysis has been applied for the entire period. At Ispra, parallel measurements of EC and OC in PM_{10} and $PM_{2.5}$ were performed for the period 2003–2005, whereas thermal-optical analysis has been applied since 2005. At Melpitz, EC and OC are measured in both $PM_{2.5}$ and PM_{10} using the VDI protocol, which do not correct for charring of OC during analysis, hence artificial EC is generated during the analysis overestimating the true EC concentration of the sample. Despite the erroneous feature of the VDI protocol, the results could still provide useful information concerning seasonal variation and time-trends.

Comparable data for EC and OC require that also the sampling protocol is harmonized. At both Birkenes (change from 6+1 days to 7 days sampling time in 2003) and at Ispra (denuder included in the sampling train in 2008) changes have been made to the sampling protocol since the measurements started. The sampling protocol (see Table 3.5) varies substantially between Birkenes, Ispra and Melpitz, with only Ispra accounting for positive and negative artefacts on a regular basis. The sampling time, differing from one week at Birkenes to 24 hours at the two

other sites, reflects the low aerosol loading experienced in the Nordic rural background environment.

Birkenes, Ispra and Melpitz represent different parts of the European rural background environment. Birkenes has typically reported the lowest annual mean concentrations for both EC and OC in Europe, while Ispra has reported the highest levels; by a fair margin. The annual mean (here: TC) observed at Melpitz is second to Ispra only, but still nowhere near the levels observed at Ispra. Birkenes has a strategic position well suited to monitor the outflow of air pollutants from the European continent. Consequently, Birkenes from time to time experience elevated concentrations. The very high level of the carbonaceous aerosol observed at Ispra is attributed to the severe regional air pollution characterizing the Po Valley region. Melpitz is situated in the eastern part of Germany, experiencing both air masses passing over densely populated areas in Western Europe, as well as polluted air masses from well-known source regions in Eastern Europe.

EC and OC also differ with respect to seasonality at the three sites. Ispra and Melpitz both experience substantially elevated concentrations of EC and OC in winter, likely reflecting increased anthropogenic emissions, but also meteorological conditions preventing dispersion of the air pollution is likely to have an influence. At Birkenes, EC and OC ($PM_{2.5}$) tend to be somewhat higher in winter due to increased levels during late winter and spring, but this is not particularly pronounced. For OC in PM_{10} increased concentrations are observed during summer due to OC in $PM_{10\text{-}2.5}$, which is attributed mostly to PBAP.

The time series of EC and OC in PM_{10} and $PM_{2.5}$ at Birkenes look rather similar (see Figure 3.12), however, the inter-annual variability is more pronounced for EC and OC in $PM_{2.5}$ compared to PM_{10}. For OC in PM_{10} this is likely due to the influence of PBAP of mostly local origin. No stepwise up- or downward trend in the annual mean concentration of OC and EC is observed for the period 2001–2010. The time series are characterised by a drop in the annual mean concentrations from 2003 to 2004 and a maximum in 2006. Note though that the increase in 2006 is most pronounced for OC and primarily for OC in $PM_{2.5}$. For the period 2007–2010, only a modest annual variation is observed for OC, although somewhat more pronounced for EC. The time series of EC and OC for PM_{10} and $PM_{2.5}$ resemble that of the secondary inorganic constituents, as well as that of the mass concentration of PM_{10} and $PM_{2.5}$ observed at Birkenes. The annual mean OC concentration observed for 2010 was 20% (PM_{10}) and 30% ($PM_{2.5}$) less compared to the first year of sampling (2001). For EC the corresponding range was 15% (PM_{10}) and 40% ($PM_{2.5}$).

The relative contribution of TCM [(TCM = Total carbonaceous matter (TCM = OC x 1.7 + EC x 1.1)] to the mass concentration of PM_{10}, $PM_{2.5}$ and $PM_{10\text{-}2.5}$ at Birkenes for the time-period 2001–2010 is shown in Figure 3.13. The relative contribution of TCM to PM_{10} and $PM_{2.5}$ shows a modest annual variation, except from 2001–2002, ranging between 25–29% for PM_{10} and 30–37% for $PM_{2.5}$. The relative contribution of TCM-to-$PM_{2.5}$ has the same temporal pattern as for TCM-to-PM_{10}. The relative contribution of TCM to $PM_{10\text{-}2.5}$ ranged from 9–21% for the actual period. While the relative contribution increased substantially from 2001–2004, the contribution has declined slightly again from 2004 and onwards.

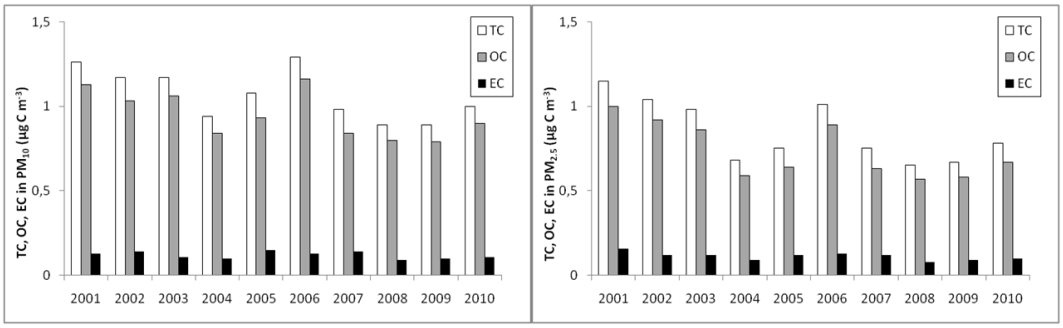

Figure 3.12: Annual mean concentrations of EC, OC and TC in PM_{10} (left) and $PM_{2.5}$ (right) at the Norwegian site Birkenes for the period 2001–2010.

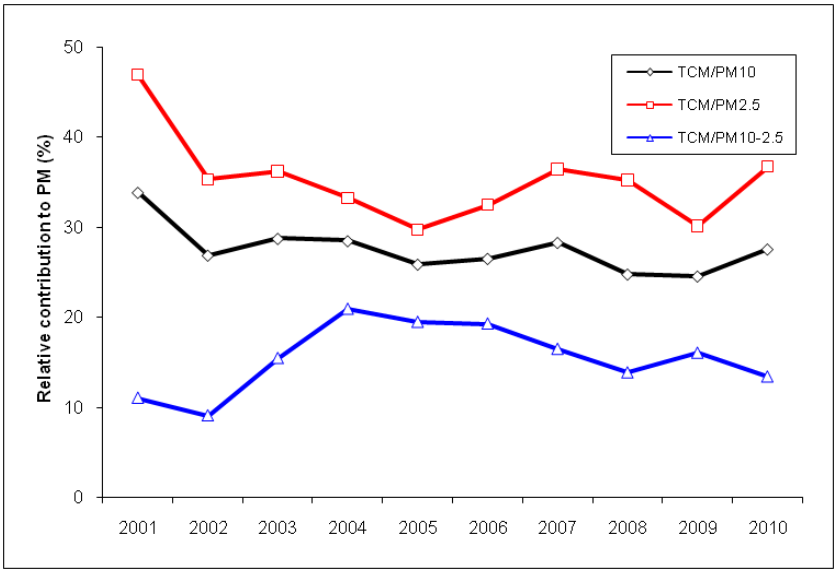

Figure 3.13: Relative contribution of TCM (Total Carbonaceous Matter) to PM_{10}, $PM_{2.5}$ and $PM_{10-2.5}$ at Birkenes for the period 2001–2010.

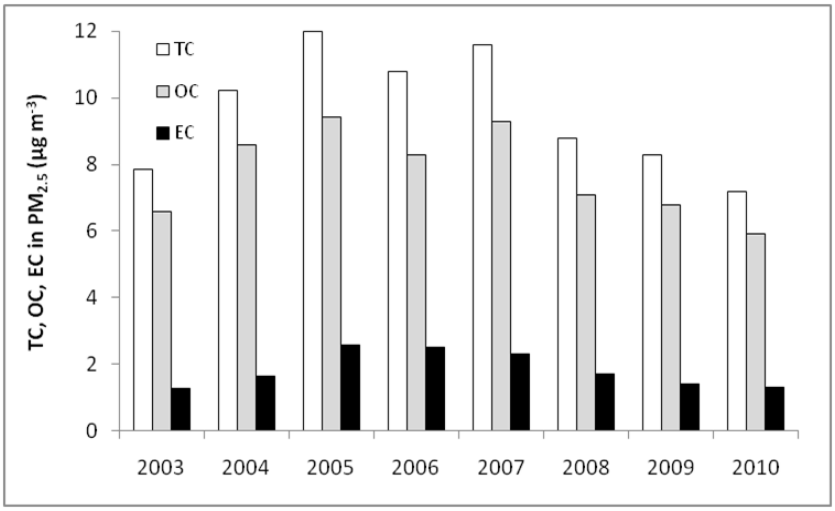

Figure 3.14: Annual mean concentrations of EC. OC and TC in $PM_{2.5}$ at the Italian site Ispra (IT0004R) for the period 2003–2010.

No stepwise up- or downward trend in the annual mean concentration of OC and EC in $PM_{2.5}$ is observed for the entire period 2003–2009 at Ispra. However, since 2005, i.e. the year thermal-optical analysis was introduced at Ispra, and until 2010, the annual mean EC concentration has decreased by a substantial 50%, with the greatest reductions taking place since 2007. The annual mean concentration of OC has a rather similar variation as seen for EC, and for the period 2005 until 2010 a nearly 40% decrease has been observed. It should be noted that the sampling approach has been changed during this period, i.e. a denuder has been introduced into the sampling train, which is likely to have caused a reduction in the observed OC level.

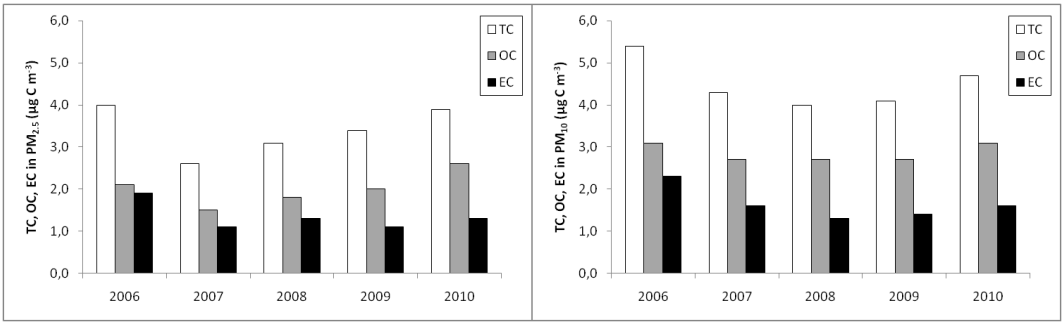

Figure 3.15: Annual mean concentrations of EC, OC and TC in $PM_{2.5}$ (left) and PM_{10} (right) at the German site Melpitz (DE0044R) for the period 2006 – 2010. Note that the data are obtained using the VDI 2465 Part 2 method, which do not correct for charring of OC.

The time series of EC, OC and TC at Melpitz goes back no more than 5 years. Given the uncertainty in the split point between EC and OC using the VDI 2465 Part 2 method, only the TC fraction will be addressed, although the EC and OC fractions both are included in Figure 3.15. For both size factions (here: $PM_{2.5}$ and PM_{10}) there is a substantial drop in the TC concentration from 2006 to 2007. For TC in $PM_{2.5}$ the concentration has steadily increased since the initial drop, and for 2010 the annual mean almost equals that of 2006, lacking 0.1 µg C/m^3, only. TC in PM_{10} decreased going from 2007 to 2008 as well, after which it increased for the two consecutive years. Unlike TC in $PM_{2.5}$, TC in PM_{10} has not equalled the annual mean TC value from 2006. Both TC in $PM_{2.5}$ and PM_{10} increased by 15% going from 2009 till 2010. From 2012 on, concentrations of EC and OC at Melpitz will be analyzed using thermal-optical analysis, thus it is unlikely that the time series presented in Figure 2.15 will be continued, at least for EC and OC. Concurrent measurements using the VDI 2465 Part 2 method and the new thermal-optical method will reveal whether the time series of TC can be continued.

3.2.4.1 Concluding remarks

The lack of a harmonized sampling- and analytical measurement protocol has been the main concern in our effort to establish a reliable picture of the regional distribution of the carbonaceous aerosol concentration within EMEP. For 2010, ten out of twelve sites reported levels of EC and OC using the EUSAAR2 thermal protocol, being an important step towards harmonized and comparable data for

EC and OC within EMEP. Only *one* site reported levels of EC and OC, which were not obtained by thermal-optical analysis, however, this site will take on thermal-optical analysis from 2012 on. Fully comparable data require that also the sampling protocol is harmonized, which is currently not the case. The final tests of the EUSAAR best affordable, "artefact-free" sampling train, is currently taking place within the EU funded project ACTRIS. Further, effort concerning how to handle samples which are impacted by carbonate carbon is currently also undertaken within ACTRIS. Guidelines for how to deal with such samples will be developed based on the results obtained in ACTRIS and will subsequently be added to the SOP for EC/OC.

The carbonaceous aerosol concentration was found to range by more than one order of magnitude within the European rural background environment. Elevated concentrations were observed in northern Italy and in Eastern Europe. Concentrations observed at sites in Scandinavia and at high altitude sites in western/south-western Europe, were substantially lower. Levels observed in the UK and in the Eastern Mediterranean should be considered intermediate. The spatial variation of the carbonaceous aerosol concentration for 2010 closely resembles that observed during the EMEP EC/OC Campaign conducted in 2002–2003 (Yttri et al., 2007).

Levels of EC were found to be increased during winter at most sites, reflecting increased emissions. e.g. from residential wood burning, as well as inversion, preventing dispersion of air pollution. Increased EC/TC ratios in winter show that EC was more pronounced in the carbonaceous aerosol in winter compared to summer. Increased summertime concentrations of OC were observed at most low and medium loading sites. Formation of secondary aerosol, both from anthropogenic and natural precursors, and primary biological aerosol particles, along with a low impact from anthropogenic OC are likely to explain the observed seasonal variation for the actual sites.

For two of the three sites with time series of EC and OC extending 5–10 years back in time, levels of EC and OC were found to be lower in 2010 compared to the year when the measurements were initiated.

3.3 Modelling of organic aerosol (OA): status and issues

By David Simpson and Robert Bergström

As of 2011, a so-called volatility basis set (VBS) approach (Robinson et al., 2007; Donahue et al., 2009) for secondary organic aerosol (SOA) has been added to the available defaults of the EMEP chemical code. This follows an extensive period of testing against observational data, with the conclusion that the adopted scheme is a reasonable first approach, suitable for policy purposes. It should be noted though that all VBS schemes (in fact, any SOA schemes) have many parameters which are not well known, and therefore we have been testing different versions of VBS schemes: this work has been described in detail in Bergström et al. (2012). We will not repeat the results of that study here, but rather wish to draw

attention to an issue which is of increasingly obvious importance – the quality and type of emissions inventory which are available.

Summarising results from a number of studies (e.g. Szidat et al., 2006; Gelencsér et al., 2007; Puxbaum et al., 2007; Simpson et al., 2007; Genberg et al., 2011; Gilardoni et al., 2011; Heal et al., 2011; Bergström et al., 2012; Denier van der Gon et al., 2012), it seems obvious that one can make the following points:

- In summertime, biogenic secondary organic aerosol (BSOA) is an important part of the total organic aerosol, and the BSOA concentration is completely dependent on emissions estimates of biogenic volatile organic compounds (BVOC).

- During the cold seasons, emissions from residential wood-combustion (RWC) are very important in large parts of Europe.

The problem is that BVOC and RWC emissions are two of the most uncertain inputs to any modelling exercise!

With regard to BVOC, the uncertainties have been discussed many times before (Simpson et al., 1995, 1999; Arneth et al., 2008), but little new data is appearing to help improve the inventories. Given that summertime SOA is a significant contributor to total OM and $PM_1/PM_{2.5}$ (and hence to both health and radiative forcing issues) there is a clear need for more measurements, so that more reliable inventories can be developed.

Problems with modelling the wood-burning component were identified in Simpson et al. (2007) for sites of the CARBOSOL network (Legrand and Puxbaum, 2007), but similar features have been found in subsequent studies (e.g. Genberg et al., 2011; Gilardoni et al., 2011; Bergström et al., 2012), usually with a suggestion that the available inventories are underpredicting wood-burning emissions. (In Norway, on the other hand, there are indications that the inventory is too high, Denier van der Gon et al., 2012.) As an illustration of the importance of RWC, Figure 3.16 shows the percentage contribution of RWC emissions to the total fine-mode organic matter, modelled for February 2008 with the EMEP VBS system (the NPAS version, discussed below). These calculations clearly show that RWC is important in many countries, sometimes accounting for more than 50% of the total fine OM. If the inventories are underpredicting RWC emissions as many studies suggest, this contribution could be much higher.

A further problem arises from the newly recognised issues surrounding the volatility of the emissions. Traditionally, emissions of primary organic aerosol (POA) and VOC were seen as very different, with POA being inert, and VOC volatile. However, Robinson et al. (2007) and subsequent papers (e.g. Donahue et al., 2009; Shrivastava et al., 2008) have made the point that the dividing line between particulate and gaseous emissions is to some extent arbitrary, since many compounds are semi-volatile (SVOC), and may be in the gas or condensed phase depending on local conditions; the partitioning will be very different in the high concentration high-temperature exhaust plume compared to the ambient air into which the plume dilutes. They also suggest that there is a class of compounds

(IVOC: intermediate volatility organic compounds) which is too volatile to be included in the PM inventory, and yet too heavy to be included in current VOC inventories.

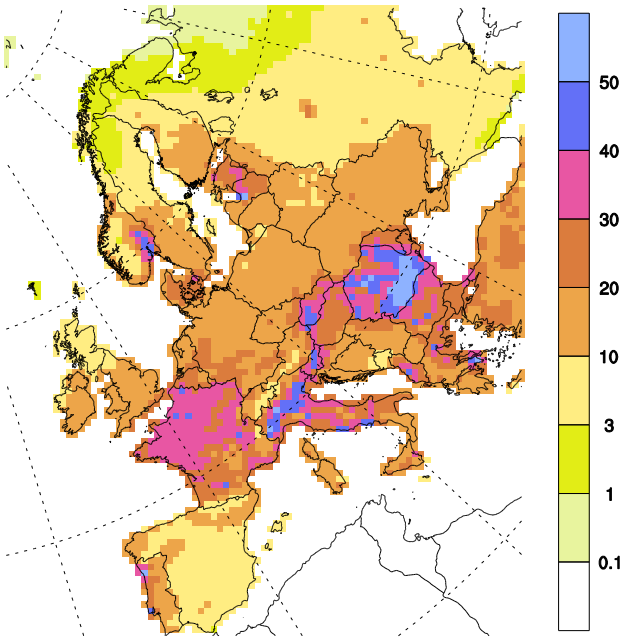

Figure 3.16: Percentage contribution of residential wood burning emissions to fine OA concentrations. Calculations for Feb., 2008. EMEP VBS (NPAS) model.

These compounds thus represent a pool of carbonaceous material from which OA can form, but which is not accounted for in current inventories. In the work of Shrivastava et al. (2008) the sum of true POA and these unaccounted-for S/IVOC compounds was estimated to be 2.5 times the official POA emission estimate. The research runs of Bergström et al. (2012) (and indeed those of e.g. Lane et al., 2008; Fountoukis et al., 2011) made use of similar assumptions. For the 'standard' EMEP model we have used a simpler scheme, the 'NPAS' scheme (**N**o **P**artitioning of POA, plus **A**ging of **S**OA). The NPAS scheme assumes that POA emissions can be treated as non-volatile, instead of treating them (and related emissions of SVOC and IVOC) as components of varying volatility.

As discussed more in Simpson et al. (2012) (revised version currently under review), there are two main reasons why we choose to use nonvolatile POA emissions in the 'standard' EMEP model code (that used for policy-associated runs): (1) The volatility distribution of POA and associated SVOC and IVOC compounds is poorly known; (2) For policy modelling it is necessary to keep these POA and VOC emission totals the same as in the official emission inventories. Model runs which make use of these extra SVOC+IVOC emissions produce OA amounts which are generally higher (up to 20%) than those with NPAS; however, in high-emission regions (within and close to large cities) the NPAS approach can give more OA than the partitioning model versions (e.g., more than 40% higher yearly average concentrations of fine OA in the Paris region with the NPAS model than with S/IVOC emissions).

In general, modelling of organic aerosol is subject to much larger problems than those of many other pollutants, something which inevitably follows from the complexity of OA itself, and our lack of understanding of the underlying science (e.g. Hallquist et al., 2009; Ng et al., 2010). It will not be possible to build or evaluate reliable SOA models though until the main model inputs, the emission inventories, are in good shape. We believe that the improvement of emission inventories for especially BVOC and POA (including RWC) should be priority areas of the modelling of OA is to be improved substantially.

4 EMEP and the Project ACTRIS - *Aerosols, Clouds, and Trace gases Research InfraStructure Network*: a Collaboration for Mutual Benefit

By Cathrine Lund Myhre, Paolo Laj, Gelsomina Pappalardo, André Prévôt, Wenche Aas

4.1 Background: From EUSAAR to ACTRIS

Collaboration and integration with other networks and frameworks working on monitoring of atmospheric constituents is an essential theme in the EMEP monitoring strategy (ECE/EB.AIR/GE.1/2009/15)[9]. One very valuable and good example of this is the collaboration and interaction with the EU 6th framework programme EUSAAR[10] over the period 2006-2011.

The synergy between EMEP and EUSAAR can be considered as a successful implementation of EMEP's strategy on collaboration between frameworks and networks. While receiving policy support for continued operation of a set of European supersites for aerosol research from EMEP, EUSAAR provided EMEP with needed standard operating procedures for aerosol parameters observed at level 2 EMEP sites improving and further developing the measurements considerably. Furthermore EUSAAR also contributed by setting up a public web-interface for the EMEP database, and an infrastructure for near-real-time data collection and dissemination. The EMEP status report 4/2011 (Fiebig et al., 2011) provides a more detailed overview of the key benefits provided by EUSAAR from an EMEP perspective. The main focus was on the optical and physical properties of aerosols but also development of reference method for EC/OC was a core activity in EUSAAR. The thermo-optical analysis using the defined EUSAAR-2 protocol (Cavalli et al., 2010). has been adapted as standard method for analysis of EC/OC within EMEP Work is currently in progress to finalize the standard operating procedure (SOP) of EC/OC measurements for subsequent inclusion to the EMEP manual. Furthermore, the EMEP manual will include guidelines improved in EUSAAR on measurements of physical and optical properties, and these will be based on the standard operation procedure outlined and summarised in the EMEP report last year (Fiebig et al., 2011). All this work for the definition of SOPs is also made in close collaboration with the Scientific Advisory Group on Aerosol of WMO.

There are considerable future challenges connected with the understanding of atmospheric change, and the effects of this. This includes the evolution and assessments of long-lived greenhouse gases (LLGHG) as well as the understanding of short-lived climate forcers (SLCF). SLCF includes aerosols and tropospheric ozone, and related gases as CO, NO_x, methane and volatile organic compounds (VOC). VOCs are key precursor gases for the formation of aerosols and tropospheric ozone. Furthermore, also the interaction between aerosols and clouds is largely uncertain. Both aerosols and several short-lived gases have adverse health effects influencing air quality. While EUSAAR focused solely on

[9] http://www.unece.org/fileadmin/DAM/env/documents/2009/EB/ge1/ece.eb.air.ge.1.2009.15.e.pdf
[10] EUSAAR: European Supersites for Atmospheric Aerosol Research, http://www.eusaar.net/. EUSAAR was an EU FP6 Integrated Infrastructures Initiative, ending March 2011.

aerosol *in situ* observations, this work will be continued in the larger follow-up project *Aerosols, Clouds, and Trace gases Research InfraStructure Network – ACTRIS* (http://www.actris.net) which started in 2011, funded by the EU 7th framework programme. This project includes a comprehensive set of atmospheric variables covering aerosol profiles, aerosol and trace gas *in situ* measurements, and cloud properties.

4.2 ACTRIS – Aerosols, Clouds, and Trace gases Research InfraStructure Network

There was recognition in the research community for the need of atmospheric supersites combining observations from a set of various measurement platforms and methods targeting aerosols, clouds and short-lived trace gases. A coordinated research infrastructure for these observations was lacking and ACTRIS (Aerosols, Clouds and Trace gases Research InfraStructure Network, http://www.actris.net/) aims to fill this observational gap (Pappalardo and Laj, 2012). ACTRIS builds a new research infrastructure on the basis of a consortium joining existing networks/observatories that are already providing consistent datasets of observations, and that are performed using state-of-the-art measurement technology and data processing. ACTRIS will be active for a period of 4 years, from 1st April 2011 to 31st March 2015. The project is coordinated by CNR (Italy) and CNRS (France) and has 29 partners. The ACTRIS consortium represents 24 European countries; and more than 60 sites are reporting ACTRIS labelled data.

The main objectives of ACTRIS are:

- To provide long-term **observational data relevant to climate and air quality research** on the regional scale produced with standardized or comparable procedures throughout the network: *ACTRIS' aim is to substantially increase the number of high-quality data accessible through the ACTRIS data centre with respect to 2010.*
- To provide a coordinated framework to support trans-national **access to large infrastructures,** strengthening high-quality collaboration in and outside the EU and access to **high-quality information and services** for the user communities (research, Environmental protection agencies, etc.). *ACTRIS aims to substantially increase the use of European advanced infrastructures for atmospheric research.*
- To develop **new integration tools** to fully exploit the use of multiple atmospheric techniques at ground-based stations, in particular for the calibration/validation/integration of satellite sensors and for the improvement of the parameterizations used in global and regional scale climate and air quality models. *ACTRIS aim is to provide time series of climate and air quality related variables not measured directly which are not presently available through the existing data centre.*
- To enhance training of new scientists and new users in particular students, young scientists, and scientists from eastern European and non-EU developing countries in the field of atmospheric observation. *ACTRIS aim is to provide training to more than 40 research personnel (Researchers/engineers/Post-doc and students) per year outside of the ACTRIS consortium.*
- To promote development of new technologies for atmospheric observation of aerosols, clouds and trace gases through close partnership with EU SMEs

(Small and Medium-sized enterprises). *ACTRIS aims, by the end of the project, to have contributed to more than 4 new operating standards for atmospheric monitoring.*

4.3 ACTRIS measurements and ACTRIS-EMEP interactions

ACTRIS is divided in 4 main data provision activities, and all measurements will be collected and available through a joint data centre. The map included in the upper panel in Figure 4.1, shows the sites included in ACTRIS (www.actris.net), and the distribution of the various types of observations; aerosol profiles, *in situ* trace gas and aerosol measurements, and measurements of cloud properties.

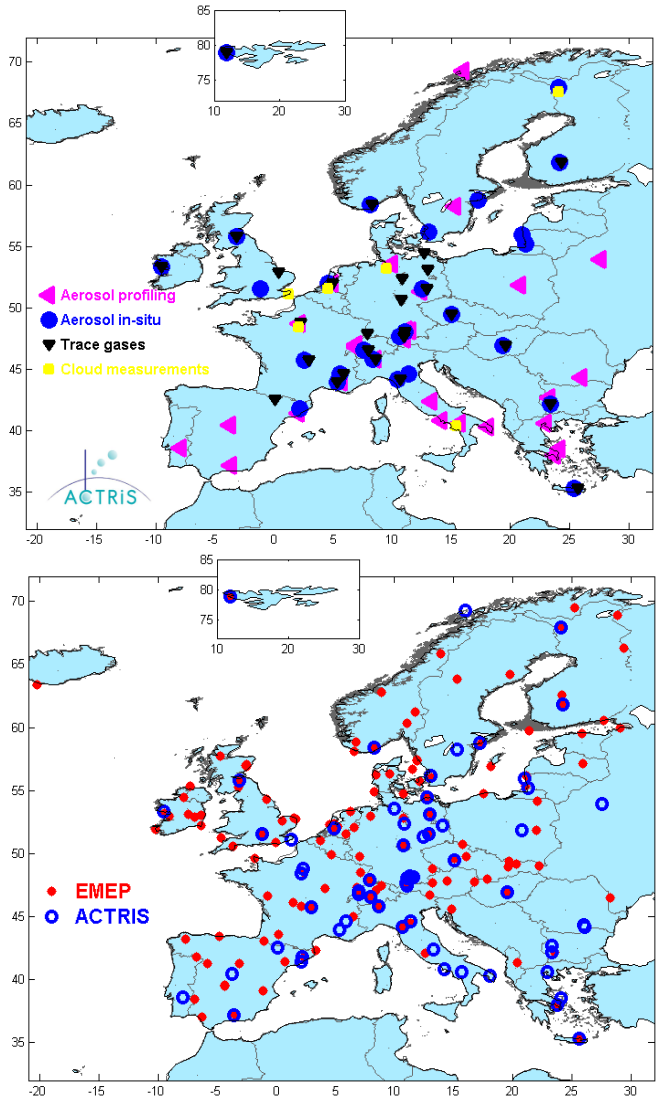

Figure 4.1: The upper panel shows the ACTRIS research infrastructure, and the distribution of various types atmospheric measurements. The lower panel shows the location of ACTRIS and EMEP sites.

ACTRIS is an infrastructure network and the research component of the existing measurement networks, EARLINET[11], EMEP, and Cloudnet[12]. Hence ACTRIS is contributing to further strengthening and developing these networks, and to the quality of their measurements. The map in the lower panel in Figure 4.1 shows the EMEP network reporting trace gas and/or aerosol measurements to EBAS by spring 2011 (the start of ACTRIS), together with the location of the ACTRIS sites. The ACTRIS sites performing aerosol *in situ* measurements were all a part of EUSAAR, and all these sites are EMEP level 2 sites. Additionally, several ACTRIS sites performing VOC measurements (not a part of EUSAAR, which focused solely on aerosol variables) are EMEP sites. ACTRIS sites not collocated with EMEP sites, are generally sites performing aerosol profiles, and a part of EARLINET.

[11] EARLINET: European Aerosol Research Lidar Network, http://www.earlinet.org/
[12] Cloudnet: http://www.cloud-net.org/

The existence of both the EMEP monitoring network, and of a research infrastructure for Aerosol, Cloud and Trace Gases such as ACTRIS clearly facilitates rapid mobilisation of atmospheric probing tools and skilled personnel at the pan-European scale. These unique tools are used in support of national or international projects or in case of emergency situations (atmospheric hazards). This organisation is unique, and was proven very efficient i.e. during the recent eruption of Grimsvotn in Iceland, also in co-operation with the EARLINET network.

The following sections summarise the 4 main measurement activities in ACTRIS, with focus on the aerosols activities, and the main relation and relevance to EMEP.

WP2: Remote sensing of vertical aerosol distribution

The main objective of this activity is to improve the observations of the vertical aerosol distribution by means of a network of advanced and coordinated lidar stations in such a way that the data they provide can be efficiently integrated with those contributed by other parts of the whole ACTRIS infrastructure. This activity is based on what is developed through the lidar network EARLINET (Pappalardo et al., 2008), and it is closely linked to this. A subset of EARLINET sites are actively involved in ACTRIS, and the improvement of methods and protocols developed within ACTRIS will be disseminated to the full EARLINET community. The core variables provided through this activity are aerosol back-scatter and extinction profiles, depolarization ratio (information about shape of the particles) and thickness and height of aerosol layer. All data are delivered to the EARLINET data base, but also available through the joint ACTRIS data portal http://actris.nilu.no/. Aerosol profile measurements are in included in the EMEP monitoring strategy9 (ECE/EB.AIR/GE.1/2009/15) as level 3 measurements, thus warranted as voluntary contributions to EMEP, and important for further progress. Within the EMEP program, level 3 observations shall contribute to the understanding of processes relevant for long-range transport of air pollutants and support model development and validation.

WP3: In-situ chemical, physical and optical properties of aerosols

The overall objective of this activity is to improve the observations of the *in situ* aerosol properties throughout a network of 23 stations in such a way that the data they provide can be efficiently integrated with those contributed by other parts of the whole ACTRIS infrastructure. The *in situ* aerosol network activities capitalize on and enhance the work initiated within the EUSAAR project. The core aerosol variables are chemical composition, optical properties (absorption and scattering coefficients), cloud condensation nuclei concentration, and particle size distribution. Except for cloud condensation nuclei, these are all level 2 measurements in EMEP, and therefore represent a core requirement of the EMEP monitoring network. Most of the ACTRIS sites involved in this activity are also reporting to EMEP, thus this activity is closely linked to EMEP and are expected to improve both the quality of and amount of data collected.

The following specific objectives are defined for this activity in ACTRIS:

- Ensure the implementation of the existing standardized protocols for high-quality-assured and – controlled aerosol number size distributions in the network and to develop procedures for its extension to the nucleation mode range
- Ensure the implementation of the existing standardized protocols of high-quality assured and – controlled aerosol measurements of scattering and absorption coefficients and the development of standardized procedures of spectral absorption measurements.
- Ensure the implementation of the existing harmonized protocols for sampling and analysis of organic/elemental carbon and to develop standardized protocols for sampling and quantification of organic tracers for source identification
- Develop standardized protocols for high-quality assured and - controlled measurements of cloud condensation nuclei.
- Ensure diffusion of information to data centres.

Also further development of near real time (NRT) observations is included, and this is central both for QA of the measurements as well as of high importance during specific events influencing the local and regional air quality e.g. heat waves, fires and volcanic eruptions. It is an important goal that the methods and protocols developed within the *in situ* aerosol activity in ACTRIS will be implemented by the EMEP network, following the successes of EUSAAR.

All data from this activity in ACTRIS will be delivered to the EMEP data base EBAS. The measurements will be public and openly available from EBAS, and also made available through the ACTRIS data portal http://actris.nilu.no/.

WP4: Trace gases networking: Volatile organic carbon and nitrogen oxides
The main objectives of this activity are

- To integrate and harmonise trace gas measurements in Europe, with the result of having a sustainable and reliable observation network for highly time-resolved data across Europe.
- To implement standardised measurement protocols (SOPs) and common European calibration scales for VOCs and NO_{xy} in support of the European EMEP and global GAW strategy and according to data quality objectives formulated by these initiatives.
- To create a protocol for merging the information of ground-based in-situ and remote sensing capacities in order to achieve more comprehensive distributions of VOCs and NO_{xy} in Europe.
- To foster the dissemination of the methods and quality assured data to scientific groups related to the analysis and modelling of air pollutants in Europe and to support EC directives relevant for air pollution and the CLRTAP abatement strategies.

The core variables resulting from this activity are a selection of VOCs and non-methane hydrocarbons (halocarbons, aldehydes, ketons, alcohols, terpenes ~30 components) and NO, NO_2 and NO_y (NO_y defined as NO, NO_2, NO_3, N_2O_5, HNO_2, HNO_3, PAN, organic nitrates and aerosol nitrates sum of oxidized nitrogen species with an oxidation number >1, both organic and inorganic). Development and implementation of standardised measurement protocols (SOPs) for these

compounds is highly needed in general, and also within EMEP. It is expected that this activity will improve the quality and amount of trace gas observations and data within EMEP, similar to the achievements during EUSAAR on the aerosol side.

All data from this activity in ACTRIS will be delivered to the EMEP data base EBAS. The measurements will be public and open and also made available through the ACTRIS data portal http://actris.nilu.no/.

WP5: Clouds and aerosol quality-controlled observations
This activity will focus on extending the scope of the FP5 EU project Cloudnet (http://www.cloud-net.org/) project to include new stations so that eight sites will have the capability to make continuous quality controlled observations of clouds and to include aerosols, all observations will have quantified errors and be available in near real time.

The core variables resulting from these measurements are cloud height and cloud thickness, and classification of liquid, ice or mixed phase clouds. The second stage is retrieval of cloud variables such as cloud fraction, cloud liquid water and ice water content held in operational models. None of these variables are included in the EMEP monitoring strategy, but the interaction between aerosols and clouds are central both for deposition and in the understanding of aerosols influence on climate in various ways, and also relevant for EMEP.

All data from this activity will be delivered to the Cloudnet data base, and also made available through the ACTRIS data portal http://actris.nilu.no/.

4.4 ACTRIS-EMEP Intensive Measurement Periods in 2012 and 2013

The EMEP intensive measurement periods (IMPs) are important supplements to the regular EMEP monitoring programme (UNECE, 2009b). The main purpose of these campaigns are to improve the spatial and temporal resolution of advanced measurements, which are highly needed to better understand transport and composition of atmospheric constituents. This is needed also for developing the chemical transport models such as the EMEP model. The first EMEP IMPs were held in June 2006 and January 2007 (Aas et al., 2012). It was quite clear from this first experience that EMEP needed to coordinate its efforts with research and infrastructure projects to get a better financial and scientific fundament, as well as improved harmonization of methodology and data reporting. The second IMPs in 2008 and 2009 were therefore coordinated together with the EUSAAR (Philippin et al., 2009) and EUCAARI (Kulmala et al., 2011) projects from the EU 6th Framework Programmes. A lesson learned from these previous IMPs is that having a close interaction between networks and research infrastructures (e.g. EMEP linked to ACTRIS) is an ideal structure to support research projects, both within EU frameworks and other initiatives. For the next periods, EMEP TFMM and ACTRIS have worked close together to plan and coordinate the IMPs for the summer 2012 and winter 2013. It was soon realised that other relevant projects were planning measurement campaigns in the same period(s), both ChArMEx (http://charmex.lsce.ipsl.fr/) and PEGASOS (http://pegasos.iceht.forth.gr/) projects. ACTRIS-EMEP joined forces with both ChArMEx and PEGASOS to support and complement these campaigns, for mutual benefit. The first

measurement period was set from 8 June to 17 July 2012. The following IMP will be arranged from 11 January to 8 February 2013.
There are several objectives and a large suit of measurements with extended measurements of aerosols and its precursors are conducted during these IMPs. There are both off and online instrumentation. Since there are few regional measurements of mineral dust in Europe, EMEP has a special focus on mineral dust in this IMP, and the chemical composition of $PM_{10.}$ Sampling with double quartz filters (QBQ) are done for determining the carbonaceous fraction, and several of these filters will be used for additional measurements to assess the importance of carbonate (done at JRC in Ispra); and for organic tracer analysis, coordinated by ACTRIS (Lund University). Regular EMEP measurements (i.e. filterpacks) are used for the inorganic fraction. A parallel PM_{10} sampler has been installed with Teflon® filters for mineral dust analysis, which will be done at one centralized laboratory, the INFN LABEC laboratory in Florence. An overview of the sites performing aerosol measurements during IMP is found in Table 4.1. In addition to EMEP and ACTRIS sites, ChArMEx has established new sites in the Mediterranean area, i.e. in Mallorca and Cape Corse.

Intensive measurements of VOC are also conducted during the IMPs, either with extended programme (parameters and/or frequency) of the regular measurements and/or additional instrumentation, like PTR-MS are installed at some sites. This work is coordinated by ACTRIS (DWD and EMPA).

To assess aerosol chemical composition and the sources/components for longer time periods, the Aerodyne™ Aerosol Chemical Speciation Monitors (ACSM) seems to be a very good tool, and ACTRIS have therefore decided to have a coordinated one year long term measurement campaign from June 2012 to May 2013 (prolonged on voluntary basis) at a number of sites; thus overlapping with the EMEO IMPs, see Table 4.1 and Figure 4.2. The red symbols in the map show the ACSM stations (and some AMS instruments) measuring full year, the yellow symbols are the stations only measuring during EMEP summer and winter campaign, the green and white symbols are stations only measuring during one of the EMEP IMPs, winter and summer campaigns, respectively. This ACSM campaign is coordinated by ACTRIS (PSI). Furthermore, the combination of the ACSM with the multi-wavelength light absorption measurements has been recommended to provide source apportionment of BC as well, and several of the sites have light absorption measurements in their regular monitoring programme, established during the EUSAAR project.

Table 4.1: Overview of the participating sites and what is planned for the joint EMEP/ACTRIS/ChArMEx intensive measurement period in 2012 and 2013.

Parties	Station		Online chemistry	VOC	PM_{10} speciation	OC tracers	Backscatter profiles	Extinction profiles
Armenia	AM0001	Amberd			Summer 2012			
Czech Rep	CZ0003	Košetice	ACSM (winter)	X				
Finland	FI0050	Hyytiälä	ACSM, Marga	GCMS		X		
Finland	FI0096	Pallas	Marga	GCFID				
Finland	FI0007	Virolahti	ACSM					
France	FI0009	Revin	AMS-TOF	Various on/off line	X	X		
France		OPE / Andra at Houdelaincourt			X			
France		Sirta	ACMS, Pils	PTRMS	X	X		
France	FR0030	Puy de Dome		Various on/off line PTRMS	X	X		
France		Cape Corse	ACSM, Pils	Various on/off line	X	X		
Germany	DE0044	Melpitz	ACSM; Marga		X			
Germany	DE0043	Hohenpeissenberg	ACSM	GCMS/GCFID	X			
Great Britain	GB0048	Auchencorth Moss	Q-AMS, Marga	X	X			
Greece	GR0002	Finokalia	ACSM		X			
Greece		Athens					X	X
Greece		Thessaloniki					X	X
Hungary	HU0002	K-puzta			X	X		
Ireland	IE0031	Mace Head	ACSM	GCMS	X			
Ireland		Cork					X	X
Italy	IT0001	Montelibretti			X			
Italy	IT0010	San Pietro Capofiume	HR-Tof-AMS		(not all comp)	X		
Italy		Ispra						
Italy		Potenza					X	X
Italy		L'Aquila					X	X
Italy (EC)	IT0004	Ispra			X	?	X	X
Latvia	LT0015	Preila						
Moldova	MD	Leova			Summer 2012			
Netherlands	NL0011	Cabauw	ACSM					
Norway	NO0001	Birkenes	ACSM	PTR-MS TOF	(not all comp.)	X		
Portugal		Evora					X	X
Slovakia	SK0006	Starina			X			
Spain	ES1778	Montseny	ACSM		X			
Spain		Palma de Mallorca			X			
Spain		Montsec			X			
Spain		Barcelona					X	X
Spain		Granada					X	X
Sweden	SE0011	Vavihill	HR-ToF-AMS	Tenax tubes	(not all comp.?)	X		
Sweden	SE0012	Aspvreten			X			
Switzerland	CH0001	Jungfraujoch	(TOF) ACSM	GCMS				
Switzerland	CH0002	Payerne	HR-TOF AMS		X			
19		**40**	**19**	**13**	**22**	**9**	**9**	**9**

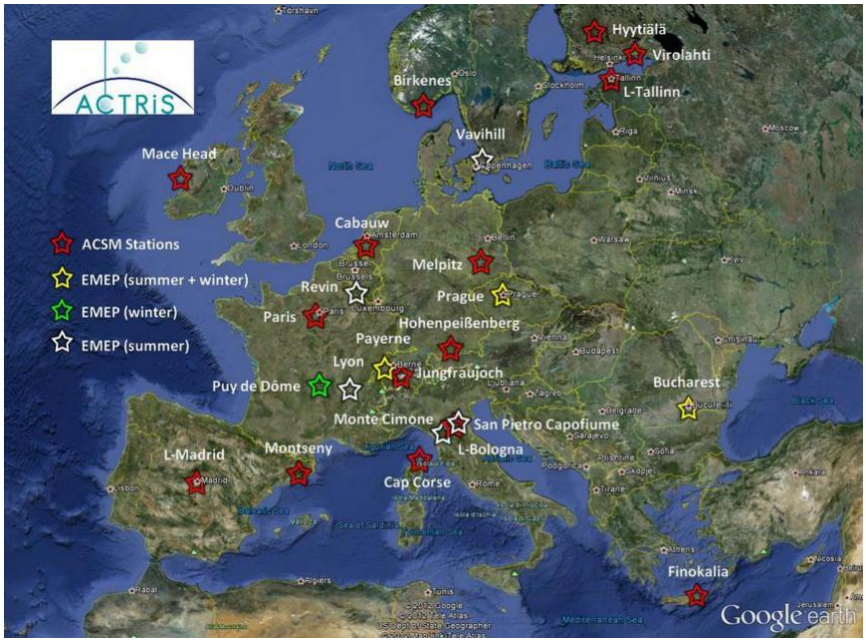

Figure 4.2: Overview over participating ACSM stations, from http://www.psi.ch/acsm-stations/acsm-and-emep-stations.

Also several lidar sites have the ambition to perform additional measurements during the EMEP/PEGASOS period. This is coordinated within ACTRIS (CNR). During June–July months, Saharan dust intrusions typically occur in Southern Europe, and lidar observations linking ground based measurements with lofted aerosol layers are particularly relevant. Additionally, biomass burnings are also typical of this season. EARLINET will perform regular measurements (17 measurements over the period for each site: 6 measurements are schedule during daytime and 11 in night time). Furthermore, additional measurements are foreseen for some specific EARLINET stations, taking into account the distance from EMEP/PEGASOS sites and the capability of the EARLINET stations to provide multi-wavelength extinction/backscatter profiles. The following stations agreed to perform additional measurements during the whole EMEP/PEGASOS campaign period: Athens (GR), Barcelona (ES), Cork (IE), Evora (PT), Granada (ES), Ispra (IT), L'Aquila (IT), Potenza (IT), Thessaloniki (ES). Barcelona, Ispra, L'Aquila, Athens are collocated with, or very close to, EMEP sites participating in the campaign, while Evora, Granada, Potenza, Thessaloniki are additional important stations for dust and burning events. Finally Cork could fill the gap related to UK where different EMEP stations will be operative during this campaign. These selected stations could perform additional measurements every day of the campaign adopting the EARLINET night-time measurements interval period, i.e. about 2 hours around the sunset.

The map in Figure 4.3 illustrates the distribution of all the sites participating in the joint campaign, and the various type of observations; aerosol *in situ* measurements: sites with PM_{10} speciation are shown as black circles, online chemistry sites (ACSM) are shown as red dots, and planned sites with organic tracer analysis are shown as green circles. Furthermore sites measuring trace gases

are shown as blue circles, and aerosol profile measurements (extinction and backscatter coefficient at most sites) are included as yellow crosses.

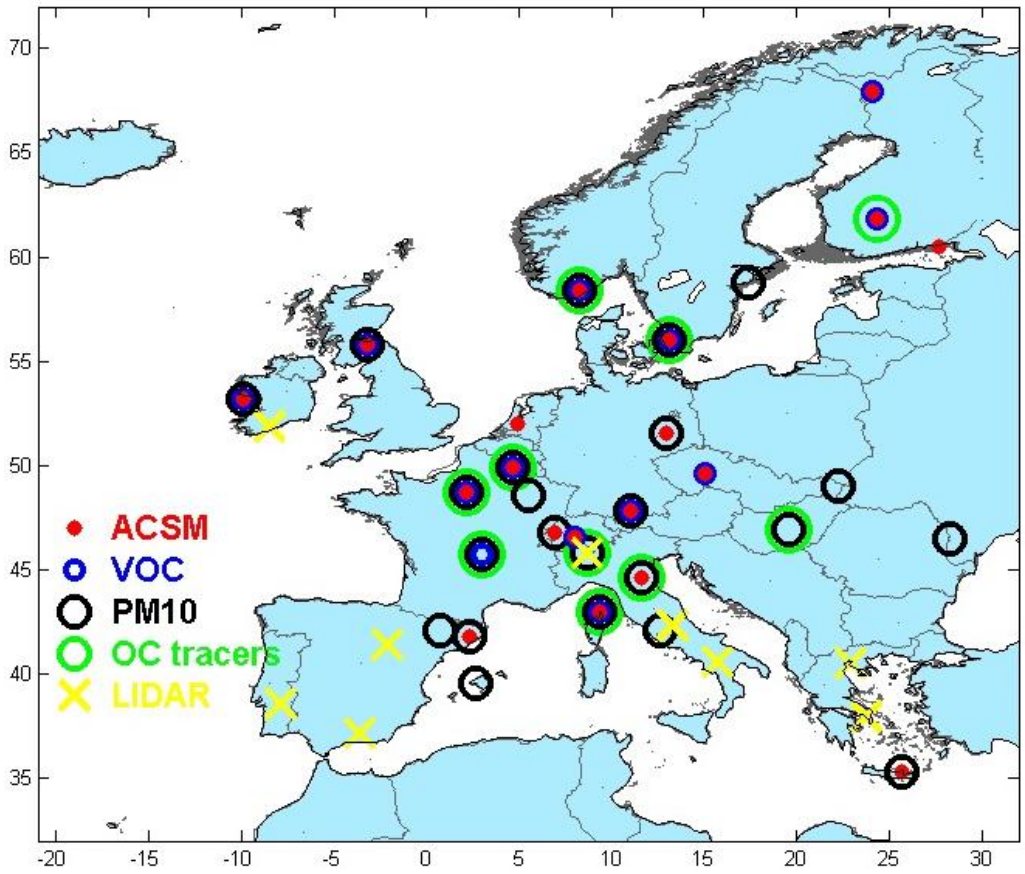

Figure 4.3: The distribution of all the sites participating in the campaign 2012 and 2013 and the various types of observations.

ACTRIS-EMEP Intensive Measurement Periods in the future

Later EMEP campaigns will be discussed and decided at TFMM, and it should be a goal to interact with ACTRIS and other EU research and infrastructure projects in the decision of the main focus of these. To facilitate interactions with ACTRIS and other EU infrastructure projects as InGOS (Integrated non-CO2 Greenhouse gas Observation System, http://www.ingos-infrastructure.eu/) at EMEP TFMM, the meetings should be announced for a broad community, with an outline of the topics to be discussed together with the invitation at an early stage.

5 Monitoring and modelling volcanic aerosols from the Eyjafjallajökull eruption

By Nina Iren Kristiansen and Svetlana Tsyro

5.1 Introduction

The eruption of the Eyjafjallajökull volcano in April and May 2010 released large amounts of volcanic ash and gases high into the atmosphere where it was transported long distances with the winds. Volcanic ash is small fragmented rock or glass particles and can lead to degradation of air quality via exceedances of air quality standards for particulate matter (PM). Volcanic ash also constitutes a serious threat to aviation. The ash was transported eastward and southwards to the European mainland in the days after the eruption onset and caused closure of airports all over Europe. 100,000 flights were canceled during the eruption period with over 10 million people affected.

5.2 Physical and chemical composition of volcanic aerosols

Volcanic ash consist mainly of silicate glass which is non-spherical, hard and sharp particles, and thus very abrasive. Ash can also transport toxic components such as fluoride, aluminium and arsenic. The density of the ash particles vary from 0.7 to 3.2 g/cm^3. During volcanic eruptions, vast amounts of sulphur dioxide (SO_2) can also be released, which during transport are transformed into sulphate particles. Sulphate particles are smaller in size than ash particles and have a typical density of ~1.5-1.8 g/cm^3.

The properties of the Eyjafjallajökull ash particles are described by Gislason et al. (2011) from samples collected during the eruption about 10-55 km from the volcano. The composition of the ash was dominated by andesitic glass with 57-58 mass % silica (SiO_2) content, thus the ash originated from trachy-andesitic magma (rather than basalt), and it contained very little quartz. The ash from the initial explosive phase of the eruption was significantly different from that of the later stage. The explosive ash was grey, soft, light and resembled the consistency of flour. This was a result of the explosive origin and the reaction between the glacial melt water and the magma which produced unusually large amounts of very fine ash (phreato-magmatic ash). At the later stages of the eruption, the ash was more typical with larger, black particles and the consistency of dry sand. The chemical composition of the ash particles observed over Europe (for example from the Jungfraujoch station as described by Bukowiecki et al., 2011) was very similar to the one found in these samples collected during the eruption close to the volcano.

5.3 Ground-based observations of volcanic aerosols

Besides monitoring volcanic ash clouds by satellite (Prata and Prata, 2012) and aircraft measurements (Schumann et al., 2011), ground-based observation networks for aerosol measurements can provide valuable information on the amount and distribution of volcanic ash in the atmosphere. Ground-based remote sensing from lidars and ceilometres can provide information about the vertical distribution of an aerosol layer like in a volcanic cloud. For an unambiguous

identification of volcanic clouds, in-situ measurements from ground-based stations, balloons and aircraft are of high value as it allows determining concentrations as well as the physical and chemical properties of the volcanic particles.

Several stations in the EMEP monitoring network and other measurement sites revealed time periods with volcanic aerosol impact in April and May 2010. In-situ measurements of volcanic clouds are typically confined to particle measurements and SO_2 concentrations in ambient air. Measurements from some selected *local*, *regional* and *remote* stations that detected volcanic components are described in the following. The positions of these stations are marked on Figure 5.4b.

5.4 Stations in the proximity of the eruption

The stations in the vicinity of the volcano were naturally affected strongly by the volcanic emissions. Thorsteinsson et al. (2012) report measurements of PM from several Icelandic stations. The Vík station is located only 38 km south-east of the volcano and on 7 May 2010 experienced 24 hour mean PM_{10} concentrations of 1230 µg/m^3 and 10 min average values over 13.000 µg/m^3 (Figure 5.1a) which is the highest ever measured in Iceland. This exceeded the air quality limit of 50 µg/m^3 (24 hours average) by several orders of magnitude.

Even after the volcanic activity had ceased, high PM concentrations were measured on several occasions, due to resuspended ash deposited during the eruption. Reykjavik, 125 km west-northwest of the volcano, was never hit directly by the eruption plume, but on 4 June an ash storm with resuspended ash reduced the visibility and measured PM_{10} concentrations reached over 2000 µg/m^3 (10 min average) (Figure 5.1b). A similar event occurred in Reykjavik on 7 September 2010 with peak values of 535 µg/m^3 (30 min average).

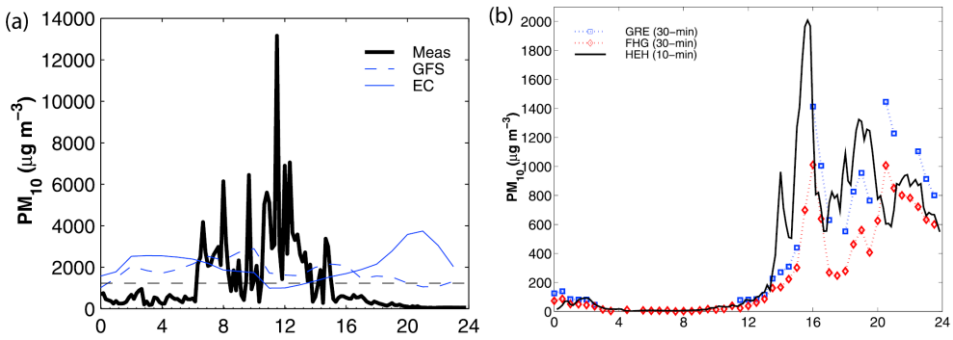

Figure 5.1: Measured PM_{10} concentrations (black lines) a) at Vík (38 km south-east of Eyjafjallajökull) on 7 May 2010. The 24 hour average PM_{10} concentration is shown with a dashed grey line. FLEXPART modelled concentrations of PM_{10} due to direct volcanic emissions are shown by blue lines (using GFS and ECMWF meteorological data), and b) at three stations near Reykjavik on 4 June 2010 when resuspended ash caused an ash storm. From Thorsteinsson et al., J. Geophys. Res. (2012).

5.4.1 Stations located in south-western Europe

The Mace Head Atmospheric Research Station on the West coast of Ireland is located about 1200 km south-southeast of the volcano and detected the volcanic plume numerous times during the eruption period. The three strongest events occurred on 20 April, 4-5 May and 17 May 2010 and are analysed in detail by O'Dowd et al. (2012). On 20 April 2010 the edge of the plume passed over Mace Head as a thin layer at 4 km altitude which subsided into the boundary layer. $PM_{2.5}$ mass concentrations increased to ~9.1 μg/m^3. The ash plume signature was confirmed by a simultaneous moderate increase in nss-sulphate mass while nitrate and organic aerosol mass remained low. The second major plume interaction on 4-5 May 2010 was connected with an almost direct flow between Iceland and Ireland/UK and the western edge of the ash plume was located over Mace Head. Three thin layers at 1, 2.5 and 3.5 km altitude were observed, total $PM_{2.5}$ increased to >10.4 μg/m^3 concomitant with a large increase in nss-sulphate aerosols without any elevation in organic or nitrate aerosol mass. The third strong event on 17 May 2010 was similar to the first event with the edge of the volcanic plume reaching the station as a thin aerosol layer at 4 km altitude descending towards the boundary layer. The highest nss-sulphate loading and the longest in duration was measured during this event. The 24-hour average PM_{10} mass was 11.45 μg/m^3 of which 33% was nss-sulphate, 39% ash and 28 % sea-salt. For $PM_{2.5}$ the average mass was 5.03 μg/m^3 of which 64% was nss-sulphate, 30% ash and 7% sea-salt.

The Eyjafjallajökull ash plume that passed over Central Europe from 16 to 26 April 2010 was observed by several stations. Figure 5.2 shows the time series of PM_{10} and SO_2 measurements at five stations in the north Alpine region (Augsburg, Innsbruck, Schauinsland, Hohenpeissenberg and Zugspitze/ Schneefernerhaus) over several days in April as presented by Schäfer et al., (2011). All stations experienced enhanced PM_{10} and SO_2 concentrations from 17 April 2010. At Schauinsland (SSL) elevated PM_{10} concentrations up to 140 μg/m^3 were observed on 17 April 2010, parallel to an increase in SO_2 concentrations. Hohenpeissenberg (HPB) observed that PM_{10} concentrations increased from 20 μg/m^3 to 40 μg/m^3 (peaks about 50 μg/m^3) on 17 April 2010 and remained elevated till 23 April 2010. Also there, the simultaneous increase in SO_2 and sulphuric acid (H_2SO_4) concentrations confirmed the presence of compounds of volcanic origin. The measured H_2SO_4 concentrations were also well above the maximum levels ever observed in April since measurements started 1998 (Flentje et al., 2010). For the measurements at Augsburg, Pitz et al. (2011) estimated that at the volcanic ash contribution to the overall PM_{10} load was on average 30 % (12 μg/m^3) for the days 17-22 April. At a single time on 19 April the maximum contribution was around 65 % (35 μg/m^3).

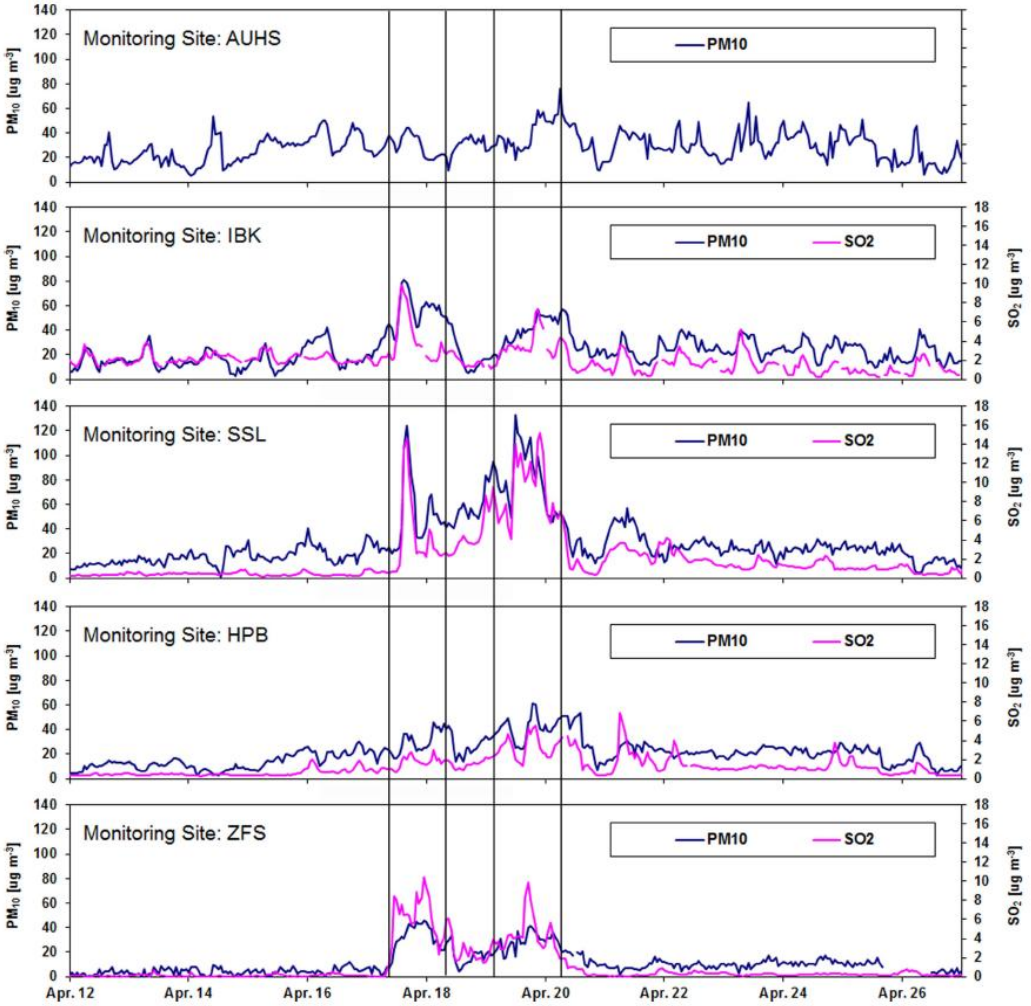

Figure 5.2: Time series of PM_{10} and SO_2 (hourly mean data) concentrations at five measurement sites Augsburg (AUHS), Innsbruck (IBK), Schauinsland (SSL), Hohenpeissenberg (HPB) and Zugspitze/ Schneefernerhaus (ZSF) in the time period from 12 April to 27 April. The two main entrainment events of the volcanic plume are marked. Note that PM_{10} and SO_2 show a strongly correlated evolution at all measurement sites. From Schäfer et al., ACP (2011).

5.4.2 Continental and distant stations

The high Alpine research station Jungfraujoch was clearly influenced by the volcanic aerosol cloud during two episodes in April and May 2010. The site did not encounter the same strong influence as compared to other sites in Europe due to its remote, elevated location and a distance of more than 2500 km from the volcano. From 17-19 April and 18-19 May 2010 simultaneous increases in PM_{10} and SO_2 concentrations indicated the presence of volcanic aerosol clouds. The study by Bukowiecki et al. (2011) presents a thorough analysis of these measurements. For the April event, the aerosol clouds were not transported directly to the station and only the diluted edge of the volcanic plume reached the station. Therefore, the measured PM_{10} concentrations were rather low reaching a maximum of 30 µg/m^3 on 18 April 2010 (Figure 5.3a). These values are in line

with the results from Hohenpeissenberg presented by Schäfer et al. (2011). For the May event, the eruption and transport characteristics were different than in April and both the SO_2 and PM_{10} concentrations exceeded those measured in April (Figure 5.3b). A maximum PM_{10} concentration of 70 µg/m^3 was measured on 18 May 2010.

The measured volume distribution exhibited a clear bimodality with peaks at 0.5 µm (accumulation mode) and 3 µm (ash mode) for both the April and May events. The first peak is associated with secondary aerosols (e.g. sulphate) and the latter ascribed to volcanic ash. The retrieved particle size distributions suggested that most of the particles larger than 10 µm had fallen out when the ash cloud reached the Swiss Alps.

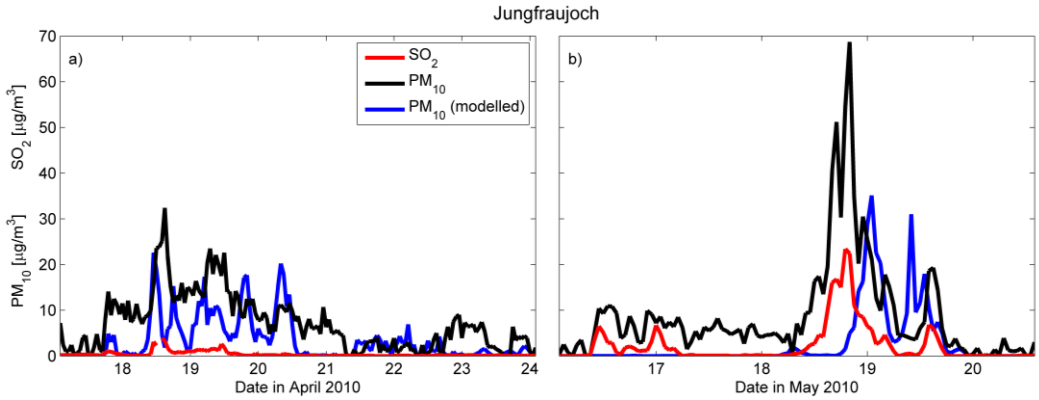

Figure 5.3: Measured SO_2 concentrations (red lines), PM_{10} concentrations (black lines) and modelled PM_{10} concentrations from the FLEXPART model (blue lines) at the Jungfraujoch station (46.55°N, 7.99°E, 3580 m a.s.l.) for a) 17–23 April 2010 and b) 16–20 May 2010. Measured values are 10-min averages while modelled values are hourly averages.

Volcanic aerosols resulting from this eruption were also detected in Lecce (Southeastern Italy) from 20 to 22 April 2010, at a distance of approximately 3500 km from the volcano. Perrone et al. (2012) show that the volcanic ash over Italy was strongly diluted but enhanced PM_{10} and SO_2 concentrations were found all over a 400 km long area of Southern Italy on 20-21 April 2010. At Lecce, the estimated enhancement of PM_{10} from volcanic particles was ~6 µg/m^3 on 21 April 2010.

5.5 Modelling of volcanic aerosol clouds

The official forecasts of the transport of the volcanic emissions are provided through the Volcanic Ash Advisory Centers (VAAC) of which the London VAAC has the responsibility for eruptions in the Icelandic region. During the Eyjafjallajökull eruption, other national Met Offices and many other research institutes also made forecasts of the transport of the volcanic ash clouds over Europe.

The modeling of volcanic eruption clouds relies on the meteorological fields that drive the models, the source emissions estimates used in the model, and the models' descriptions of physical processes (e.g. parameterizations of wet and dry deposition). All these issues make quantifying the uncertainties in the model forecast challenging. For the source emissions estimates, both the temporal and vertical variations in the ash emission rates are important for providing accurate forecasts of ash concentrations. Direct observations of the emission rates are almost impossible and modelers must rely on crude estimates, or use inversion techniques that indirectly constrain the models with observations.

The EMEP/MSC-W chemical transport model was shortly after the start of the Eyjafjallajökull eruption, adapted for calculating volcanic PM by implementing a first provisional scheme. In the following year, the volcano module was further developed and improved. Calculations of volcanic SO_2 and ash pollution have been included in the operational version of the model. The default emission parameters for volcanic ash are based on Mastin et al. (2009) and Mastin et al. (2010). The volcanic emission module was extended for emergency simulations of volcanic eruptions. Also, specific emission parameters can be given for the study of historical eruptions, such as the Eyjafjallajökull eruption. Emissions of SO_2, $PM_{2.5}$ and PM_{10} from the Eyjafjallajökull eruption in April-May 2010 were reported to EMEP/CEIP by Iceland this year. Those emissions were used in the EMEP/MSC-W model simulations this year. Maximum plume heights were taken from reports by the London VAAC (http://www.metoffice.gov.uk/aviation/vaac/), and the temporal variation of emission was based on expert estimates (Pfeffer M. A., UiO, personal communications). Further descriptions of the model set-up can be found on https://wiki.met.no/emep/emep_volcano_plume.

The FLEXPART model is a Lagrangian particle dispersion model that was used to simulate the transport of volcanic ash particles from the Eyjafjallajökull eruption. These simulations used ash emissions constrained by satellite observations using inverse modelling as described by Stohl et al. (2011). Some results from the volcanic ash transport calculations from the both the EMEP/MSC-W and FLEXPART models and the effect of PM levels are presented here.

Model calculated concentrations of PM_{10} using both the EMEP/MSC-W and FLEXPART models are shown in Figure 5.4. Both models are driven with ECMWF meteorology. On 17 May at 5 km height, the ash particles were dispersed across Europe and a dense ash plume was located over the United Kingdom and the North Sea. On this day, several monitoring sites and research aircraft (e.g. Schumann et al., 2011) observed the ash cloud. The notable differences in the two model simulations in Figure 5.4 are mainly due to the different emissions used in the two models, differences in the horizontal and

vertical resolutions of the models, and their descriptions of wet and dry deposition processes.

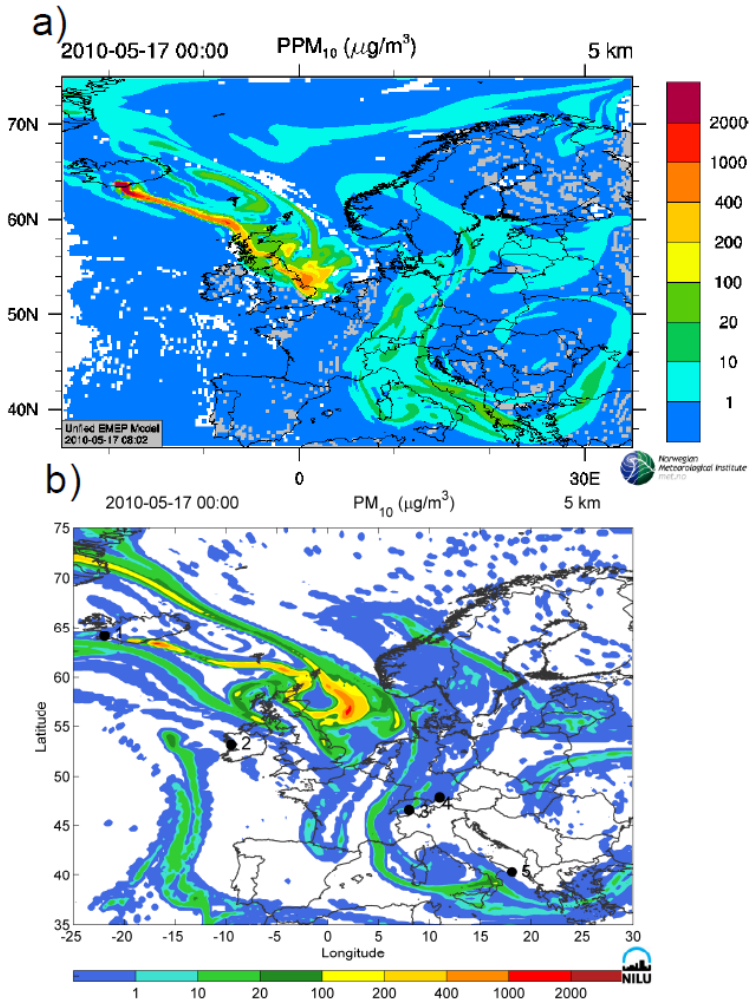

Figure 5.4: Modelled PM_{10} concentrations on 17 May 2010 at 00 UTC from a) the EMEP/MSC-W model and b) the FLEXPART model, and coordinates for ground-based stations (1: Reykjavik, 2: Mace Head, 3: Jungfraujoch, 3: Hohenpeissenberg, 5: Lecce).

5.5.1 Comparison of modelled and observed PM_{10} concentrations

Comparison of calculated PM_{10} concentrations using the FLEXPART model with measured PM_{10} concentrations from the Vík station on 7 May 2010 are presented in Figure 5.1 (thin blue lines using two different meteorological data, ECMWF and GFS, for driving the model). The model correctly simulates the ash plume travelling directly over Vík with elevated PM_{10} concentrations, but clearly underpredicts the measured concentrations. This is mostly due to the resolution of the model and emissions which is not sufficient to capture the high spatiotemporal variability of measured ash concentrations in the vicinity of the volcano. Further, resuspension of ash is not treated in the model and will cause further discrepancies between modeled and measured ash concentrations.

Measured PM_{10} concentrations for the Jungfraujoch station during April and May 2010 are shown in Figure 5.3. Also the PM_{10} concentrations as modelled by FLEXPART are shown. In general, FLEXPART models similar ash concentrations peaks as observed at the station. For the May event (Figure 5.3b), the model produces an ash signal over Jungfraujoch but while the magnitude of the observed PM_{10} concentration peak is simulated quite well, there is a time delay of roughly 12 hours between the measured and modelled peaks indicating that the modelled transport is too slow toward the Alps.

Similarly, Figure 5.5 shows the measured time-series at Jungfraujoch and EMEP/MSC-W modelled PM_{10}, SO_2 and volcanic ash in PM_{10}. The EMEP/MSC-W model captures well the episode of high PM_{10} on 19 April, though predicting PM_{10} larger than observed. The volcanic ash time-series reveals that more than half of the calculated PM_{10} is due to volcanic ash pollution. Also SO_2 concentrations are enhanced. During the second episode 18-19 May, the PM_{10} peak is larger in the model, and the modelled peak of PM_{10} daily concentrations is one day behind the observations, indicating slightly later calculated arrival of the volcano plume to the site as compared to observations. This was also seen for the FLEXPART model (Figure 5.3). It is typical that model errors and uncertainty increase with distance from the emission source and for simulations over complex terrain such as over the Alps.

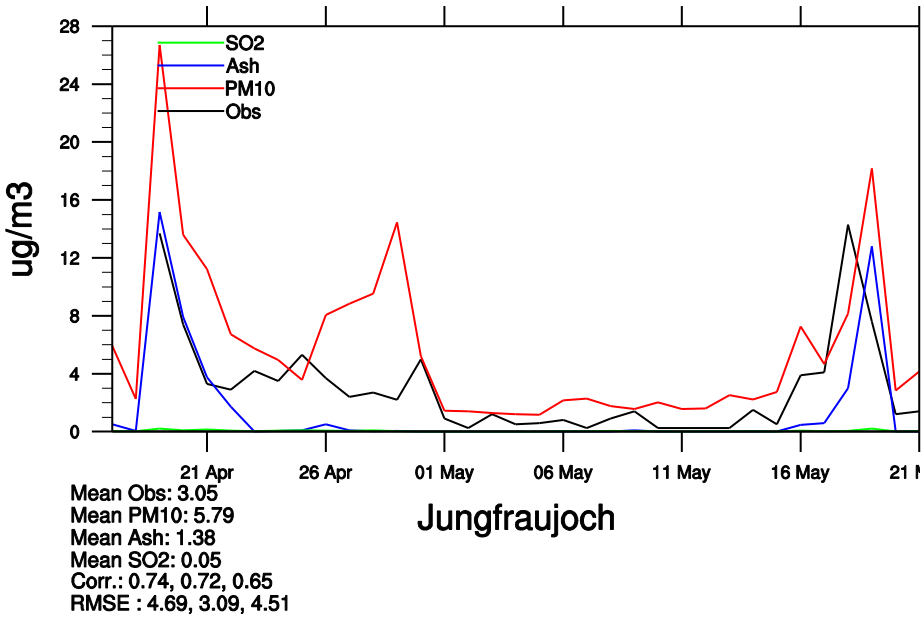

Figure 5.5: Daily time-series of measured PM_{10} and calculated with the EMEP/MSC-W model concentrations of PM_{10}, SO_2 and volcanic ash in PM_{10} at Jungfraujoch in April-May 2010.

As described above, the Eyjafjallajökull ash plume passed over Central Europe in the period 16 to 26 April 2010. Figure 5.6 shows EMEP/MSC-W model calculated ash clouds on 17, 19 and 24 April, whereas Figure 5.7 shows daily time-series of observed PM_{10} and calculated PM_{10} and volcanic ash at British and German sites.

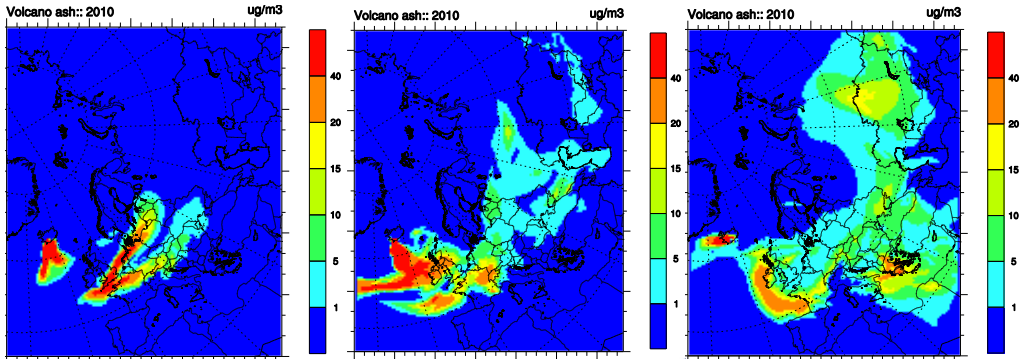

Figure 5.6: Concentrations of volcanic ash with particle size within 10 μm, calculated with the EMEP/MSC-W model for: 17 (left), 19 (middle) and 24 (right) April 2010.

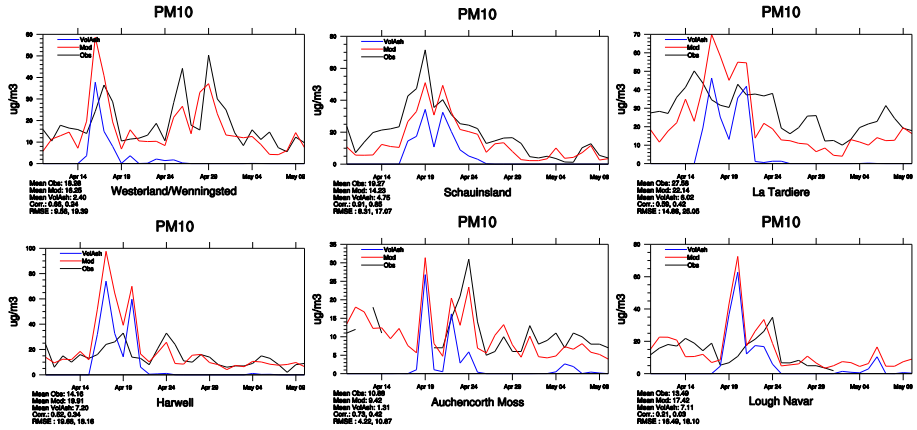

Figure 5.7: Daily time-series of measured PM_{10} and calculated with the EMEP/MSC-W model concentrations of PM_{10} and volcanic ash in PM_{10} at: upper panel - Westerland (DE0001), Schauinsland (DE0003), La Tardière (FR0015), lower panel - Harwell (GB0036), Auchencorth Moss (GB0048) and Lough Navar (GB0006) in April-May 2010.

The episode registered 16-18 April at German sites, related to volcanic pollution, is quite well calculated by the model, though calculated plume arrives a day too early than observed to Westerland site. The ash cloud, traversing northern Germany 17 April is clearly seen in Figure 5.7. On April 19, south-western parts of Germany were mostly influenced by the volcanic ash, which was observed and calculated at Schauinsland. Enhanced PM_{10} due to volcanic ash are calculated for the French site La Tardiere for 16-22 April and corresponds with observations, though measured PM_{10} started to increase 1-2 days earlier and was somewhat lower than calculated.

For the British sites, the model reproduces the occurrence of volcanic ash episode in the northern parts of England and Ireland (Auchencorth Moss and Lough Navar) during 22-24 April, but it underestimated observed PM_{10}. On the other hand, the time-series for British sites reveal that the calculated strong volcanic

cloud over southern England on 17 April and then over central-northern parts of England and Ireland on 19 April is not confirmed by observations.

Summarizing briefly, the models were able to reproduce the occurrence of most of pollution episodes associated with emissions from the Eyjafjallajökull eruption in April-May 2010. However, the levels of PM_{10} concentrations are not always calculated accurately, and in some cases model calculated episodes (or concentration peaks) are slightly shifted in time compared to observations. There are also cases when modelled volcanic ash episodes are not found in observational data, or oppositely. Good quality of meteorological input is crucial for the transport model to correctly predict the direction and speed of ash cloud propagation. Also, good estimates of volcanic emissions are important for accurate modelling of the effects of volcanic eruption clouds on air pollution.

6 References

Aas, W., Tsyro, S., Bieber, E., Bergström, R., Ceburnis, D., Ellermann, T., Fagerli, H., Frölich, M., Gehrig, R., Makkonen, U., Nemitz, E., Otjes, R., Perez, N., Perrino, C., Prévôt, A.S.H., Putaud, J.-P., Simpson, D., Spindler, G., Vana, M., Yttri, K. E. (2012) Lessons learnt from the first EMEP intensive measurement periods. *Atmos. Chem. Phys. Discuss., 12*, 3731-3780, doi:10.5194/acpd-12-3731-2012.

Amann, M., Bertok, I., Borken-Kleefeld, J., Cofala, J., Heyes, Ch., Höglund-Isaksson, L., Klimont, Z., Rafaj, P., Schöpp, W., Wagner, W. (2011a) An updated set of scenarios of cost-effective emission reductions for the revision of the Gothenburg Protocol; Background paper for the 49th Session of the Working Group on Strategies and Review. Geneva, September 12-15, 2011. Laxenburg, Centre for Integrated Assessment Modelling (CIAM), International Institute for Applied Systems Analysis (IIASA). (CIAM report 4/2011).

Amann, M., Bertok, I., Borken-Kleefeld, J., Cofala, J., Heyes, C., Höglund-Isaksson, L., Klimont, Z., Nguyen, B., Posch, M., Rafaj, P., Sandler, R., Schöpp, W., Wagner, F., Winiwarter, W. (2011b) Cost-effective control of air quality and greenhouse gases in Europe: modeling and policy applications. *Environ. Model. Software*, *26*, 1489–1501.

Amann, M., Bertok, I., Borken-Kleefeld, J., Cofala, J., Heyes, Ch., Höglund-Isaksson, L., Klimont, Z., Rafaj, P., Schöpp, W., Wagner, W. (2012) Environmental improvements of the revision of the Gothenburg Protocol. Laxenburg, Centre for Integrated Assessment Modelling (CIAM), International Institute for Applied Systems Analysis (IIASA). (CIAM report 1/2012).

Arneth, A., Monson, R.K., Schurgers, G., Niinemets, Palmer, P.I. (2008) Why are estimates of global terrestrial isoprene emissions so similar (and why is this not so for monoterpenes)? *Atmos. Chem. Phys., 8*, 4605-4620, doi:10.5194/acp-8-4605-2008.

Barmpadimos, I., Keller, J., Oderbolz, D., Hueglin, C., Prevot, A.S.H. (2012) One decade of parallel fine ($PM_{2.5}$) and coarse (PM_{10}–$PM_{2.5}$) particulate matter measurements in Europe: trends and variability. *Atmos. Chem. Phys., 12*, 3189–3203, doi:10.5194/acp-12-3189-2012.

Bergström, R., Denier van der Gon, H., Prevot, A., Yttri, K., Simpson, D. (2012) Modelling of organic aerosols over Europe (2002-2007) using a volatility basis set (VBS) framework with application of different assumptions regarding the formation of secondary organic aerosol. *Atmos. Chem. Phys. Discuss., 12*, 5425–5485, doi:10.5194/acpd-12-5425-2012.

Bukowiecki, N., Zieger, P., Weingartner, E., Jurányi, Z., Gysel, M., Neininger, B., Schneider, B., Hueglin, C., Ulrich, A., Wichser, A., Henne, S., Brunner, D., Kaegi, R., Schwikowski, M., Tobler, L., Wienhold, F. G., Engel, I., Buchmann, B., Peter, T., Baltensperger, U. (2011) Ground-based and airborne in-situ measurements of the Eyjafjallajökull volcanic aerosol plume in Switzerland in spring 2010. *Atmos. Chem. Phys., 11*, 10011-10030, doi:10.5194/acp-11-10011-2011.

Cavalli, F., Viana, M., Yttri, K.E., Genberg, J., Putaud, J.-P. (2010) Toward a standardised thermal-optical protocol for measuring atmospheric organic and elemental carbon: the EUSAAR protocol. *Atmos. Meas. Tech., 3*, 79-89. doi:10.5194/amt-3-79-2010

Denier van der Gon, H., Visschedijk, A., Pandis, S., Fountoukis, C., Bergström, R., Simpson, D., Johansson, C. (2012) Particulate emissions from residential wood combustion in Europe - revised estimates and an evaluation. In prep.

Donahue, N.M., Robinson, A.L., Pandis, S.N. (2009) Atmospheric organic particulate matter: From smoke to secondary organic aerosol. *Atmos. Environ., 43*, 94–106, doi:10.1016/j.atmosenv.2008.09.055.

EEA (2009) Proposed gap-filling procedure for the European Community LRTAP Convention emission inventory. Technical paper for the meeting of the Air and Fuels Committee under Directive 96/62/EC, concerning 'Information on the Member States' reporting under the National Emission Ceilings Directive 2001/81/EC'. 28 September 2009, Brussels. European Environment Agency. Available upon request.

Elbir, T. (2003) Comparison of model predictions with the data of an urban air quality monitoring network in Izmir, Turkey. *Atmos. Environ., 37*, 2149-2157.

EMEP (2012) Transboundary acidification, eutrophication and ground level ozone in Europe in 2009. Oslo, Norwegian Meteorological Institute (EMEP MSC-W & CCC & CEIP Status Report 1/2012).

EMEP/EEA (2009) EMEP/EEA Air pollutant emission inventory guidebook 2009. Copenhagen, European Environment Agency (EEA technical report, 9/2009). **URL**: http://www.eea.europa.eu/publications/emep-eea-emission-inventory-guidebook-2009 [07.08.2012]

EMEP/EEA (2011) Inventory review 2011. Review of emission data reported under the LRTAP Convention and NEC Directive. Stage 1 and 2 review. Review of emission inventories from shipping. Status of gridded and LPS data. By Mareckova K., Wankmueller, R., Murrels, T., Walker, H., Tista, M. Vienna, Umweltbundesamt (Technical report CEIP 1/2011).

EMEP/EEA (2012) Inventory review 2012. Vienna, Umweltbundesamt (in preparation). **URL:** http://www.ceip.at/review-of-inventories/review-2012/ [07.08.2012]

Fiebig, M., Laj, P., Wiedensohler, A., Fjæraa, A.M. (2011) EMEP and the project EUropean Supersites for Atmospheric Aerosol Research (EUSAAR): a collaboration for mutual benefit. In: *Transboundary particulate matter in Europe*. Kjeller, NILU - Norwegian Institute for Air Research (EMEP status report 4/2011), pp. 62-72.

Flentje, H., Claude, H., Elste, T., Gilge, S., Köhler, U., Plass-Dülmer, C., Steinbrecht, W., Thomas, W., Werner, A., Fricke, W. (2011) The Eyjafjallajökull eruption in April 2010 – detection of volcanic plume using in-situ measurements, ozone sondes and lidar-ceilometer profiles. *Atmos. Chem. Phys., 10*, 10085-10092, doi:10.5194/acp-10-10085-2010.

Fountoukis, C., Racherla, P.N., Denier van der Gon, H.A.C., Polymeneas, P., Haralabidis, P.E., Wiedensohler, A., Pilinis, C., Pandis, S.N. (2011) Evaluation of a three-dimensional chemical transport model (PMCAMx) in the European domain during the EUCAARI May 2008 campaign. *Atmos. Chem. Phys, 11*, 10 331–10 347, doi:10.5194/acp-11-10331-2011.

Gelencser, A., May, B., Simpson, D., Sanchez-Ochoa, A., Kasper-Giebl, A., Puxbaum, H., Caseiro, A., Pio, C., Legrand, M. (2007) Source apportionment of $PM_{2.5}$ organic aerosol over Europe: primary/secondary, natural/anthropogenic, fossil/biogenic origin. *J. Geophys. Res., 112*, D23S04, doi:10.1029/2006JD008094.

Genberg, J., Hyder, M., Stenström, K., Bergström, R., Simpson, D., Fors, E. O., Jönsson, J.Å., Swietlicki, E. (2011) Source apportionment of carbonaceous aerosol in southern Sweden. *Atmos. Chem. Phys., 11*, 11387-11400, doi:10.5194/acp-11-11387-2011.

Gilardoni, S., Vignati, E., Cavalli, F., Putaud, J.P., Larsen, B.R., Karl, M., Stenström, K., Genberg, J., Henne, S., Dentener, F. (2011) Better constraints on sources of carbonaceous aerosols using a combined ^{14}C – macro tracer analysis in a European rural background site. *Atmos. Chem. Phys., 11*, 5685–5700, doi:10.5194/acp-11-5685-2011.

Gíslason, S.R., Hassenkam, T., Nedel, S., Bovet, N., Eiriksdottir, E.S., Alfredsson, H.A., Hem, C.P., Balogh, Z.I., Dideriksen, K., Oskarsson, N., Sigfusson, B., Larsen, G., Stipp, S.L.S. (2011) Characterization of the Eyjafjallajökull volcanic ash particles and a protocol for rapid risk assessment. *Proc. Natl. Acad. Sci., 108*, 7307–7312.

Hallquist, M., Wenger, J.C., Baltensperger, U., Rudich, Y., Simpson, D., Claeys, M., Dommen, J., Donahue, N.M., George, C., Goldstein, A.H., Hamilton, J.F., Herrmann, H., Hoffmann, T., Iinuma, Y., Jang, M., Jenkin, M.E., Jimenez, J.L., Kiendler-Scharr, A., Maenhaut, W., McFiggans, G., Mentel, T.F., Monod, A., Prevot, A.S.H., Seinfeld, J.H., Surratt, J.D., Szmigielski, R., Wildt, J. (2009) The formation, properties and impact of secondary organic aerosol: current and emerging issues. *Atmos. Chem. Phys., 9*, 5155–5236, doi:10.5194/acp-9-5155-2009.

Heal, M.R., Naysmith, P., Cook, G.T., Xu, S., Duran, T.R., Harrison, R.M. (2011) Application of 14C analyses to source apportionment of carbonaceous $PM_{2.5}$ in the UK. *Atmos. Environ., 45*, 2341–2348, doi:10.1016/j.atmosenv.2011.02.029.

Hjellbarekke, A.-G., Fjæraa, A.M. (2012) Data Report 2009. Acidifying and eutrophying compounds and particulate matter. Kjeller (EMEP/CCC-Report 1/2012).

Kulmala, M., Asmi, A., Lappalainen, H.K., Baltensperger, U., Brenguier, J.-L., Facchini, M.C., Hansson, H.-C., Hov, Ø., O'Dowd, C.D., Pöschl, U., Wiedensohler, A., Boers, R., Boucher, O., de Leeuw, G., Denier van der Gon, H.A.C., Feichter, J., Krejci, R., Laj, P., Lihavainen, H., Lohmann, U., McFiggans, G., Mentel, T., Pilinis, C., Riipinen, I., Schulz, M., Stohl, A., Swietlicki, E., Vignati, E., Alves, C., Amann, M., Ammann, M., Arabas, S., Artaxo, P., Baars, H., Beddows, D.C.S., Bergström, R., Beukes, J.P., Bilde, M., Burkhart, J.F., Canonaco, F., Clegg, S.L., Coe, H., Crumeyrolle, S., D'Anna, B., Decesari, S., Gilardoni, S., Fischer, M., Fjaeraa, A.M., Fountoukis, C., George, C., Gomes, L., Halloran, P., Hamburger, T., Harrison, R.M., Herrmann, H., Hoffmann, T., Hoose, C., Hu, M., Hyväarinen, A., Hõrrak, U., Iinuma, Y., Iversen, T., Josipovic, M., Kanakidou, M., Kiendler-Scharr, A., Kirkevåg, A., Kiss, G., Klimont, Z., Kolmonen, P., Komppula, M., Kristjánsson, J.-E., Laakso, L., Laaksonen, A., Labonnote, L., Lanz, V.A., Lehtinen, K.E.J., Rizzo, L.V., Makkonen, R., Manninen, H.E., McMeeking, G., Merikanto, J., Minikin, A., Mirme, S., Morgan, W.T., Nemitz, E., O'Donnell, D., Panwar, T.S., Pawlowska, H., Petzold, A., Pienaar, J.J., Pio, C., Plass-Duelmer, C., Prévôt, A.S.H., Pryor, S., Reddington, C.L., Roberts, G., Rosenfeld, D., Schwarz, J., Seland, Ø., Sellegri, K., Shen, X.J., Shiraiwa, M., Siebert, H., Sierau, B., Simpson, D., Sun, J.Y., Topping, D., Tunved, P., Vaattovaara, P., Vakkari, V., Veefkind, J.P., Visschedijk, A., Vuollekoski, H., Vuolo, R., Wehner, B., Wildt, J., Woodward, S., Worsnop, D.R., van Zadelhoff, G.-J., Zardini, A.A., Zhang, K., van Zyl, P.G., Kerminen, V.-M., Carslaw, K., Pandis, S.N. (2011) General overview: European integrated project on Aerosol Cloud Climate and Air Quality interactions (EUCAARI) – integrating aerosol research from nano to global scales. *Atmos. Chem. Phys., 11*, 13061–13143, doi:10.5194/acp-11-13061-2011

Lane, T.E., Donahue, N.M., Pandis, S.N. (2008) Simulating secondary organic aerosol formation using the volatility basis-set approach in a chemical transport model. *Atmos. Environ., 42*, 7439–7451, doi:10.1016/j.atmosenv.2008.06.026.

Legrand, M., Puxbaum, H. (2007) Summary of the CARBOSOL project: Present and retrospective state of organic versus inorganic aerosol over Europe. *J. Geophys. Res., 112*, D23S01, doi:10.1029/2006JD008271.

Mastin, L.G., Guffanti, M., Ewert, J.E., Spiegel, J. (2009) Preliminary spreadsheet of eruption source parameters for volcanoes of the world. U.S. Geological Survey. (Open-File Report, 2009-1133).
URL: http://pubs.usgs.gov/of/2009/1133/ [07.08.2012]

Mastin, L.G., Guffanti, M., Servranckx, R., Webley, P. Barsotti, S., Dean, K., Durant, A., Ewert, J.W., Neri, A., Rose, W.I., Schneider, D., Siebert, L., Stunder, B., Swanson, G., Tupper, A., Volentik, A., Waythomas, C. F. (2010) Erratum to `A multidisciplinary effort to assign realistic source parameters to models of volcanic ash-cloud transport and dispersion during eruptions' by Mastin et al. J. Volcanol. Geotherm. Res. 188(2009), 1-21. *J. Volcanol. Geotherm. Res., 191*, 245-245.

Mihalopoulos, N., Kerminen, V.M., Kanakidou, M., Berresheim, H., Sciare, J. (2007) Formation of particulate sulfur species (sulfate and methanesulfonate) during summer over the Eastern Mediterranean: A modelling approach. *Atmos. Environ., 41*, 6860-6871.

Ng, N.L., Canagaratna, M.R., Zhang, Q., Jimenez, J.L., Tian, J., Ulbrich, I.M., Kroll, J.H., Docherty, K.S., Chhabra, P.S., Bahreini, R., Murphy, S.M., Seinfeld, J.H., Hildebrandt, L., Donahue, N.M., DeCarlo, P.F., Lanz, V.A., Prevot, A.S.H., Dinar, E., Rudich, Y., Worsnop, D.R. (2010) Organic aerosol components observed in Northern Hemispheric datasets from Aerosol Mass Spectrometry. *Atmos. Chem. Phys.*, *10*, 4625–4641, doi:10.5194/acp-10-4625-2010.

O'Dowd, C.D., Ceburnis, D., Ovadnevaite, J., Martucci, G., Bialek, J., Monahan, C., Berresheim, H., Vaishya, A., Grigas, T., Jennings, S.G., McVeigh, P., Varghese, S., Flanagan, R., Martin, D., Moran, E., Lambkin, K., Semmler, T., Perrino, C., McGrath, R. (2012) The Eyjafjallajökull ash plume - part I: physical, chemical and optical characteristics. *Atmos. Environ.*. *48*, 129-142.

Pappalardo, G., Boesenberg, J., Amodeo, A., Ansmann, A., Apituley, A., Arboledas, L.A., Balis, D., Böckmann, C., Chaikovsky, A., Comeron, A., D'Amico, G., Freudenthaler, V., Grigorov, I., Hansen, G., Linnè, H., Kinne, S., Mattis, I., Mona, L., Mueller, D., Mitev, V., Nicolae, D., Papayannis, A., Perrone, M.R., Pietruczuk, A., Pujadas, M., Putaud, J.-P., Ravetta, F., Rizi, V., Simeonov, V., Spinelli, N., Trickl, T., Wandinger, U., Wiegner, M. (2008) EARLINET for long term observations of aerosol over Europe. In: *24th International Laser Radar Conference 2008, Boulder, Colorado, June 23rd - 27th, 2008. Proceedings.* Red Hook, NY, Curran Associates. Vol. 2, pp. 711-714.

Pappalardo, G., Laj, P. (2012) ACTRIS Research Infrastructure for coordinated long-term observation of aerosols, cloud-aerosol interactions, and trace gases in Europe. European Aerosol Conference, Granada, Spain September 2012.

Perrone, M.R., De Tomasi, F., Stohl, A., Kristiansen, N.I. (2012) Characterization of Eyjafjallajökull volcanic aerosols over Southeastern Italy. *Atmos. Chem. Phys. Discuss*., *12*, 15301-15335, doi:10.5194/acpd-12-15301-2012.

Philippin, S., Laj, P., Putaud, J.-P., Wiedensohler, A., de Leeuw, G., Fjaeraa, A.M., Platt, U., Baltensperger, U., Fiebig, M. (2009). EUSAAR – An unprecedented network of aerosol observation in Europe. *Earozoru Kenkyu, 24*, 78–83.

Pio, C.A., Legrand, M., Oliveira, T., Afonso, J., Santos, C., Caseiro, A., Fialho, P., Barata, F., Puxbaum, H., Sanchez-Ochoa, A., Kasper-Giebl, A., Gelencsér A., Preunkert, S., Schock. M. (2007) Climatology of aerosol composition (organic versus inorganic) at non-urban areas on a west-east transect across Europe. *J. Geophys. Res.*, *112*, D23S02, doi:10.1029/2006JD008038.

Pitz, M., Gu, J., Soentgen, J., Peters, A., Cyrys, J. (2011) Particle size distribution factor as an indicator for the impact of the Eyjafjallajökull ash plume at ground level in Augsburg, Germany. *Atmos. Chem. Phys.*, *11*, 9367-9374, doi:10.5194/acp-11-9367-2011.

Prata, A.J., Prata, A.T. (2012) Eyjafjallajökull volcanic ash concentrations determined using Spin Enhanced Visible and Infrared Imager measurements. *J. Geophys. Res.*, *117*, 1-24, doi:10.1029/2011JD016800.

Puxbaum, H., Caseiro, A., Sanchez-Ochoa, A., Kasper-Giebl, A., Claeys, M., Gelencser, A., Legrand, M., Preunkert, S., Pio, C. (2007) Levoglucosan levels at background sites in Europe for assessing of the impact of biomass combustion on the European aerosol background. *J. Geophys. Res., 112*, D23S05, doi:10.1029/2006JD008114.

Robinson, A.L., Donahue, N.M., Shrivastava, M.K., Weitkamp, E.A., Sage, A.M., Grieshop, A.P., Lane, T.E., Pierce, J.R., Pandis, S.N. (2007) Rethinking Organic Aerosols: Semivolatile Emissions and Photochemical Aging. *Science, 315*, 1259–1262, doi:10.1126/science.1133061.

Schäfer, K., Thomas, W., Peters, A., Ries, L., Obleitner, F., Schnelle-Kreis, J., Birmili, W., Diemer, J., Fricke, W., Junkermann, W., Pitz, M., Emeis, S., Forkel, R., Suppan, P., Flentje, H., Gilge, S., Wichmann, H. E., Meinhardt, F., Zimmermann, R., Weinhold, K., Soentgen, J., Münkel, C., Freuer, C., Cyrys, J. (2011) Influences of the 2010 Eyjafjallajökull volcanic plume on air quality in the northern Alpine region. *Atmos. Chem. Phys., 11,* 8555-8575, doi:10.5194/acp-11-8555-2011.

Schumann, U., Weinzierl, B., Reitebuch, O., Schlager, H., Minikin, A., Forster, C., Baumann, R., Sailer, T., Graf, K., Mannstein, H., Voigt, C., Rahm, S., Simmet, R., Scheibe, M., Lichtenstern, M., Stock, P., Rüba, H., Schäuble, D., Tafferner, A., Rautenhaus, M., Gerz, T., Ziereis, H., Krautstrunk, M., Mallaun, C., Gayet, J.-F., Lieke, K., Kandler, K., Ebert, M., Weinbruch, S., Stohl, A., Gasteiger, J., Groß, S., Freudenthaler, V., Wiegner, M., Ansmann, A., Tesche, M., Olafsson, H., Sturm, K. (2011) Airborne observations of the Eyjafjalla volcano ash cloud over Europe during air space closure in April and May 2010. *Atmos. Chem. Phys*, *11,* 2245-2279, doi:10.5194/acp-11-2245-2011.

Sciare, J., Oikonomou, K., Favez, O., Markaki, Z., Liakakou, E., Cachier, H., Mihalopoulos, N. (2008) Long-term measurements of carbonaceous aerosols in the Eastern Mediterranean: Evidence of long-range transport of biomass burning. *Atmos. Chem. Phys., 8*, 5551-5563.

Shrivastava, M.K., Lane, T.E., Donahue, N.M., Pandis, S.N., Robinson, A.L. (2008) Effects of gas particle partitioning and aging of primary emissions on urban and regional organic aerosol concentrations. *J. Geophys. Res., 113*, D18301, doi:10.1029/2007JD009735.

Simpson, D., Benedictow, A., Berge, H., Bergström, R., Emberson, L.D., Fagerli, H., Hayman, G.D., Gauss, M., Jonson, J.E., Jenkin, M.E., Nyıri, A., Richter, C., Semeena, V.S., Tsyro, S., Tuovinen, J.-P., Valdebenito, A., Wind, P. (2012) The EMEP MSC-W chemical transport model – Part 1: Model description. *Atmos. Chem. Phys. Discuss., 12*, 3781–3874, doi:10.5194/acpd-12-3781-2012.

Simpson, D., Guenther, A., Hewitt, C., Steinbrecher, R. (1995) Biogenic emissions in Europe 1. Estimates and uncertainties. *J. Geophys. Res., 100*, 22 875–22 890, doi:10.1029/95JD02368.

Simpson, D., Winiwarter, W., Börjesson, G., Cinderby, S., Ferreiro, A., Guenther, A., Hewitt, C.N., Janson, R., Khalil, M.A.K., Owen, S., Pierce, T.E., Puxbaum, H., Shearer, M., Skiba, U., Steinbrecher, R., Tarrason, L., Öquist, M.G. (1999) Inventorying emissions from Nature in Europe. *J. Geophys. Res., 104*, 8113–8152, doi:10.1029/98JD02747.

Simpson, D., Yttri, K., Klimont, Z., Kupiainen, K., Caseiro, A., Gelencser, A., Pio, C., Legrand, M. (2007) Modeling Carbonaceous Aerosol over Europe. Analysis of the CARBOSOL and EMEP EC/OC campaigns. *J. Geophys. Res.*, *112*, D23S14, doi:10.1029/2006JD008158.

Stohl, A., Prata, A. J., Eckhardt, S., Clarisse, L., Durant, A., Henne, S., Kristiansen, N. I., Minikin, A., Schumann, U., Seibert, P., Stebel, K., Thomas, H. E., Thorsteinsson, T., Tørseth, K., Weinzierl, B. (2011) Determination of time- and height-resolved volcanic ash emissions for quantitative ash dispersion modeling: The 2010 Eyjafjallajokull eruption (2011). *Atmos. Chem. Phys.*, *11*, 4333-4351, doi:10.5194/acp-11-4333-2011.

Szidat, S.,Jenk, T.M., Synal, H.-A., Kalberer, M., Wacker, L., Hajdas, I., Kasper-Giebl, A., Baltensperger, U. (2006) Contributions of fossil fuel, biomass burning, and biogenic emissions to carbonaceous aerosols in Zürich as traced by ^{14}C. *J. Geophys. Res.*, *111*, D07206, doi:10.1029/2005JD006590.

Thorsteinsson, T., Johannsson, T., Stohl, A., Kristiansen, N.I. (2012) High levels of particulate matter in Iceland due to direct ash emissions by the Eyjafjallajökull eruption and resuspension of deposited ash. *J. Geophys. Res.*, *117*, B00C05. doi:10.1029/2011JB008756.

Tørseth, K., Aas, W., Breivik, K., Fjæraa, A.M., Fiebig, M., Hjellbrekke, A.G., Lund Myhre, C., Solberg, S., Yttri, K.E. (2012) Introduction to the European Monitoring and Evaluation Programme (EMEP) and observed atmospheric composition change during 1972–2009. *Atmos. Chem. Phys.*, *12*, 5447-5481, doi:10.5194/acp-12-5447-2012.

UNECE (2009a) Guidelines for reporting emission data under the Convention on Long-Range Transboundary Air Pollution. Geneva (ECE/EB.AIR/97). **URL:** http://www.ceip.at/fileadmin/inhalte/emep/reporting_2009/Rep_Guidelines_ECE_EB_AIR_97_e.pdf [07-08-2012]

UNECE (2009b) Progress in activities in 2009 and future work. Measurements and modelling (acidification, eutrophication, photooxidants, heavy metals, particulate matter and persistent organic pollutants). Draft revised monitoring strategy. Geneva (ECE/EB.AIR/GE.1/2009/15). **URL:** http://www.unece.org/env/documents/2009/EB/ge1/ece.eb.air.ge.1.2009.15.e.pdf [16.08.2012]

UNECE (2012) Parties to UNECE Air Pollution Convention approve new emission reduction commitments for main air pollutants by 2020. Press release 04 May 2012. Geneva, United Nations Economic Commission for Europe. **URL:** http://www.unece.org/index.php?id=29858 [07-08-2012]

WHO (2005) Air quality guidelines for particulate matter, ozone, nitrogen dioxide and sulfur dioxide - Global update 2005. Copenhagen, World Health Organization. **URL:** http://www.who.int/phe/health_topics/outdoorair_aqg/en/ [2011-08-16].

Yttri, K.E., Aas, W., Bjerke, A., Ceburnis, D., Dye, C., Emblico, L., Facchini, M.C., Forster, C., Hanssen, J.E., Hansson, H.C., Jennings, S.G., Maenhaut, W., Putaud, J.P., Tørseth, K. (2007) Elemental and organic carbon in PM10: a one year measurement campaign within the European Monitoring and Evaluation Programme EMEP. *Atmos. Chem. Phys.*, *7*, 5711-5725.

Yttri, K.E., Simpson, D., Nøjgaard, J.K., Kristensen, K., Genberg, J., Stenström, K., Swietlicki, E., Hillamo, R., Aurela, M., Bauer, H., Offenberg, J.H., Jaoui, M., Dye, C., Eckhardt, S., Burkhart, J.F., Stohl, A., Glasius, M. (2011a) Source apportionment of the summer time carbonaceous aerosol at Nordic rural background sites. *Atmos. Chem. Phys., 11*, 13339-13357, doi:10.5194/acp-11-13339-2011.

Yttri, K.E., Simpson, D., Stenström, K., Puxbaum, H. Svendby, T. (2011b**)** Source apportionment of the carbonaceous aerosol in Norway – quantitative estimates based on ^{14}C, thermal-optical and organic tracer analysis. *Atmos. Chem. Phys. Discuss., 11*, 7375-7422.

APPENDIX A

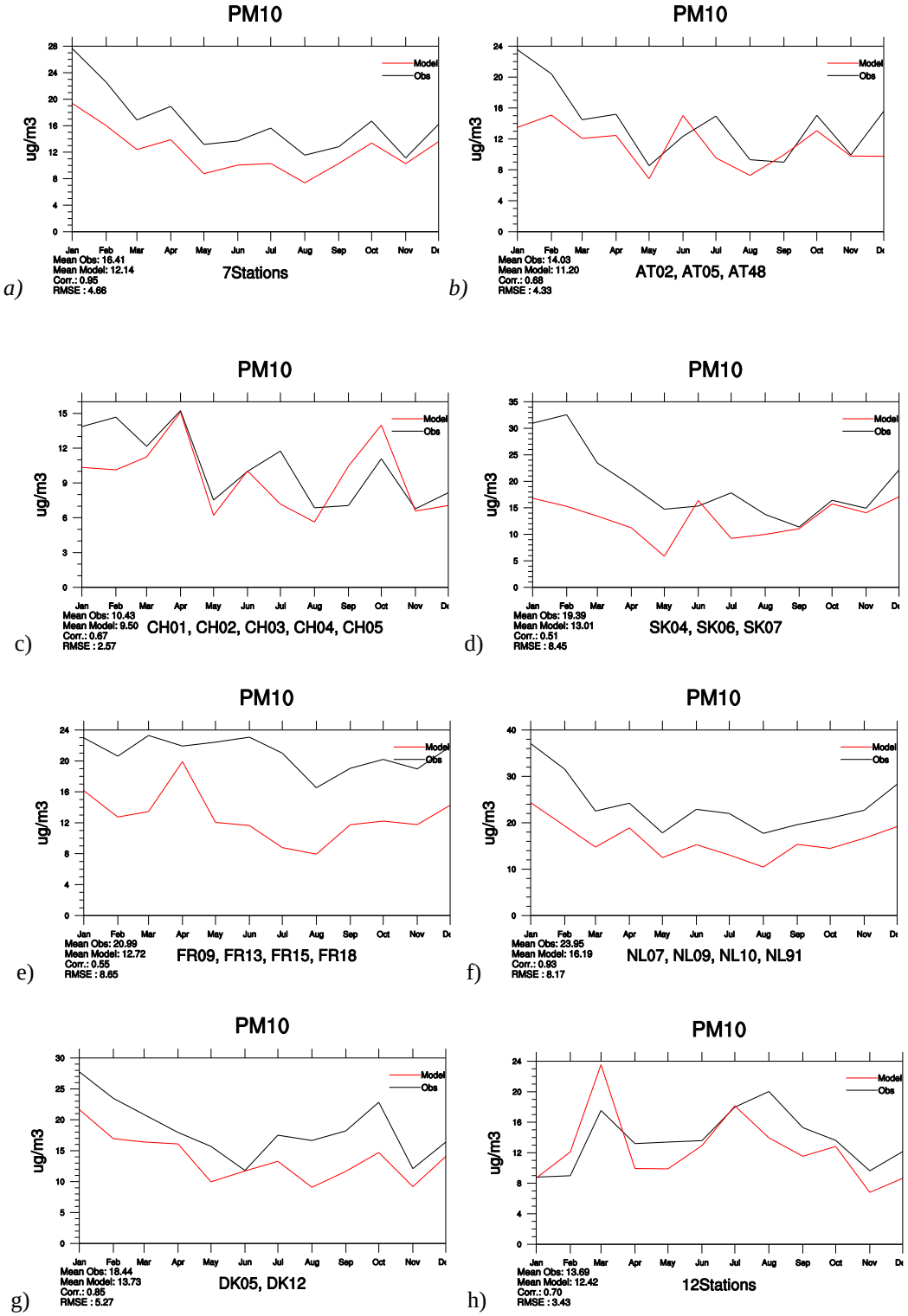

Figure A.1: Monthly time-series of observed and calculated of PM_{10} concentrations in 2010 at the sites in different countries. Here: a) German sites; h) Spanish sites; i) based on daily and j) on hourly observations at British sites.

i)

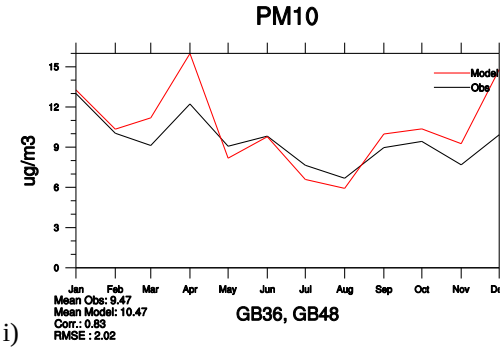

j)

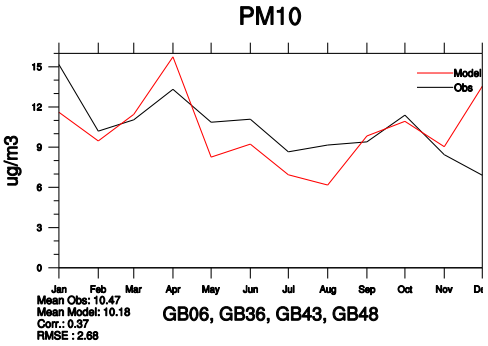

k)

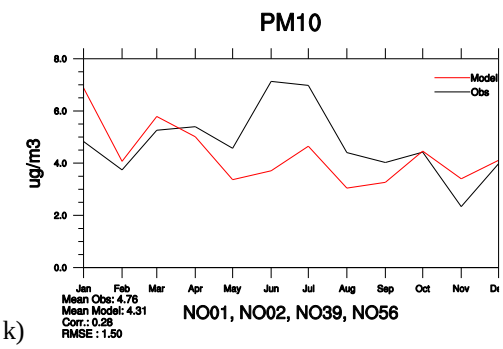

l)

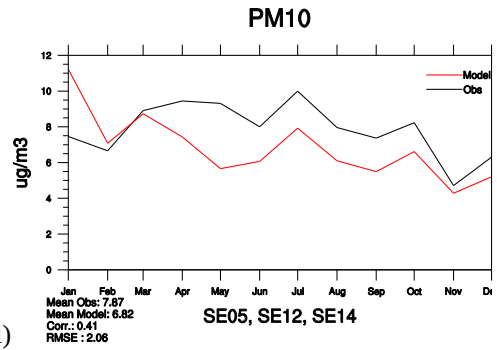

Figure A.1, cont.

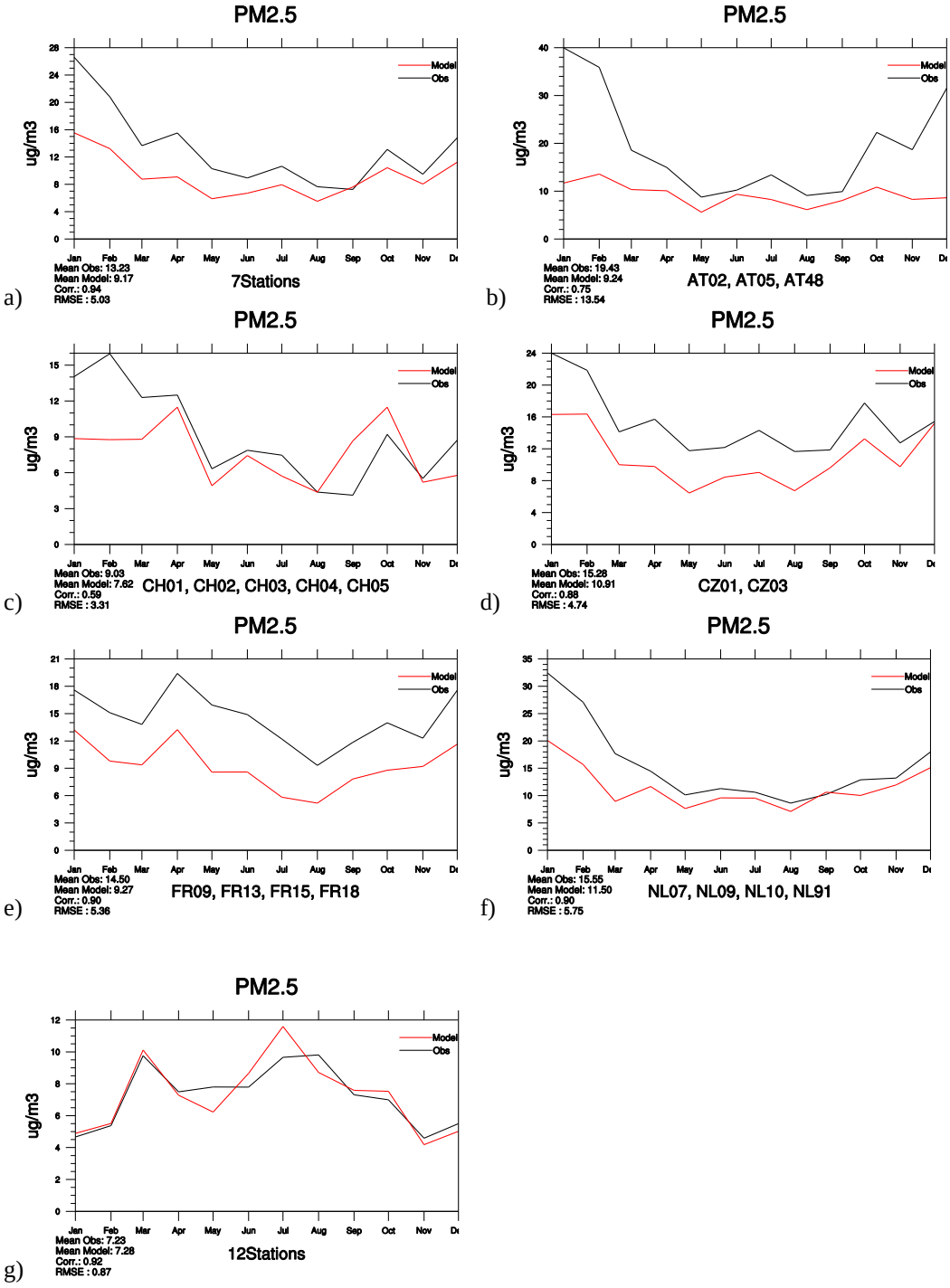

Figure A.2: Monthly time-series of observed and calculated of $PM_{2.5}$ concentrations in 2010 at the sites in different countries. Here: a) German sites; g) Spanish sites; h) based on daily and i) on hourly observations at British sites.

h)

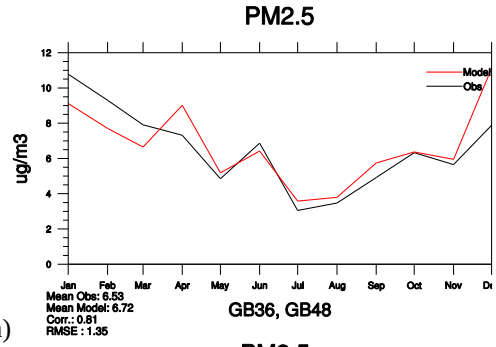

i)

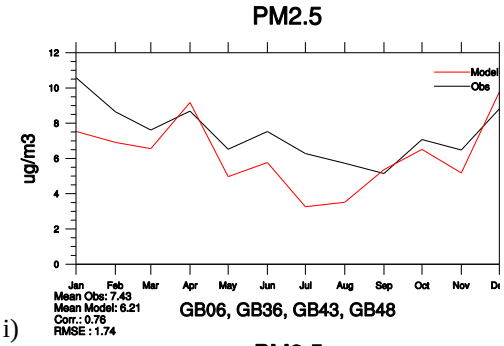

j)

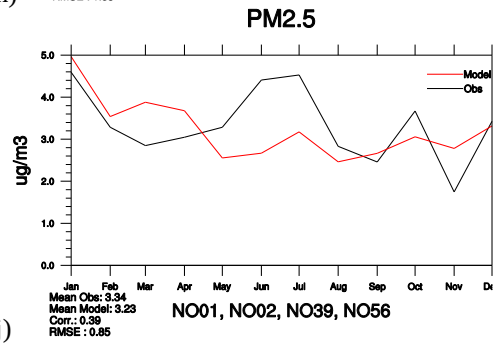

k)

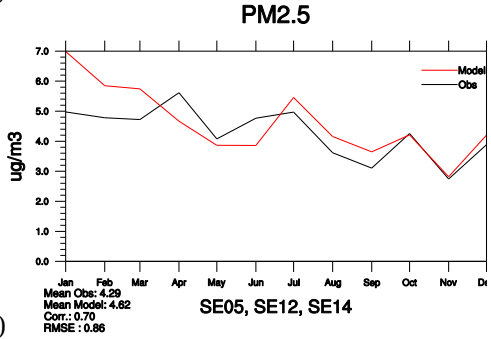

Figure A.2, cont.

Table A.1: Statistic analysis of model calculated PM_{10} against observations in 2010.

Site	Name	Obs	Mod	Bias	R	RMSE	IOA
AT02	Illmitz	23.79	12.99	-45	0.55	18.22	0.59
AT05	Vorhegg	8.99	8.23	-8	0.44	7.93	0.66
AT48	Zoebelboden	9.31	11.48	23	0.61	7.25	0.76
CH01	Jungfraujoch	2.20	5.40	145	0.29	6.33	0.47
CH02	Payerne	16.31	10.38	-36	0.53	11.21	0.65
CH03	Tänikon	16.30	11.20	-31	0.51	11.64	0.66
CH04	Chaumont	8.55	10.46	22	0.60	6.86	0.75
CH05	Rigi	8.57	9.52	11	0.64	6.59	0.79
CY02	Ayia Marina	30.32	35.98	19	0.46	29.49	0.63
CZ01	Svratouch	15.97	12.75	-20	0.62	7.50	0.75
CZ03	Košetice	16.95	12.19	-28	0.69	8.64	0.76
DE01	Westerland/Wenningsted	18.36	13.49	-27	0.72	8.97	0.78
DE02	Langenbrügge/Waldhof	18.04	12.53	-31	0.71	10.67	0.73
DE03	Schauinsland	10.05	9.28	-8	0.68	6.60	0.80
DE07	Neuglobsow	16.52	11.64	-30	0.73	9.74	0.76
DE08	Schmücke	11.38	11.43	0	0.49	7.29	0.69
DE09	Zingst	17.03	11.12	-35	0.72	9.92	0.72
DE44	Melpitz	23.40	13.46	-42	0.68	16.18	0.64
DK05	Keldsnor	17.42	14.63	-16	0.46	13.68	0.57
DK12	Risoe	19.69	10.81	-45	0.57	12.87	0.62
ES01	Toledo	11.00	7.93	-28	0.65	8.88	0.70
ES06	Mahón	25.38	16.11	-37	0.30	16.63	0.48
ES07	Víznar	15.95	12.81	-20	0.53	11.51	0.70
ES09	Campisábalos	11.01	6.76	-39	0.68	9.27	0.63
ES10	Cabo de Creus	16.45	13.32	-19	0.34	10.09	0.56
ES11	Barcarrota	15.18	9.57	-37	0.28	13.40	0.46
ES12	Zarra	11.89	10.10	-15	0.66	6.86	0.79
ES13	Penausende	8.72	6.61	-24	0.55	7.23	0.60
ES14	Els Torms	12.61	10.89	-14	0.62	6.99	0.76
ES16	O Saviñao	8.77	7.64	-13	0.65	3.93	0.79
ES17	Doñana	15.75	12.95	-18	0.45	8.98	0.66
ES1778	Montseny	18.24	15.54	-15	0.68	9.73	0.78
GB36	Harwell	11.40	12.51	10	0.50	8.78	0.66
GB48	Auchencorth Moss	7.79	8.62	11	0.61	4.86	0.77
IT01	Montelibretti	26.99	12.26	-55	0.48	18.15	0.54
LV10	Rucava	14.55	9.76	-33	0.34	10.66	0.57
LV16	Zoseni	15.79	8.30	-47	0.48	12.26	0.59
MD13	Leova II	4.73	14.3	202	0.06	17.01	0.26
NL07	Eibergen	27.01	16.14	-40	0.64	15.77	0.65
NL09	Kollumerwaard	21.82	15.14	-31	0.68	11.68	0.73
NL10	Vreedepeel	24.31	15.87	-35	0.75	11.76	0.74
NL91	De Zilk	22.54	16.77	-26	0.68	11.39	0.73
PL05	Diabla Gora	18.73	11.59	-38	0.44	13.17	0.61
RO08	Poiana Stampei	17.46	9.52	-45	0.43	14.3	0.60
SE05	Bredkälen	3.63	2.95	-19	0.40	2.99	0.59
SE12	Aspvreten	8.29	6.24	-25	0.57	5.52	0.68
SE14	Råö	11.73	10.21	-13	0.72	5.30	0.83
SI08	Iskrba	14.4	11.17	-22	0.58	8.77	0.72

Hourly							
CZ03	Košetice	19.28	12.66	-34	0.69	10.46	0.71
ES09	Campisábalos	10.92	6.63	-39	0.59	8.37	0.62
ES12	Zarra	13.03	10.55	-19	0.57	7.73	0.73
ES13	Penausende	8.50	6.59	-22	0.44	4.75	0.64
ES16	O Saviñao	11.26	7.72	-31	0.61	5.47	0.68
FR09	Revin	25.70	12.47	-51	0.45	15.84	0.49
FR13	Peyrusse Vieille	21.65	11.33	-48	0.27	13.58	0.46
FR15	La Tardière	20.24	13.39	-34	0.51	11.15	0.64
FR18	La Coulonche	16.50	12.53	-24	0.66	7.98	0.76
GB06	Lough Navar	10.29	8.39	-18	0.55	6.61	0.70
GB36	Harwell	16.03	11.99	-25	0.54	9.42	0.68
GB43	Narberth	8.36	11.66	39	0.63	6.69	0.75
GB48	Auchencorth Moss	7.25	8.47	17	0.66	4.58	0.79
GR02	Finokalia	25.72	49.99	94	0.74	49.24	0.75
HU02	K-puszta	27.61	14.64	-47	0.63	19.36	0.61
MK07	Lazaropole	17.08	17.19	1	0.50	20.67	0.62
NL07	Eibergen	27.06	16.06	-41	0.64	15.80	0.65
NL09	Kollumerwaard	21.84	15.14	-31	0.68	11.69	0.73
NL10	Vreedepeel	24.68	16.07	-35	0.76	11.98	0.74
NL91	De Zilk	22.60	16.77	-26	0.68	11.40	0.73
SE11	Vavihill	13.76	9.00	-35	0.67	7.61	0.71
Weekly							
NO01	Birkenes	5.38	4.62	-14	0.47	2.53	0.67
NO02	Birkenes II	5.13	4.41	-14	0.56	2.54	0.72
NO39	Kårvatn	3.89	2.21	-43	0.28	2.78	0.51
NO56	Hurdal	4.84	4.81	-1	0.1	2.68	0.39
SK04	Stará Lesná	13.1	10.13	-23	-0.01	7.17	0.44
SK06	Starina	15.45	11.28	-27	0.36	7.55	0.54
SK07	Topolniky	23.86	14.82	-38	0.53	12.91	0.58

Here, Obs – the measured mean, Mod – the calculated mean, Bias is calculated as Σ(Mod-Obs)/Obs x 100%, R– the temporal correlation coefficient and RMSE – the Root mean Square Error= $1/Ns \times \Sigma(Mod-Obs)^2]^{1/2}$. Cells marked in grey are sites with less than 75% data coverage

Table A.2: Statistic analysis of model calculated daily $PM_{2.5}$ against observations in 2010.

Site	Name	Obs	Mod	Bias	R	RMSE	IOA
AT02	Illmitz	19.33	10.56	-45	0.65	15.16	0.61
CH02	Payerne	14.75	9.06	-39	0.55	11.89	0.64
CH05	Rigi	7.92	8.23	4	0.74	5.79	0.85
CY02	Ayia Marina	15.71	19.27	23	0.32	14.64	0.52
CZ03	Košetice	15.24	10.37	-32	0.71	7.49	0.75
DE02	Langenbrügge/Waldhof	15.09	9.78	-35	0.75	10.59	0.73
DE03	Schauinsland	8.16	7.39	-9	0.59	5.67	0.73
DE07	Neuglobsow	11.50	8.24	-28	0.73	6.52	0.80
DE08	Schmücke	6.87	9.14	33	0.45	6.08	0.64
DE44	Melpitz	19.30	10.87	-44	0.72	14.01	0.68
ES01	Toledo	5.93	4.82	-19	0.71	3.01	0.78
ES07	Viznar	9.22	6.73	-27	0.59	5.08	0.71
ES09	Campisábalos	5.65	4.54	-20	0.75	2.35	0.82
ES10	Cabo de Creus	7.87	7.71	-2	0.52	4.57	0.69
ES11	Barcarrota	7.64	5.45	-29	0.46	5.71	0.57
ES12	Zarra	5.47	6.87	26	0.71	3.42	0.78
ES13	Penausende	4.86	4.42	-9	0.75	2.51	0.82
ES14	Els Torms	7.32	7.96	9	0.63	4.60	0.77
ES16	O Saviñao	6.20	5.35	-14	0.68	2.88	0.80
ES1778	Montseny	12.32	12.17	-1	0.67	5.47	0.81
GB36	Harwell	8.64	8.15	-6	0.62	5.72	0.77
GB48	Auchencorth Moss	4.31	5.04	17	0.71	3.12	0.83
IT04	Ispra	17.92	12.00	-33	0.37	16.57	0.60
LV10	Rucava	11.95	7.69	-36	0.64	7.80	0.71
LV16	Zoseni	10.49	6.84	-35	0.51	7.22	0.66
NL09	Kollumerwaard	13.61	10.54	-23	0.76	9.02	0.82
NL10	Vreedepeel	16.37	12.07	-26	0.75	9.61	0.79
NL11	Cabauw	17.22	11.88	-31	0.74	10.23	0.78
PL05	Diabla Gora	15.21	9.74	-36	0.44	11.64	0.61
SE05	Bredkälen	2.07	2.23	8	0.53	1.49	0.71
SE14	Råö	6.52	6.24	-4	0.50	4.51	0.70
SI08	Iskrba	11.61	9.10	-22	0.62	7.44	0.72
Hourly							
FR09	Revin	18.43	10.37	-44	0.52	11.29	0.59
FR13	Peyrusse Vieille	13.53	8.09	-40	0.43	8.87	0.57
FR15	La Tardière	14.92	9.66	-35	0.58	8.57	0.68
FR18	La Coulonche	11.56	8.34	-28	0.68	6.48	0.76
GB36	Harwell	10.26	7.92	-23	0.68	5.60	0.78
GB48	Auchencorth Moss	4.35	5.86	35	0.67	3.92	0.79
SE11	Vavihill	7.26	6.57	-10	0.67	4.97	0.78
SE12	Aspvreten	5.79	4.88	-16	0.58	4.02	0.72
Weekly							
NO01	Birkenes	3.49	3.26	-7	0.29	1.83	0.51
NO02	Birkenes II	3.41	3.10	-9	0.40	2.23	0.50
NO39	Kårvatn	3.19	1.72	-46	0.24	2.61	0.46
NO56	Hurdal	3.85	4.10	6	-0.02	2.62	0.26

Cells marked in grey are sites with less than 75% data coverage.

Table A.3: Statistic analysis of model calculated daily EC, OC and TC in PM_{10} and $PM_{2.5}$ against observations in 2010.

Site	Name	Obs	Mod	Bias	R	RMSE	IOA
	EC in PM_{10}						
DE44	Melpitz	1.60	0.54	-66	0.68	2.62	0.33
ES09	Campisábalos	0.12	0.11	-8	0.53	0.08	0.64
ES1778	Montseny	0.23	0.58	152	0.16	0.40	0.31
NO02	Birkenes II*)	0.11	0.08	-27	0.55	0.06	0.64
SE11	Vavihill*)	0.20	0.20	0	0.39	0.12	0.61
SE12	Aspvreten	0.31	0.21	-32	0.62	0.26	0.62
	EC in $PM_{2.5}$						
CZ03	Košetice	0.49	0.32	-35	0.67	0.29	0.70
DE02	Langenbrügge/Waldhof	0.33	0.30	-9	0.55	0.20	0.66
DE03	Schauinsland	0.16	0.25	56	0.35	0.15	0.53
DE08	Schmücke	0.22	0.30	36	0.57	0.19	0.70
DE44	Melpitz	1.34	0.38	-72	0.68	2.28	0.33
ES09	Campisábalos	0.11	0.09	-18	0.57	0.05	0.71
ES78	Montseny	0.22	0.56	155	0.05	0.40	0.29
IT04	Ispra	1.27	0.74	-42	0.37	1.06	0.54
NO02	Birkenes II*)	0.10	0.07	-30	0.56	0.07	0.57
SI08	Iskrba	0.38	0.37	-3	0.51	0.31	0.66
	OC in PM_{10}						
DE44	Melpitz	3.08	1.22	-60	0.55	3.19	0.43
ES09	Campisábalos	1.87	0.91	-51	0.79	1.08	0.66
ES1778	Montseny	1.74	1.57	-10	0.50	0.81	0.70
NO02	Birkenes II*)	0.90	0.88	-2	0.27	0.39	0.48
SE11	Vavihill*)	1.71	1.08	-37	-0.1	1.14	0.42
SE12	Aspvreten	1.63	1.07	-34	0.43	1.53	0.48
	OC in $PM_{2.5}$						
CZ03	Košetice	3.17	1.31	-59	0.24	3.35	0.44
DE03	Schauinsland	1.82	1.10	-40	0.72	1.13	0.67
DE08	Schmücke	1.83	1.10	-40	0.63	1.17	0.65
DE44	Melpitz	2.61	1.16	-56	0.47	3.00	0.40
ES09	Campisábalos	1.78	1.14	-36	0.80	0.81	0.72
ES1778	Montseny	1.53	1.55	1	0.07	1.10	0.36
IT04	Ispra	5.81	2.02	-65	0.12	6.57	0.45
NO02	Birkenes II*)	0.67	0.87	30	0.32	0.42	0.46
SI08	Iskrba	3.38	1.54	-54	0.31	2.64	0.47
	TC in PM_{10}						
DE44	Melpitz	4.68	1.69	-64	0.67	5.69	0.39
ES09	Campisábalos	1.98	0.99	-50	0.79	1.13	0.66
ES1778	Montseny	1.97	2.14	9	0.43	0.94	0.65
NO02	Birkenes II*)	1.00	0.96	-4	0.00	1.22	0.42q
SE11	Vavihill*)	1.94	1.28	-33	0.00	1.22	0.42
SE12	Aspvreten	1.94	1.23	-37	0.45	1.78	0.47
	TC in $PM_{2.5}$						
CZ03	Košetice	3.66	1.67	-54	0.42	3.53	0.47
DE03	Schauinsland	1.97	1.36	-31	0.67	1.14	0.68
DE08	Schmücke	2.05	1.41	-31	0.64	1.16	0.69
DE44	Melpitz	3.95	1.53	-61	0.63	5.12	0.38
ES09	Campisábalos	1.88	1.22	-35	0.79	0.83	0.73
ES1778	Montseny	1.75	2.17	24	0.08	1.28	0.32
IT04	Ispra	7.08	2.67	-62	0.19	7.57	0.46
NO02	Birkenes II*)	0.77	0.94	22	0.36	0.45	0.48
SI08	Iskrba	3.76	1.93	-49	0.41	2.75	0.49

*) Weekly observations

Cells marked in grey are sites with less than 75% data coverage

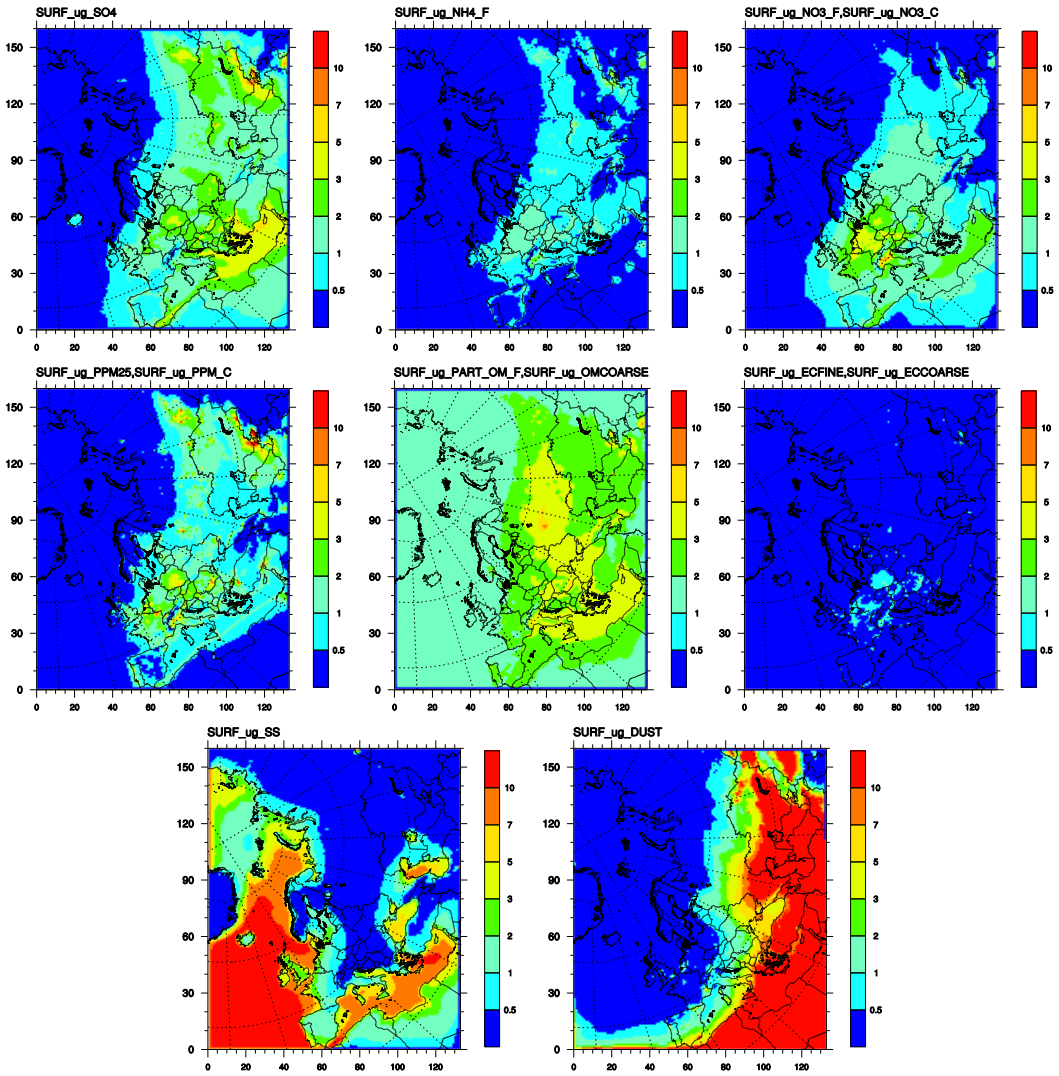

Figure A.3: Annual mean concentrations of the individual aerosol components of PM_{10} in 2010 calculated with the EMEP/MSC-W model. Here, upper panel: SO_4^{2-}, NO_3^-, NH_4^+; middle panel: primary PM_{10}, elemental carbon, organic aerosols; lower panel: sea salt and mineral dust. Units: $\mu g/m^3$.

emep

Chemical Co-ordinating Centre of EMEP
Norwegian Institute for Air Research
P.O. Box 100, N-2027 Kjeller, Norway

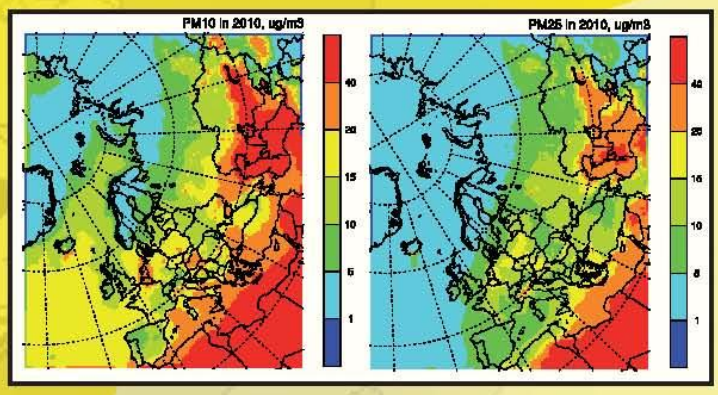

ccc
NILU
Norwegian Institute for Air Research
P.O. Box 100
NO-2027 Kjeller
Norway
Phone: +47 63 89 80 00
Fax: +47 63 89 80 50
E-mail: kjetil.torseth@nilu.no
Internet: www.nilu.no

ciam
International Institute for
Applied Systems Analysis
(IIASA)
Schlossplatz 1
A-2361 Laxenburg
Austria
Phone: +43 2236 807 0
Fax: +43 2236 71 313
E-mail: amann@iiasa.ac.at
Internet: www.iiasa.ac.at

ceip
Umweltbundesamt GmbH
Spittelauer Lände 5
1090 Vienna
Austria
Phone: +43-(0)1-313 04
Fax: +43-(0)1-313 04/5400
E-mail:
emep.emissions@umweltbundesamt.at
Internet:
http://www.umweltbundesamt.at/

msc-e
Meteorological Synthesizing
Centre-East
Krasina pereulok, 16/1
123056 Moscow
Russia
Phone +7 495 981 15 66
Fax: +7 495 981 15 66
E-mail: msce@msceast.org
Internet: www.msceast.org

msc-w
Norwegian Meteorological
Institute (met.no)
P.O. Box 43 Blindern
NO-0313 OSLO
Norway
Phone: +47 22 96 30 00
Fax: +47 22 96 30 50
E-mail: emep.mscw@met.no
Internet: www.emep.int